A THESIS SUBMITTED TOWARD THE DEGREE OF DOCTOR OF PHILOSOPHY

Biomaterials with Antimicrobial and Regenerative Properties for The Fabrication of Custom Medical Devices for Treatment of Medication-Related Osteonecrosis of The Jaw (MRONJ)

Abdullah Musaed S Alghamdi

MARCH 2024

SUPERVISORS:

Professor Paul Hatton,

Dr Ilida Ortega Asencio,

Professor Graham Stafford

School of Clinical Dentistry in the Faculty of Health

Abstract

Medication-related osteonecrosis of the jaw (MRONJ) is a complex disease that affects oral soft tissues and bone, especially the mandible. It occurs in patients who have used certain types of medication, especially anti-resorptive and anti-angiogenic drugs. The precise aetiology of MRONJ is still subject to research and debate, but it is now generally agreed that microorganisms play a crucial role in its progression. Many bacterial species have been isolated from clinical sites, including anaerobic, aerobes, and Gram-positive and negative organisms. Current treatments are based on antimicrobial wash followed by broad spectrum antibiotics and finally by surgical removal of necrotic bone. MRONJ is still not considered to be reversible or preventable and causes bone loss and a demonstrable negative impact on quality of life. Therefore, it is a significant unmet and growing clinical challenge, and new therapeutic approaches are needed. In recent years, advances in dental technology and biomaterials science suggest that it is possible to fabricate custom shaped devices using antimicrobial materials. These might have a wide range of potential clinical applications. This study aimed to evaluate the potential custom prosthetics that can locate a modified biomaterial to promote healing at a site of MRONJ. A range of potentially antimicrobial bio-active glasses have been fabricated and characterized. Antimicrobial activities have also been conducted using *E. coli*. However, this part of the project will be further explored using various test organisms commonly associated with MRONJ including clinical isolates. Bioactive glasses based on the substitution of CaO with CuO in 45S5 bioactive glass were designed at (0, 1, .2.5, and 5 mol% substitution). Glasses were prepared using melt route and post melt component determine using XRF and SEM/EDS. Further structural characterisations include XRD

to determine lack of crystallinity and thermal analysis (differential scanning calorimetry, DSC).

Ion release was performed with all glass in the form of powder in deionised water prior to antibacterial study and biocompatibility assessment. Agar disc diffusion antimicrobial testing was carried out using Gram positive *Actinomyces oris* (laboratory strain MF1) and a clinical isolate from MRONJ patient, and Gram negative clinical isolate *Prevotella buccae*, both considered as one of the key pathogens in the development of MRONJ. This work demonstrates that the 5 mol% and 2.5 mol% copper substituted bioactive glass exhibited the greatest antimicrobial activity against the *Actinomyces sp*. The *Prevotella* bacteria were unsuccessful to show result due to difficulties growing the bacteria on the plate for testing

Maximum loading of bioactive glass into an acrylic (PMMA) denture base material were assessed. Composite of 30% (w/w) composite were obtained. Biocompatibility was investigated using the 30% (w/w) composite with all glass composition with two cell lines (MG63 and L929). In simple terms, invitro biocompatibility decreased with increased copper substitution, with 5 mol% copper substituted glass-acrylic composites appearing to kill all cells after 48h of direct contact. This result was interesting as the highest copper glass (5 mol%) release the least sodium ions which are classically associated with the cytotoxicity. It is therefore likely that a different mechanism as responsible, potentially related to copper ions release (as the 5 mol% substituted released the most copper ions). This does not though exclude the potential for synergic effect between establishment of a basic pH via Na^+ release and the copper ions (Cu I + Cu II) in solution. It was concluded that copper-substituted bioactive

glasses have potential for use in preparation of antimicrobial composite, but further work is required to optimise formulation and take forward to additive manufacturing.

Covid impact statement

The pandemic arrived in the UK just as I was starting my PhD, with the lockdown interrupting my early training that was necessary to commence laboratory work. Much of my time in lockdown was spent reading the literature (especially the consideration of the role of microbial infection in MRONJ) and learning about subjects relevant to my PhD with my supervisors. Working closely with Professor Hatton and other PhD students, we also undertook a specific study of how to read and interpret published papers and design and write scientific documents.

Access to the laboratory for further training and research was exceptionally difficult until they opened partially in the summer of 2021 but even then, restriction impacted on practical instruction for laboratory.

Periodic lockdown further impacted, and this update lack of family contact (via travel restrictions) also impacted on my mental wellbeing.

Acknowledgement

First and most I would like to express my gratitude and thanks to my parent and sibling for the continuous support and encouragements throughout this PhD journey and to family.

I would like to thank my sponsors King Saud University and the Saudi Cultural Bureau in London, for making this valuable PhD happening for me.

I am hugely grateful to my supervisory team Professor Paul Hatton, Professor Graham Stafford, and Dr Ilida Ortega Asencio, for their support and superb guidance and advice in this PhD project, especially throughout the pandemic periods. I would also like to thank all the school's technical staff, especially Jason Heath, for much training in microbiology and Dr Emilia Barker for the guidance and help in the material lab and Lisa ling for helping in the cell culture laboratory. I would like to share my gratitude to Dr Aileen Crawford for the support and help with the cytotoxicity study for providing the cell and the protocol. I am grateful to Rayan Binduhayyim for sharing his glass-making skills and characterization techniques, as well as providing bioactive glass composition that I have evolved in this study. My thanks and best wishes to all the PGR students' community in the school and the faculty of health for the support and the activity which was an important to me during this PhD experience to share and support each other.

List of abbreviation in ascending order:

Abbreviation / symbols:	In full
°	Degree.
°C	Degree Celsius.
µl	Microlitres.
µm	Micrometres.
µm	Micrometres.
3D	Three dimensional.
Ag	Silver.
ANOVA	Analysis of variance.
ATCC	American type culture collection.
$CaCO_3$	Calcium carbonate.
$CaHPO_4$	Calcium phosphate dibasic.
CaO	Calcium oxide.
CaP	Calcium phosphate.
Na_2O	Sodium carbonate anhydrous.
Cu	Copper.
CuO	Copper oxide.
DSC	Differential scanning calorimetry.
Fe_2O_3	Iron (iii) oxide.
FTIR	Fourier transform infrared spectroscopy.
HA	Hydroxyapatite.
ICP-OES	Inductive coupled plasma - optical emission spectroscopy.
Kα	K alpha (k) electrons shell.
Kβ	K beta (k) electrons shell.

L929	Cell line.
Li	Lithium.
MAS-NMR	Magic angle spinning nuclear magnetic resonance.
mg	Milligrams.
MG63	Cell line.
ml	Millilitres.
mm	Millimetres.
MRONJ	Medication-related osteonecrosis of the jaw.
Na_2O	Sodium oxide.
nHA.	Nano hydroxyapatite.
Ni	Nitrogen.
P_2O_5	Phosphorus pentoxide.
PMMA	Poly (methyl methacrylate).
Psi	Pound per square inches.
Rpm	Round per minute.
SEM	Scanning electron microscopy.
SiO_2	Silicon dioxide.
Sp.	Species.
Tc	Crystallization temperature.
TCP	Tricalcium phosphate.
Tg	Glass transition temperature.
Ti	Titanium.
W/g	Watt per gram.
Wt.%	Weight per cent.
XRD	X-ray diffraction.

XRF	X-ray fluorescence.
PCR	Polymerase chain reaction.
pH	Power of hydrogen.
BO	Bridging oxygen.
NBO	Non-bridging oxygen.
NC	Network connectivity.
BAG	Bioactive glass
BG	Bioglass

Contents

1 Introduction. 1

2 Literature review. 4

2.1 A healthy mouth. 4

2.2 Bone and turnover process 5

2.3 Medication-related osteonecrosis of the jaw (MRONJ). 7

2.3.1 The role of microorganisms in medication-related osteonecrosis of the jaw. 9

2.3.2 Medication related osteonecrosis of the jaw MRONJ site environment 13

2.4 Antimicrobial materials and related technologies that have the potential for use in an oral custom device. 14

2.5 Bioactive glasses 24

2.5.1 Glasses' structure 26

2.5.2 Mechanisms of bioactive glasses 29

2.5.3 Evidence on the ion dissolution, antimicrobial, and angiogenic activity of bioactive glass: 31

2.5.4 Bioactive glasses manufacturing 37

2.6 Poly (methyl methacrylate) PMMA 45

3 Aim and objectives. 48

4 Materials and Methods. 50

4.1 Glasses synthesis and substitution. 50
4.2 Bioactive glass characterization. 54
4.2.1 Differential Scanning calorimetry (DSC) 54
4.2.2 X-ray diffraction (XRD). 54
4.2.3 X-ray fluorescence XRF 55
4.2.4 Scanning Electron Microscopy SEM and Energy Dispersive Spectroscopy (EDS). 56
4.2.5 Fourier transform infrared spectroscopy (FTIR). 58
4.2.6 Inductively coupled plasma optical emission spectroscopy ICP-OES. 59
4.3 PMMA and bioactive glass composite. 61
4.3.1 Composite Characterization. 61
4.4 Antimicrobial activity. 63
4.4.1 Materials and preparation. 63
4.4.2 Antimicrobial testing 64
4.5 Cell viability assay 65
5 Results 72
5.1 Bioactive glass synthesis. 72
5.2 Bioactive glasses characterisation. 73
5.2.1 X-ray diffraction (XRD). 73
5.2.2 X-ray fluorescence (XRF) 75
5.2.3 Differential scanning calorimetry (DSC). 77

5.2.4 Scanning electron microscopy (SEM / EDS). 81

5.2.5 Fourier transform infrared spectroscopy (FTIR). 83

5.2.6 Inductively coupled plasma optical emission spectroscopy ICP-OES. 84

5.3 PMMA and bioactive glass composite. 93

5.3.1 Composite Characterization. 94

5.4 Antimicrobial activity. 100

5.5 In vitro biocompatibility of composite. 105

6 Discussion 108

6.1 Glasses composition and characterization: 108

6.2 Inductively coupled plasma optical emission spectroscopy ICP-OES. 112

6.3 Antibacterial activity of the glasses 114

6.4 Composite characterisation 117

6.5 Composite Cell viability study 119

7 Conclusion 122

8 Future work 125

9 References 128

List of figures

Figure 2-1. Illustration of healthy mouth and the underling bone structure BarCharts, Inc., 2016. 5

Figure 2-2 Image show illustration of osteoclast (Ocl) and osteoblast (Ob) cells in the bone remodelling cycle [1]. 6

Figure 2-3. Image of MRONJ site (S. Ruggiero. Multinational Association of Supportive Care in Cancer / MASCC meeting, Vienna 2018) 8

Figure 4-1. Sample images show the design of the experiment and the composites discs in the wells. the ladling was used to identify the well during the experiments. In the white box the designed experiment: 1st row experimental samples materials and cells, 2nd row control 1 materials with no cells, 3rd Control 2 cells only, 4th row Control 3 culture media only. Labels (C) Cell, (NC) no cell, (CM) Culture media only, (PBS) phosphate-buffered saline, (DMSO) Dimethyl sulfoxide_ not used in the study..... 68

Figure 4-2. Sample image from the experiment (L929 Vs Cu 5 composite) show the Prestoblue dye in the wells. The colour change from blue to the purple indicate cell viability. There is no colour change in the Cell with the discs first row because there was no cell activity in the Cu 5 composite sample indicate no cell viability. 70

Figure 4-3. Sample images from the experiment of the 96 well plate properad for the TECAN. Top images obtained from the same plate in Figure 4-2 Cu 5 composite, only the 4th row has purple colour as described in the previous figure. Bottom image represent the 45S5-PMMA Vs MG63 plate, the first row has a slight colour change form blue to purple. 71

Figure 5-1. The glass frit after melt quench processes at the top, left white is 45S5 and the right blue is 1%mol Cu, the bottom dried sample glass frit with a ruler reference for the frit size. 72

Figure 5-2 The XRD pattern of the glasses shows the amorphous state. No signs of crystallisation (sharp peak). 73

Figure 5-3. The one hump XRD pattern of the high Na_2O glasses shows the amorphous state. No signs of crystallisation (sharp peak)..... 74

Figure 5-4. Differential scanning calorimetry (DSC) graph of all glass obtained by SDT 650® (Waters™). The sample run at 10°C /min ramp rate to 1000°C for DSC under N gas. The top show the typical DSC curve of glasses. Bottom left shows the glass transition (Tg) analysis and the onset of the (Tg). Bottom right show the peak hight and the onset of glass crystallisation analysis. The analysis performed in Trios TA® (Waters™) software provided from the company. The second indentation is clearly visible on the bottom left specially on the Cu 1 and Cu 5 glasses, where there is no sign of indentation on the 45S5 after the glass transition dip..... 79

Figure 5-5. The DSC graph of the 4530 and the 305 shows the analysis of the onset of Tg and Tc and the also the hight peak of Tc. The Tg onset for 4530 glass is around 501 C and the Tc onset around 690 °C, the 503 glass Tg onset is around 443 °C and the onset of Tc is around 611 °C..... 80

Figure 5-6. SEM images of the glass's frits in the study and the corresponding EDS analysis in the blue boxes showing the weight percentage of the elemental analysis of the bioactive glass composition Si, Ca, Na, P, and Cu. (A) 45S5, (C) Cu 1, (E) Cu 2.5, and (G) Cu 5. 82

Figure 5-7. FTIR spectra for all glasses showing the band and their group signed by vertical line from left 1460 (carbonate group $(CO_3)^{2-}$),1000 and 910 (Si-O-Si stretch), 700 (amorphous phosphate), 580, and 480 (Si-O-Si bend). 83

Figure 5-8. Silica [Si] concentration in deionised water measured from series 1 glasses dissolution over time determined using ICP-OES..... 84

Figure 5-9. Sodium [Na] concentration in deionised water measured from series 1 glasses dissolution over time determined using ICP-OES..... 85

Figure 5-10. Calcium [Ca] concentration in deionised water measured from series 1 glasses dissolution over time determined using ICP-OES..... 86

Figure 5-11. Phosphorus [P] concentration in deionised water measured from series 1 glasses dissolution over time determined using ICP-OES..... 87

Figure 5-12. Copper [Cu] concentration in deionised water measured from series 1 glasses dissolution over time determined using ICP-OES..... 88

Figure 5-13. Silicon [Si] Concentration in deionised water measured from series 2 glasses dissolution over time determined using ICP-OES..... 89

Figure 5-14. Sodium [Na] concentration in deionised water measured from series 2 glasses dissolution over time determined using ICP-OES..... 90

Figure 5-15. Calcium [Ca] Concentration in deionised water measured from series 2 glasses dissolution over time determined using ICP-OES..... 91

Figure 5-16. Phosphorus [P] Concentration in deionised water measured from series 2 glasses dissolution over time determined using ICP-OES..... 92

Figure 5-17. Copper [Cu] Concentration in deionised water from series 1 glasses containing Cu (Cu 1, Cu 2.5, and Cu 5) and series 2 glass containing Cu (305) over time determined using ICP-OES. 93

Figure 5-18. Image of the composites disc sample of the four different composites of 30 % w/w glass PMMA. From the left, 0 PMMA (control), 45S5 PMMA, Cu 1 PMMA, Cu 2.5 PMMA, and Cu 5 PMMA..... 94

Figure 5-19. Bars chart for the surface roughness of the four composites and the PMMA control. The bars compare the surface hardness of the composite in

comparison to the PMMA control. There is a slight decrease in surface roughness among the study group. significant difference between 0 PMMA and Cu 5 PMMA. Each bar represents an average of three reading on three sample (n = 3). 97

Figure 5-20. Bars chart for the surface hardness of the four composites and the PMMA control. The bars compare the surface hardness of the composite in comparison to the PMMA control. There is a slight increase in surface hardness but no significant difference between or among the control and the study group. Each bar represents an average of three reading on three sample (n = 3). 98

Figure 5-21. Pictures of the Agar disc diffusion assay of two different *Actinomyces oris* strain on fastidious anaerobe blood agar blates for series 1 glasses. A-D *Actinomyces* MF1 laboratory strain, E-H *Actinomyces oris* clinical Isolate. A, E 45S5, B, F Cu 1, C, G Cu 2.5, D, H Cu 5. The inhibition zone appears as a clear halo around the bioactive glass samples. 101

Figure 5-22. Inhibition of two strains of *Actinomyces oris* by Cu-substituted bioactive glasses. The data shown is the inhibition zones around glass samples using (A) *Actinomyces oris MF1* and (B) clinical isolate *Actinomyces oris* from an MRONJ patient. The data shown is an average of three sample (n = 3) for each bioactive glass and the error bar is standard deviation. All bioactive glasses showed an inhibition zone greater than 20 mm for both strains. The asterisks denote the statistically significant (P value <0.05) obtained by one way ANOVA test and Tukey's multi comparison test. 102

Figure 5-23. Pictures of the Agar disc diffusion assay of *Actinomyces Oris* MF1 laboratory strain on fastidious anaerobe blood agar blates against series 2 glasses: A 45S5. B Cu 5, C 4530, and D 305 103

Figure 5-24. Antibacterial activity bars chart comparing antimicrobial activity between high Na_2O (4530), and Cu containing glass (305) and the 45S5 bioglass and Cu 5 glasses against *Actinomyces Oris* MF, by agar disc diffusion test measuring the inhibition zone in mm. The bars chart shows an upward trend of inhibition as the Cu

and Na increased. The asterisk denotes the statistically significant (P value <0.05) obtained by one-way ANOVA test and Tukey's multi-comparison test. Error bars for standard deviation..... 104

Figure 5-25. Cell viability percentage Prestoblue® assay of 48 - hours period. The lines show the cell viability percentage between the four bioactive glasses PMMA composite 30% w/w and the control 0 PMMA with two cell lines (A) MG63 and (B) L929. The lines downward trends demonstrate a dose dependent between the Cu content and cell viability. The asterisk denotes the statistically significant (P value <0.05) obtained by one-way ANOVA test and Tukey's multi comparison test. Error bars are of the standard deviation..... 106

Figure 5-26. Images of cells after 48h of cell contact assy. images taken next to the disc (black shadow in the images). 107

List of tables

Table 2-1. Summary of microorganisms isolated from cases of BRONJ and MRONJ reported in the scientific and clinical literature. 10

Table 2-2. Antimicrobial materials and technologies associated with potential treatments for oral, bone, and related device-associated infections. 15

Table 2-3. Specific search for *Actinomyces* and bioactive glasses research article from web of science and pub med database. *Actinomyces* (*A*) strains against bioactive glass. 20

Table 2-4. List of the categories of the raw materials used in manufacturing the bioactive glass by melt-quench rout. 26

Table 2-5. An example of studies involved doping and substitution methodolgy and weather if the title matches the methodology for doping and substitution. The unmatched method to title are highlited with notes. 40

Table 4-1. Reagents used in glass synthesis. 51

Table 4-2. The mol % and wt. % composition of the synthesised glasses. 53

Table 4-3. Reagents batch calculation in grams for each glass series. 53

Table 4-4. List of the bacteria used in the antimicrobial activity and their origin. 63

Table 4-5. Materials used to prepare the agar and the broth in 400 ml Deionized water (DH_2O) volume..... 64

Table 4-6. Show the cell lines and the materials used in the. 66

Table 5-1. XRF data shows the mol % composition of the glasses post melting (XRF mol %) in comparison to the theoretical mol % (T mol%). (Nd) not detectable (N/A) not applicable. 75

Table 5-2. XRF molar percentage post melt (XRF mol%) and theoretical molar percentage (T mol%) of the high Na_2O glass 4530 and 305. XRF data obtained by (Primus IV XRF instrument). 76

Table 5-3. XRF molar percentage post melt (XRF mol%) and theoretical molar percentage (T mol%) of the high Na_2O glass 4530 and 305. XRF data obtained by Niton XL3t the Na sodium is not detectable (Nd) with this machine. 77

Table 5-4. Shows DSC analysis approximate Tg and Tc onset and Tc peak for the glasses rounded to the nearest true number. 78

Table 5-5. DSC temperature for the 4530 and 305 glasses rounded to the nearest true number obtain from the analysis of the DSC graph. The second indentation clearly seen after the glass transition dip in the 4530 and in the 305 closer to the Tc peak. 81

Table 5-6. The average measurement of the roughness of different glass and PMMA composites. The asterisk denotes the significant difference ($p<0.05$) between PMMA, and the Cu 5 composite determined by one-way ANOVA analysis and Tukey's test. 96

Table 5-7. Elements concentration (mg/L) in deionised water measured from glass / PMMA composite over seven days determined using ICP-OES. 99

Table 5-8 Mean inhibition zone from agar disc diffusion in (mm). 101

1 Introduction.

Medication-related osteonecrosis of the jaw (MRONJ) is formerly known as bisphosphonate-related osteonecrosis (BRONJ). It is a disease that affects the oral soft tissues and underlying skeletal tissues in patients. The term is used as it is associated with treatments using medications, typically anti-resorptive or anti-angiogenic drugs. In simple terms, anti-resorptive medications inhibit the bone remodelling processes for the patient with osteoporosis by preventing the osteoclast from resorbing the bone during remodelling. Anti-angiogenic drugs decrease the growth of new blood vessels to cut blood supply to the tumour site. There is no definite link between these medications and osteonecrosis of the jaw. However, the evidence that links anti-resorptive and anti-angiogenic drugs and MRONJ is strong.

The complexity of the MRONJ pathology makes it challenging to determine how the disease was initiated or progressed. Early MRONJ is frequently associated with either invasive dental procedures, e.g., tooth extraction, implant placement, or severe periodontitis. Several research studies aimed at studying the pathology of MRONJ suggested that the prevalence of a spectrum of microbiota may explain either the start or the progression of the MRONJ. However still, no clear path to explain the cause of MRONJ has been elucidated.

The impact of the MRONJ on the patient is rigorous in several aspects. Pain, often severe, is associated with the exposed necrotic bone, leading to the use of strong pain killers. The patient's quality of life is affected negatively, especially for patients in the late stages of the MRONJ, as bone necrosis and soft tissue damage may not be reversible. The number of the reported cases showed exponential growth in the last

few years, and most of the patients were above 60 years old. The MRONJ affected both maxillary and mandibular jawbone with slightly more mandibular cases reported, and females appear to be more susceptible to MRONJ than males.

Although the precise aetiology of MRONJ is not fully understood, recent papers largely agree that microbial infection plays a key role in its progression (see literature review, section 2.3.1). A wide range of pathogens, mainly bacterial but also some Candida species, have been isolated from sites of active disease. Any new therapeutic approach might reasonably incorporate an antimicrobial strategy to halt or reverse tissue destruction.

The currently available treatment options depend on the severity of the MRONJ. The classifications fall into four stages: zero, one, two and three. The ranking indicates the severity of the disease, from the patient being at risk stage 0 toward the patient with exposed necrotic bone associated with infection and pain at stage 3. Managing MRONJ ranges from taking good care of oral health and hygiene of patients at risk, using antiseptic mouthwashes, antibiotics with pain relief in mild MRONJ, and surgical procedures in severe necrotic bone with antibiotics. The current treatments do not generally give a satisfactory result. The antibiotics appear only to slow down the disease, and the surgery negatively impacts the patient health and well-being. To summarise, MRONJ is a growing challenge that does not yet have a proven therapeutic approach to reverse or even halt progression. Therefore, it is necessary to consider new approaches in developing an innovative and effective treatment.

Advances in materials science, drug delivery, and "digital dentistry" together offer potential new strategies for the treatment of MRONJ. There is a wide range of

materials available that have the potential to inhibit microbial growth while stimulating healing in bone and soft tissues (e.g., modified bioactive glasses). Biomaterials might be further enhanced and loaded with drugs or other therapeutic agents. "Digital dentistry" describes the combination of intraoral scanning, in silico design of prosthetics, and the fabrication of a custom part for a specific application in a unique patient (ideally using additive manufacturing). Combining these technologies would be feasible to produce a custom medical device that could protect sites deemed to be at risk of developing MRONJ and deliver therapeutic molecules to combat the disease and reverse its development. This approach has not been reported to date, and the aim of this PhD is to consider a combinatorial approach based on these technologies.

With the resulting combination of dental technology and the development of biomaterials, we could improve the current approaches in the fields of regenerative medicine, drug delivery and tissue engineering. Regenerative medicine could benefit from producing manufactured dressing to regenerate the tissues with the help of tissue engineering and modified antimicrobial biomaterials to produce therapeutic dressings or devices. However, before combining the approach taken in this project, it is important to review the key papers in MRONJ disease and biomaterials' manufacture.

2 Literature review.

As described in Chapter 1, MRONJ is a debilitating, painful disease for which there appear to be no effective treatments. However, understanding of the aetiology of MRONJ and the biological processes underlying the disease has increased. There is widespread agreement that microorganisms play a central role in the development of the disease. Advances in the development of antimicrobial biomaterials could therefore be used to develop therapies that suppress bacterial growth while promoting healing by utilising advances in manufacturing technology to produce customised prostheses for specific disease sites. This approach may therefore provide the first – opportunity to create advanced, customised devices to treat MRONJ lesions at all stages of the disease, with the aim of preventing disease progression or even reversing tissue destruction. Before outlining the progress made, this chapter of the literature review details the basics of MRONJ, the state of antimicrobial biomaterials and the general rationale for this proposed approach. First, however, it is important to briefly review the biology of the healthy mouth.

2.1 A healthy mouth.

The mouth is part of the human head and neck region. It consists of various and complex tissues that are necessary for the normal basic functions of life, including chewing, swallowing, speaking, and breathing with the help of the various anatomical parts of the surrounding tissue, facial and cranial muscles for example. The oral tissue and the surrounding tissue must always be in optimal condition, free from infection and destruction. In MRONJ, two tissues are probably the most important: the soft epithelial surfaces and the underlying bone tissue. These two tissues are heavily

vascularised with blood vessels and nerves to ensure the functioning of the immune and nervous systems against any infection and to deliver nutrients and oxygen. For a detailed understanding of oral anatomy and histology, the reader is recommended to read Oral Anatomy, Histology and Embryology by B. K. B. Berkovitz. However, the illustrations in Figure 2-1 (a) and (b) briefly and simply show the diversity of oral tissues. Bone, as it serves as the structure of the head and neck is briefly described in the next section.

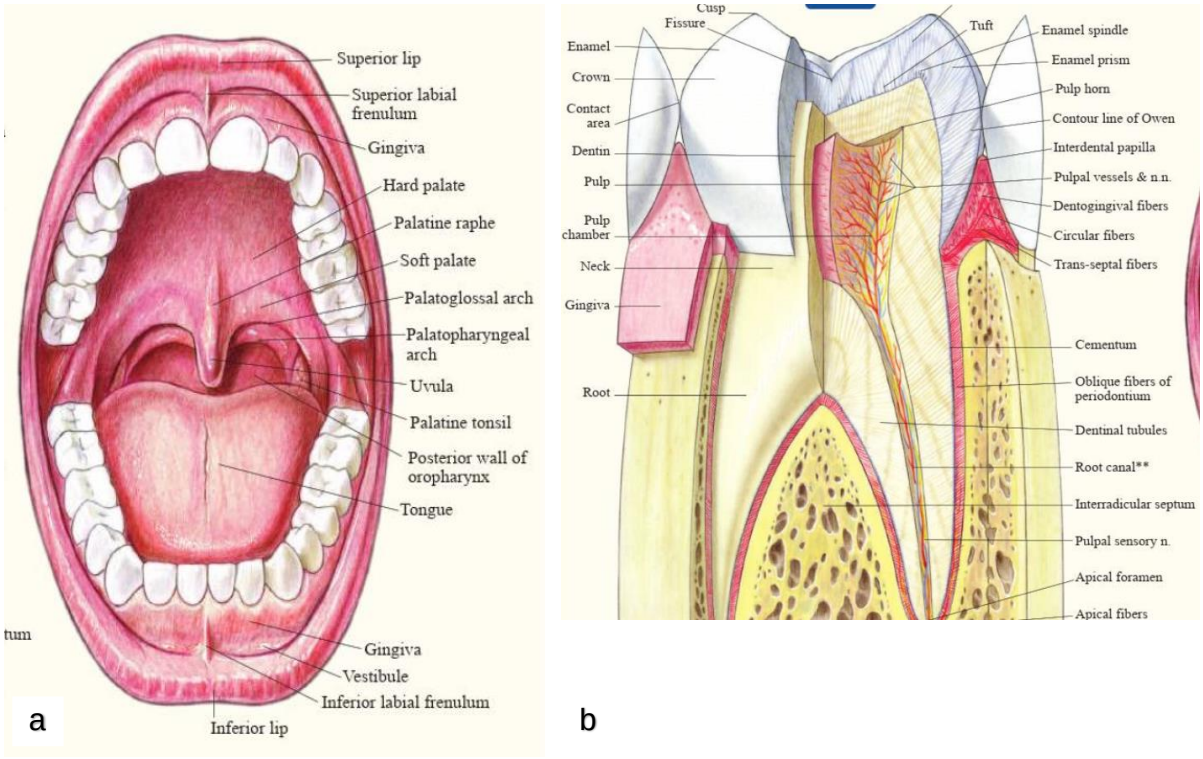

Figure 2-1. Illustration of healthy mouth and the underling bone structure BarCharts, Inc., 2016.

2.2 Bone and turnover process

Bone is a stiff mineralised tissue that forms the skeletal system. A crucial system that serves as the structural support of human body and movement. The cranial and the jawbone are an important part of the skeletal system. They house the brain and the

mouth. Hence it is important to keep the cranial and the jawbone in optimal condition. With the respect to the jawbone, in general healthy bones are in a constant state of remodelling by process called bone turnover. It is a physiological process in which the osteoclast cells, which are responsible for the resorption of bone tissue, and osteoblast cells, which build new bone, are constantly working to dissolve and produce bone tissue. These important physiological phenomena keep bone tissue fresh and healthy throughout the human lifespan. To keep bone healthy, it is also important to emphasise the need for adequate mineralisation, especially calcium, which contributes to bone strength and density. Therefore, any alteration to the bone turnover process would disturb the bone health leading to unwanted complications.

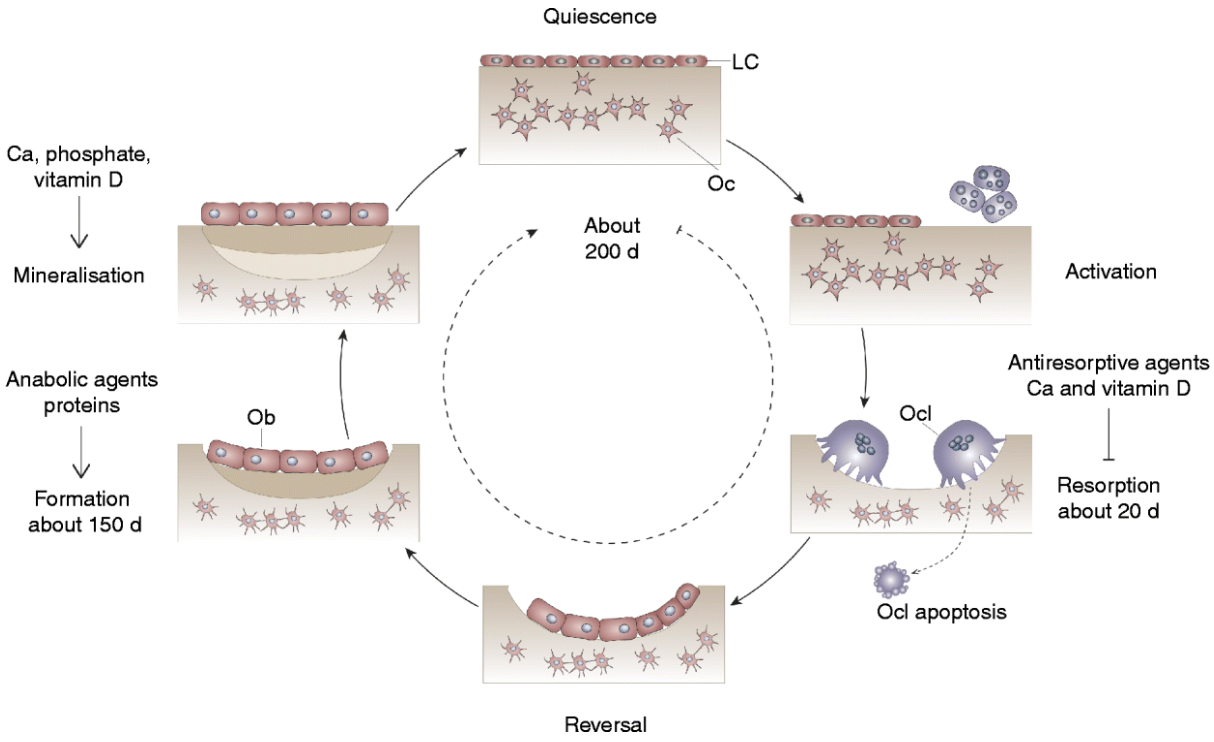

Figure 2-2 Image show illustration of osteoclast (Ocl) and osteoblast (Ob) cells in the bone remodelling cycle [1].

Although bone turnover is constant, it responds to signals such as the healing process of the bone after a fracture or trauma and to external signals such as changes in the jawbone during orthodontic treatment. This is a positive utilisation of bone turnover. However, there are sometimes unavoidable, urgent disruptions to this natural process that can lead to inadequate bone regeneration and debilitating results in the jaw.

One of these disruptions are caused by taking or undergoing a treatment with specific drugs that interfere with the bone turnover (modelling) process. The antiresorptive (e.g., bisphosphonates) intervene in the bone turnover by inhibiting osteoclast activity to preserve bone density in patient with or at risk of osteoporosis [2] [3]. Also, anti-angiogenesis drugs (e.g., bevacizumab) interfere with formation of new blood supply, indirectly affecting bone tissue [4] [5]. This conditions to the jawbone known as medication-related osteonecrosis of the jaw (MRONJ).

In conclusion, maintaining balanced bone remodelling is important for bone health with an adequate mineralization, minimising the external intervention, and avoidance unless necessary of certain drugs, contribute to the overall health of the skeletal system.

2.3 Medication-related osteonecrosis of the jaw (MRONJ).

First reported in 2003 [6], MRONJ known as BRONJ bisphosphonate related osteonecrosis of the jaw is rare but a severe soft and bone tissue deterioration due to bone necrosis result from undergoing but not exclusive an antiresorptive or angiogenesis treatment in patients with osteoporosis or cancer related bone disease [7]. Even though there is a clear connection between the drugs and the MRONJ. The onset and cause of MRONJ are unknown and debatable.

MRONJ Figure 2-3 usually occurs after an invasive dental procedure, tooth extraction or prevalence of severe oral health problems such as severe periodontitis and failed implants [8]. Although this is a simplified description, other factors are important and vary from patient to patient. These factors include poor oral hygiene, smoking, vitamin D deficiency, further trauma, diabetes, immunosuppression, and poor vascularisation. Many of these factors are interrelated, adding to the complexity of an already complex condition [9] [3] [8].

Figure 2-3. Image of MRONJ site (S. Ruggiero. Multinational Association of Supportive Care in Cancer / MASCC meeting, Vienna 2018)

BRONJ / MRONJ worsens oral health-related quality of life [10], prevents optimal dental treatment and limits activities of daily living due to impaired masticatory function and damage to the jaw bones caused by surgical treatment and / or pathological progression of MRONJ. Therefore, clarifying the exact mechanisms and defining

treatment strategies for MRONJ is essential. However, the scientific data on the pathophysiology and definitive treatment strategies for MRONJ are limited [11].

The simple explanation for MRONJ is that the related drugs inhibit bone turnover and prevent vascularisation. This leads to a lack of blood supply - which is essential for the supply of immunity, nutrition and possibly antibiotics - makes the tissue susceptible to bacterial colonisation. This favourable environment for microbial growth is associated with bone necrosis in the jaw [12]. The half-life of some of the drugs associated with MRONJ especially bisphosphonate is long and the tissue stores for extended periods of time [4] [13], where subsequent environmental changes (e.g., pH) may alter behaviour or stimulate release from the tissues [14].

Although it is difficult to establish a therapeutic regime for such a complex disease, the most recent recognition of the role of infectious microorganisms suggests that these are an important target for any new treatment. Therefore, the next two sub-sections consider, first, the role of microorganisms in MRONJ and second, the pH condition in the section afterword.

2.3.1 The role of microorganisms in medication-related osteonecrosis of the jaw.

Bacteria may not initiate MRONJ in most cases, but they cause inflammation and tissue damage, including bone loss. Therefore, significant effort by researchers directed at identifying the key pathogens. Although with limited sources, key papers identifying different microorganisms in patients with MRONJ have been reviewed by researchers in Table 2-1.

Table 2-1. Summary of microorganisms isolated from cases of BRONJ and MRONJ reported in the scientific and clinical literature.

Bacteria (sp.) (genus)	References	Gram +/-	Anaerobic or Aerobic
Actinomyces sp.	[15] [16] [17] [18] [19] [20]	+	Facultative anaerobic
Actinomyces israelii	[18]	+	Obligate anaerobic
Actinomyces odontolyticus	[21]	+	Facultative anaerobic
Actinomyces viscosus	[21]	+	Facultative anaerobic
Actinomycetaceae	[22]	+	Facultative anaerobic
Aggregatibacter actinomycetemcomitans	[21]	-	Facultative anaerobic
Atopobium sp.	[23] [15]	+	Anaerobic
Bacteroides sp.	[15] [19] [19] [22]	-	Anaerobic
Bacteroidetes Bactrium	[23] [18]	-	Anaerobic
Bifidobacterium dentium	[15] [18]	+	Anaerobic
Campylobacter concisus	[21]	-	Facultative anaerobic
Campylobacter gracilis	[21]	-	Facultative anaerobic
Campylobacter rectus	[21]	-	Anaerobic
Candida albicans	[24] [25]	Fungus	Aerobic
Capnocytophaga sp.	[21] [15]	-	Facultative anaerobic
Clostridiaceae	[22]	+	Anaerobic
Dialister invisus	[23]	-	Anaerobic
Escherichia coli	[15]	-	Facultative anaerobic
Eikenella sp.	[20]	-	Facultative anaerobic
Eikenella corrodens	[21] [15]	-	Facultative anaerobic
Enterobacter sp.	[15] [19]	-	Facultative anaerobic
Enterobacteriaceae	[22]	-	Facultative anaerobic
Enterococcaceae	[22]	+	Facultative anaerobic
Enterococcus sp.	[19]	+	Facultative anaerobic
Enterococcus faecalis	[15]	+	Facultative anaerobic
Eubacterium sp.	[16] [18]	+	Anaerobic
Eubacterium nodatum	[21]	+	Anaerobic
Eubacterium sp.	[16] [18]	+	Anaerobic
Finegoldia magna	[23]	+	Anaerobic
Fusobacterium nucleatum, ss vincentii	[21] [18]	-	Anaerobic
Fusobacterium sp.	[16]	-	Anaerobic
Klebsiella sp.	[15]	-	Facultative anaerobic
Lachnospiraceae[G-7] sp.	[18]	-	Anaerobic
Lactobacillus sp.	[16] [18]	+	Facultative anaerobic
Lactobacillaceae	[22]	+	Facultative anaerobic
Moryella indoligenes	[23]	+	Obligate anaerobic
Moraxella	[20]	-	Obligate anaerobic
Neisseriaceae	[22]	-	Anaerobic

Oribacterium sp.	[23]	+	Anaerobic
Parvimonas micra	[21] [15]	+	Anaerobic
Pasteurellaceae sp.	[22]	-	Facultative anaerobic
Peptostreptococcus stomatis	[18]	+	Anaerobic
Porphyromonas enodontalis	[23]	-	Obligate anaerobic
Porphyromonas gingivalis	[21]	-	Obligate anaerobic
Prevotella sp.	[15] [16] [19]	-	Anaerobic
Prevotella denticola (T)	[23] [18]	-	Anaerobic
Prevotella intermedia	[21]	-	Anaerobic
Prevotella nigrescens	[23] [21]	-	Anaerobic
Prevotella tannerae	[23]	-	Anaerobic
Porphyromonas sp.	[16]	-	Anaerobic
Saccharomycetaceae	[22]	Fungus	Aerobic
Selenomonas infelix	[23]	-	Anaerobic
Selenomonas sputigena	[18]	-	Anaerobic
Shuttleworthia satelles	[23]	+	Anaerobic
Slackia exigua	[15]	+	Anaerobic
Staphylococcaceae	[22]	+	Facultative anaerobic
Streptococcus sp.	[15] [16] [18] [19]	+	Facultative anaerobic
Streptococcaceae	[22]	+	Facultative anaerobic
Streptococcus constellatus	[21] [18]	+	Facultative anaerobic
Streptococcus gordonii	[21]	+	Facultative anaerobic
Streptococcus mitis	[23] [21]	+	Facultative anaerobic
Streptococcus vestibularis	[18]	+	Facultative anaerobic
Tannerella forsythia	[21]	-	Anaerobic
Treponema denticola	[21]	-	Facultative anaerobic
Treponema sp.	[16]	-	Anaerobic
Veillonella sp.	[15]	-	Anaerobic
Veillonella parvula	[21]	-	Anaerobic

In Table 2-1, there are approximately sixty species of bacteria and at least one opportunist yeast that have been isolated from active disease sites and most likely more. Even some microorganisms are repeatedly reported and may prove to be "cornerstone" infectious agents no single species appears responsible. Some are more strongly associated, including *Actinomyces sp., Bacteroides sp., Prevotella sp., and streptococcus sp*. Details of some representative microorganisms that more frequently appear are as follow:

Actinomyces sp. is a gram-positive facultative/obligate Anaerobic bacterium. It is common to be found in the mouth, and it is increasingly believed to be a cornerstone species in MRONJ [26] also as it is appeared frequently in multiple studies on clinical isolates from MRONJ sites [12] as noted in Table 2-1.

Due to its nature to grow under anaerobic condition it seems that the abundance of this species is not coincidence in MRONJ lesion that lack the blood supply strongly suggested they play important role in MRONJ. They tend to be hard to be identified with regular microbiology identification from patient swap but PCR technique is highly recommended when trying to identify [27].

Bacteroides sp. is a genus of the gram-negative obligate anaerobic bacterium. It has a very significant clinical-pathological infection, including abscesses in multiple body sites [28]. *Bacteroides sp.* is related to gingivitis, endodontic infection in the oral cavity [29].

Prevotella sp. is gram-negative facultative Anaerobic bacteria. They are most prevalence in the oral cavity, vagina, respiratory tract, gut, and skin. *Prevotella sp*. is abundant in the microbiome in the oral cavity. *Prevotella* plays a role in stabilising biofilm formation, which leads to different oral infections [30].

Streptococcus sp. is gram-positive facultative Anaerobic bacteria. One famous example from the species is *Streptococcus pneumoniae* is notably known for causing pneumonia and meningitis [31]. The species are also commonly found in the oral environment as *Streptococcus mutans* it helps develop dental caries and form biofilms [32].

While Table 2-1.

Table 2-1. Summary of microorganisms isolated from cases of BRONJ and MRONJ reported in the scientific and clinical literature.

and the key species summarised above appear to be very diverse, it is noteworthy that many are facultative or obligate Anaerobic. Finally, it was noted that commensal bacteria, for example, *E. coli*, are commonly encountered in MRONJ.

2.3.2 Medication related osteonecrosis of the jaw MRONJ site environment

In the previous section, it was stated that the microorganism is clearly playing a role in the MRONJ, and as in any bacterial infection, the bacterial infections site tends to have a lower pH value. One study conclude this change in the pH believed to be a major step in understanding BRONJ / MRONJ [33]. One study investigates acid environments promote MRONJ progression in an animal model. In this study the Bisphosphonate were observed to be released from the bone increases when pH decreases in an MRONJ infection environment. The author claims the result from this study is in line with the clinical observation form previous studies concluded the association of BP's disassociation form the bone in MRONJ infection sites. Demonstration that an acidic environment is an important factor in increasing the cytotoxicity of BPs. "An explanation for this finding is the protonated activation of the nitrogen-containing groups at low pH levels (e.g., NH_2 to NH_3^+), thereby increasing the activity/cytotoxicity, which differs among the individual BPs" [34].

The underlying reasons for MRONJ development in patients using antiresorptive agents and angiogenesis inhibitors remain unclear. Additionally, the lack of understanding of these mechanisms has hindered the development of definitive treatment strategies [35]. Therefore, the next section will discuss the various materials and technology able to be used as antimicrobial agent or as drug delivery medium.

With respect to informing the approach to be taken in this PhD. The wide range of microbial species and the MRONJ site condition (pH) suggest a) any antimicrobial agent used should be broad-spectrum, and b) preferred to perform some pH increase to inhibit cytotoxicity of BP drugs c) later, a stratified or patent specific device may be optimum.

2.4 Antimicrobial materials and related technologies that have the potential for use in an oral custom device.

In response to complex diseases with board spectrum of microorganisms such as MRONJ, and the alarming raise in bacterial resistance to antibiotics, one traditional treatment method is to increase the dose or use multiple antibiotics have proven to be harmful to the patients. To address this, researchers are exploring alternative natural and artificial approaches to combat resistance and tackle complex diseases. Several alternative technologies are candidates to be utilized for such challenges.

One prevalent method explores changing the delivery route of the drugs by coating or loading the antibacterial agents on or within the materials. Such materials have to be antimicrobial inherently and/or are capable of damaging microorganism's walls, and changing the environment by increasing oxidative stress (increasing oxygen species in the surrounding environment) using nano materials on the microorganisms, enabling the drug or the intrinsic antibacterial materials to have an effect [36] [37].

Other methods are aiming to localize and controlled release delivery of the drug using patches made from materials that has degradation properties when it is contact with body fluid such as naturals polymers [38]. The literature provides a wide range of options of to be utilized in the manufacture of a therapeutic custom device. Listed in

Table 2-2 are a range of materials and technology possible to treat diseases site such as MRONJ.

Table 2-2. Antimicrobial materials and technologies associated with potential treatments for oral, bone, and related device-associated infections.

Substance or antimicrobial technology	Specific example and reference(s)	Notes including microorganisms tested where relevant
Natural substances	Nanoparticles of chitosan & quaternary ammonium chitosan [39].	Added to PMMA cement. Tested using Staphylococcus aureus or Staphylococcus epidermidis cells.
	Fatty acid (short, medium and log chains) [40].	Aggregatibacter actinomycetemcomitans is resistant to most of the fatty acid in the article.
	Polytoxinol ™ containing oils from Eucalyptus, Thyme, and Tea Tree plants [41].	Tested against methicillin-resistant Staphylococcus aureus (MRSA) in a clinical case, reported a successful treatment using this commercial preparation.
	Frankincense (resin from Boswellia sacra), myrtle (Myrtus communis), thyme (Thymus vulgaris), lemon (Citrus limon), oregano (Origanum vulgare) and lavender (Lavandula angustifolia) essential oils [42].	Methicillin sensitive *Staphylococcus aureus* (ATCC 29213), methicillin resistant *Staphylococcus aureus* MRSA (ATCC 43300), Enterococcus faecalis (ATCC 29212), Escherichia coli (ATCC 25922), *Klebsiella pneumoniae* (ATCC 13883), and *Pseudomonas aeruginosa* (ATCC 27853) were used. All oils exhibited some activity.
Bioactive glasses (BG)	Sol-gel Ag-BAG, in the glass system SiO_2-CaO-P_2O_5-Ag_2O [43]	First reported silver doped bioactive glass with antibacterial effect in 2000. CFU count used to test the antimicrobial activity of the glass against *E. coli* (MG1655).

	45S5 vs. Ag doped BG [44]	Measuring bacteria growth in media methods. AgBG shows an antibacterial effect against: *Escherichia coli, Pseudomonas aeruginosa, and Staphylococcus aureus,* while 45S5 and BG has not.
	S53P4 bioactive glass [45].	Tested in vitro against several strains of methicillin-resistant *Staphylococcus aureus* (MRSA), *Pseudomonas aeruginosa* and *Klebsiella pneumoniae*. Similar antimicrobial activity as vancomycin or gentamicin loaded PMMA bone cement.
	(SBA3) glass composition: 48% SiO_2, 26% Na_2O, 22% CaO, 3% P_2O_5, 0.43% B_2O_3, and 0.57% Al_2O_3 Copper-doped bioactive glass [46].	Used as a filler for PMMA cement. Tested on clinical isolate Staphylococcus epidermidis. Cu doping has 50% bacterial inhabitation effect.
	Nanometric 45S5 Bioglass® [47].	Compared to regular 45S5 bioglass, nano 45S5 showed greater antibacterial activity by 99% against Enterococcus faecalis. First reported on nanometric bioglass.
	Li-doped bioglass® 45S5 [48].	Tested against common bacteria in oral environment that cause caries and periodontal disease, Streptococcus mutans, Aggregatibacter actinomycetemcomitans, and Porphyromonas gingivalis.

Metal / ions	Copper substituted HA and FA [49].	Tested using Escherichia coli, Staphylococcus aureus and Candida albicans. CuF showed more antimicrobial activity against the bacteria but not C.albicans Where the CuOH showed better C.albicans antimicrobial activity but not against Escherichia coli.
	Ag–TCP, AgZn–TCP and AgCu–TCP [50]	Tested against Escherichia coli & Staphylococcus aureus. AgCu-TCP showed the least MBC measurement.
	Metal oxide: ZnO, CuO, Fe_2O_3 [51].	Tested on Gram-negative Escherichia coli and Pseudomonas aeruginosa and Gram-positive Staphylococcus aureus and Bacillus subtilis bacteria ZnO showed the most antibacterial activity
	Copper oxide nano particles [52]	Zone of inhibiton aginst Gram-negative *Pseudomonas aeruginosa* CB1and Gram-positive *Bacillus subtilis* CN2
Modified calcium phosphate CaP	Silver doped nano hydroxyapatite nHA [53].	Tested on Staphylococcus aureus and Pseudomonas aeruginosa.
	CaP loaded with antimicrobial peptide AMP [54].	Coated on Ti surface.
	3D printed hydroxyapatite Biphasic calcium phosphate with berberine [55].	Berberine tested against Staphylococcus aureus (ATCC29523).
	Calcium phosphate (HAP) Poly-(D,L-lactide-co-glycolide)-coated calcium phosphate [56].	Investigated as a treatment for osteomyelitis, tested using Staphylococcus Aureus (ATCC 25923, a clinical isolate).

	HAP loaded with antibiotics (Vancomycin and Ciprofloxacin) [57].	Tested against Staphylococcus aureus (ATCC 27661), Escherichia coli (ATCC 14948) and Pseudomonas aeruginosa (ATCC 27853)

Table 2-2 summarizes four groups of materials from sixteen studies of different antimicrobial technologies reported to be effective against a wide range of organisms associated with bone infections (e.g., osteomyelitis) or dental/oral infections, where many of the organisms have also been associated with cases of MRONJ. It is evident that many of these have potential for incorporation into a medical device, specifically a custom medical device designed to be located over a clinical site in the oral cavity. These categories are each considered here individually, for specific consideration for use in the treatment of MRONJ.

(a) Natural antimicrobial substances. While many substances are natural including antibiotics, the focus of this section is on plant extracts that are largely unmodified prior to application to an infection (whereas modern antibiotics are frequently processed and modified prior to use). As shown in Table 2-2 above, many essential oils from plants can inhibit bacterial and fungal growth and may also have antiviral properties. This class of compounds has been extensively reviewed in recent years including by Swamy et al in 2016 [58] and Chouhan et al in 2017 [59]. Several even more recent papers have considered the activity of the most promising oils against known pathogens, with some cited in Table 2-2. These studies show other promising features of essential oils, including low toxicity of many oils to humans (e.g., with many used in foods) and low regulatory barriers to their use in unmodified forms. These should therefore be considered for incorporation into – or addition to – a custom device

to slow or reverse progression of MRONJ in the mouth. It is known that some essential oil components can inhibit free radical polymerization, for example of PMMA, and this needs to be considered in designing experiments and new therapeutic tools.

(b) Bioactive glasses (BG). Bioactive glasses are silicate-based materials first introduced in the 1960s by Hench. The basic composition of BG's are silicon dioxide, calcium oxide, and phosphate. It is osteoconductive material vastly used in bone reconstruction surgeries treatments. Bioactive glasses form hydroxyapatite by precipitating a calcium phosphate layer on its surface when it contacts body fluid, making it a strong bone substitute material. First reported to have antimicrobial activity by Bellantone et al [43, 44], proven that it has some antimicrobial activity against multiple microorganisms. The beauty of bioactive glass appears in its different manufacturing routes that give it the ability to be loaded and substitute its composition with varied materials. For example, substituting metal ion oxides through melt quench could improve the antimicrobial activity and enhance vascularization, e.g., copper oxide. This gives it a possibility to manufacture the bioactive glass in different particle sizes and compositions, which could then be added to denture materials to enhance its antimicrobial activity and mechanical properties. Therefore, this new composite material could help reverse or minimize the chance of the onset of MRONJ.

In specific review of bioactive glass were investigated against MRONJ and *Actinomyces* bacteria, the articles presented in the Table 2-3 highlight a significant gap in research on the antibacterial effects of bioactive glass targeting *Actinomyces* bacteria in the context of MRONJ. Existing studies primarily focus on periodontal diseases and dental caries using *actinomyces naeslundii* as it plays a role in the early stages of oral biofilm formation. In these cases, bioactive glasses are typically used in

combination with other materials, such as composites, pastes. One study uses ultrasonic aids to deliver surface pre-treated glass ionomer (SPRG). Given this lack of research on specific bacterial strains, bioactive glass presents a promising medium for delivering antibacterial effects in the treatment of MRONJ.

Table 2-3. Specific search for *Actinomyces* and bioactive glasses research article from web of science and pub med database. *Actinomyces* (*A*) strains against bioactive glass.

Titles	Glass type: alone or not. / Test used	Bacteria / Bacterial viability	Other comments	Year
Interactions between Bioactive Glass and Periodontal Pathogens [60].	S53P4 glass granules: adhesion test, growth inhibition test, and Agglutination test.	*Actinomyces viscosus* used to coat the glass for adhesion test (the methodology did not specify testing the strain) It has no effect on the result and does not eliminate the coagulation with *P. gingivalis*.	_pH effect from the BG was mentioned, how it is important for antibacterial test. _Agar disc diffusion is commonly used in BG antibacterial effects.	March 1996
Antibacterial effects of a bioactive glass paste on oral microorganisms [61]	S53P4 powder in suspension.	*Actinomyces naeslundii* within 10 min lost viability.		Jul 1998
Assessment of antimicrobial effect of Biosilicate® against anaerobic, microaerophilic and facultative anaerobic	_Biosilicate powder composition of 23.75 Na_2O, 23.75 CaO, 48.5 SiO_2, and 4 P_2O_5 (wt%). _Agar diffusion (double	*Actinomyces naeslundii* 15.7 ± 2.0 and *after* no viability after 60 minutes (CFU) incubation.	Agar disc diffusion	May 2011

microorganisms [62].	layered), direct contact			
Effects of silver diamine fluoride on dentine carious lesions induced by *Streptococcus mutans* and *Actinomyces naeslundii* biofilms [63].	Silver diamine (fluoride SDF). Colony forming unit (log CFU) Dead: live bacteria raion.	*Actinomyces naeslundii.* SDF reduced CFU counts.	pH were higher in the SDF group were high.	June 2012
Bioactive resin-based composite with surface pre-reacted glass-ionomer filler and zwitterionic material to prevent the formation of multi-species biofilm [64].	SPRG-filled RBC (Beautiful, Shofu, Kyoto, Japan) + 2-methacryloyloxyethyl phosphorylcholine (MPC) composite. SPRG is a bioactive glass ionomer (Calcium silicate) Bacterial attachment.	*Actinomyces naeslundii* Bacterial attachment and CFU. protein-repellent properties of MPC. "The RBC containing SPRG filler along with 3% MPC inhibited multi-species bacterial attachment and biofilm formation. This inhibition is due to the protein-repellent properties of the hydrophilic surface with MPC, while both the release of ions and acid neutralisation properties related to SPRG were maintained or even improved with the addition of MPC."	Abbrv: Surface pre-reacted glass-ionomer (SPRG) Resin-based composites (RBC) 2-methacryloyloxyethyl phosphorylcholine (MPC).	Septem ber 2019

Ultrasonic irrigation of periodontal pocket with surface pre-reacted glass-ionomer (S-PRG) nanofiller dispersion improves periodontal parameters in beagle dogs [65].	Ultrasonic + S-PRG. “Surface pre-reacted glass-ionomer (S-PRG) nanofiller, an antibacterial ion-releasing bioactive glass”. Live dead viability assay. Fluorescence intensity and colony count on BHI agar plates of 10-fold dilution from collected swap from cementum.	*Actinomyces naeslundii,* “Ultrasonic irrigation with S-PRG nanofiller dispersion using an ultrasonic scaler system could deliver S-PRG nanofiller to the cementum surface, thereby providing antibacterial effects. In support of this hypothesis, irrigation using S-PRG nanofiller dispersion in an in vivo model improved the parameters of experimental periodontitis and modified the composition of subgingival periodontal microflora.”		June 2022
Using Copper-Doped Mesoporous Bioactive Glass Nanospheres to Impart Anti-Bacterial Properties to Dental Composites [66].	Cu-MBGN (SiO_2 84.8%, CaO 9.4%, CuO 5.8%) wt% glass particles in BisGMA and TEGDMA resin. 45S5 as bioactive control.	*Actinomyces naeslundii.* Biofilm formation CFU counting “Still, despite the somewhat weaker anti-bacterial effect on A. naeslundii than a strong antimicrobial action on *S. mutans*, the preventive effect of 10-CuBG on secondary caries is still adequate”.	Sterilized sample using UV.	October 2022

Studies presented in Tables 2-2 and 2-3 on bioactive glass composites with PMMA, as well as study [Cu-MBGN in BisGMA and TEGDMA resin] as antimicrobial agents, indicate that BAGs (Bioactive Glasses) are effective materials for delivering antibacterial effects, whether in their original (S53P4) form or when doped with copper (45S5). Although copper incorporation in glass has been previously reported, the methods and techniques in this project will differ significantly from those in existing studies see section 2.2.5 on different manufacturing techniques and materials and method section 4.1.

The referenced articles primarily utilised doping techniques with bacteria commonly associated with bone and oral diseases, including *Staphylococcus*, *Pseudomonas*, and *Streptococcus* strains. However, Table 2-3 highlights a notable gap in research on *Actinomyces* bacteria, believed to play a central role in MRONJ, as indicated in Table 2-1 (Section 2.3.1). Research involving bioactive glasses and *Actinomyces* remains rare, with significant gaps in both focus and time.

(c) Metals and metal ions. Many metals are antimicrobial, with the most common examples primarily Ag, Cu, Zn, Fe [51] [67]. These have been used historically, and while largely displaced by antibiotics, some are still used in a range of applications such as using silver in wound dressings [67]. The mechanisms for their action are complex and differ between ions and the form of presentation, but they affect bacterial and fungal cell metabolism (via direct effects on enzymes and damage to cell membranes, including interference with energy production in the cell). Metal ions frequently have effects on mammalian cells too, and maybe cytotoxic. However, they

may also have beneficial effects at optimized concentrations; for example, copper can stimulate new blood vessel formation, also termed "angiogenesis"[68] [69].

(d) Modified calcium phosphates. Calcium phosphates are among the most common bone graft substitutes. While they have few demonstrable antimicrobial properties, they can be modified for example, using metal ion doping from the elements in (c) above. One recent example is the modification of a nanoscale calcium phosphate where zinc oxide was added to introduce antimicrobial activity [70]. Calcium phosphates have also been used to carry other antimicrobial substances, including antibiotics and antiseptics, to infected sites in the bone. They have the further advantage of adsorbing some of the drugs associated with MRONJ [71].

Each of these material groups present distinct advantages in combating infections associated with bone and oral health, suggesting their potential integration into custom medical devices tailored for treating conditions like MRONJ. For this project the choice of the materials is the bioactive glass based on the Hench's Bioglass, the next section will explain in detail the bioactive glasses.

2.5 Bioactive glasses

Bioactive glass is a type of bio-ceramic that is solid and porous/ nonporous [72]. The most common types of bioactive glasses are silicate-based glasses, such as the well-known Hench's Bioglass, which can degrade in body fluids and release ions beneficial for healing. Silicate based bioactive glasses consists of silicon dioxide (silicate) as the main component, along with sodium dioxide, calcium oxide, and phosphate. The components silicon dioxide (SiO_2), sodium dioxide (Na_2O), calcium oxide (CaO), and phosphorous pentoxide (P_2O_5) allow bioactive glass to be a solid, porous or nonporous

hard material. By varying the glass components and adding of various ions different forms of bioactive glasses can be produced, each with its own specific properties and applications [68]. When the bioactive glass encountered the bodily fluid, it can form silica gel layer on the surface of the contact, then the amorphous calcium phosphate precipitates on the gel layer and then the calcium phosphate crystallises into hydroxycarbonate apatite (HCA), a key component of natural bone. Such investigation is studied by immersing the glass in two type of solution, simulated body fluid (SPF) and Tris buffer solution, also dissolution and bioactivity studies help in understanding the profile and dosage concentration of the bioactive glass [73] [74] [75].

In Addition to the silicate-based glass (SiO_2), there are different types of bioactive glasses investigated for antimicrobial and bioactivity, including phosphate-based glass (P_2O_5) [76, 77], and borate-based glass (B_2O_3) [78].

The primary clinical applications of bioactive glasses have involved osteo-stimulation, which refers to the activation of progenitor cells in the body, producing more bone. This process is based on in vivo data showing that bioactive glasses stimulate more rapid bone repair than other bioactive ceramics. Bioactive glass used in dentine-repairing toothpaste with and its ability to remineralize caries and form apatite on the surface of enamel and dentine have also been reported [79].

The next sections will illustrate the glasses structures and properties of bioactive glasses.

2.5.1 Glasses' structure

All glasses have similar structure, the glass raw materials which give the structure are categorised into five categories based on their role in the process of the making the glass are: network former, flux, network modifier, and fining agent. listed in Table 2-4.

Table 2-4. List of the categories of the raw materials used in manufacturing the bioactive glass by melt-quench rout.

Raw materials categories	Functions	Example (origin)
Network former	Most important materials in forming the glass and function as the backbone of the glass. Usually, the name of the glass follows the network former Silicate for example if the former is SiO_2.	Silica SiO_2. Boric oxide B_2O_3. Phosphoric bento Oxide P_2O_5.
Network modifier	Presented in the batch to change or adjust the properties of the glass. (i.e. thermal, physical, dissolution).	Na_2O CaO MgO
Flux	Decreasing the melt temperature during the making of the glass.	Na_2O K_2CO_3

Network formers

In bioactive glasses network formers SiO_2, P_2O_5, B_2O_3 are the main building blocks of the glass structure and contribute to its overall stability and strength and contribute to the glass's ability to resist crystallization. They form the backbone of the glass network and provide structural integrity [80] [81]. In the most common silicate bioactive glasses, the SiO_2 form tetrahedral bond with the oxygen Si-O-Si this bond called a bridging oxygen (BO) it is important in glass stability, The (BO) bonds are disrupted by the

network modifiers in the glass to form non bridging oxygen (NBO's) which gives the bioactive glasses the dissolution and bio-reactivity properties on the glass surfaces.

Network modifiers

Network modifiers, alkali metals CaO, Na_2O and transition metal CuO, AgO, and FeO, play a role in modifying the properties of the glass by disrupting the glass network by breaking and reducing the oxygen bridging bond Si-O-Si which lead to the forming of the non-bridging oxygen (NBO) Si-O-NBO such effect contribute to the dissolution of the bioactive glasses depending on the concentration of the non-bridging oxygen [82]. CaO and Na_2O help in controlling the glass's melting temperature, viscosity, and bioactivity. Network modifiers also influence the porosity and textural properties of the glass, which can affect its performance in applications such as bone tissue engineering [80]. The presence of network modifiers can also affect the dissolution kinetics and bioactivity of the glass, making them important for understanding the behaviour of bioactive glasses in biological environments [83]. The addition of small amounts of network modifiers, such as alkali and alkaline earth oxides, can reduce the glass stability and reduce the tendency for crystallization [84]. However, the substitution of sodium oxide with alkaline earth oxides in bioactive glasses has been shown to improve the sintering ability and mechanical properties of the glass while maintaining biocompatibility [85]. The increased interconnection of fragmented chains by alkaline earth cations makes the substituted glasses stiffer and harder than traditional bioactive glasses [86]. Network modifiers also influence the surface reactivity of the glasses, with different amounts of alkali cations and undercoordinated species affecting the reactivity at the glass surfaces. Overall, network modifiers and

network formers have distinct effects on the properties and behaviour of bioactive glasses.

Compositional modifications of bioactive glasses have been carried out to improve their thermal stability, bioactivity, and antibacterial properties [87] [43] [88]. These modifications have helped identify the structural role of each incorporated component and its effects on the thermal and bioactive behaviour of the glasses.

Network connectivity (NC)

Following the review of the structure and composition of bioactive glasses there is an important concept related to the bioactivity of the glasses. The network connectivity (NC), NC is calculated by model proposed by Brauer and Hench in 2011 based on the molar composition for the simple SiO_2–$P2O_5$–MO–M_2O glass [89]:

$$\mathrm{NC}=\frac{4[\mathrm{SiO_2}]-2\left[\mathrm{M_2^{I}O}+\mathrm{M^{II}O}\right]+6[\mathrm{P_2O_5}]}{\mathrm{SiO_2}}$$

Where $\mathrm{M^{I}_2O}$ and $\mathrm{M^{II}O}$ represent monovalent and divalent glass modifiers mol % respectively, and [SiO_2] is the mol % of the silicate in the composition. The equation calculates the average of the bridging oxygen (BO) in the network. According to the equation the Hench's Bioglass (SiO_2 46.1 %, Na_2O 24.3 %, CaO 26.9 %, P_2O_5 2.6 %) network connectivity is about 2.11. The maximum limit for bioactive glass bioactivity is (NC = 2.6), where any increase in the NC value will indicate high number of bridging oxygen species Si-O-Si which will lead to stiffer glass and less bioactive [79, 81]. Although the network connectivity is helpful to determine the bioactivity in this simple glass formula, when designing complex glass other method could be considered for example split network by Edén and Watts [90].

Network connectivity is a crucial factor when designing new bioactive glass. For example, substituting 1 mol% of Na_2O with ZnO can increase the sintering window by 5 °C, while keeping the network connectivity around NC = 2, as the substitutions is made in the same mol%. This ensures the glass remains within the bioactivity window, similar to the original bioglass [79].

2.5.2 Mechanisms of bioactive glasses

Since the introduction of Bioglass new terms has introduced to describe the process of the materials that react with body specifically with bone's cells. It is important to familiarise oneself with the following terms. First, *osteostimulation* is a term approved by the United States Food and Drug Administration (FDA) after the introduction of biogalss, indicate the ability of a materials or its dissolution products to signal the progenitor cells to produce more bone [91]. Second term is o*steogenesis* refers to the process of bone formation and development. Third term is o*steoinduction*: are the process which osteogenesis is induced, that involve the stimulation of osteoprogenitor cells (stem cells) to differentiate into osteoblast for new bone formation. Lastly *osteoconduction:* it is the ability of biomaterial to support the growth of bone tissue over the surface, porous, channels, and pipes of implant or graft by allowing the bone forming cell to proliferate and forming new bone in the structure of the substrate [92].

The bioactive ceramics and glasses undergo solution-mediated surface reactions and serum protein adsorption events when immersed in biological fluids, which contribute to their bioactivity [72] [80]. Additionally, the effect of ionic dissolution products of bioactive ceramics on intracellular signalling pathways involved in osteogenesis has been studied.

The fundamental mechanisms of bioactive glasses involve a series of inorganic reactions when the glass is in contact with body fluids, leading to the formation of a layer of hydroxyapatite on the glass surface. This layer then interacts with biological entities, promoting osteo-conduction and osteo-stimulation, which ultimately results in the growth of new bone onto and between the bioactive glass structures [80].

Bioactive glasses exhibit bioactivity through various mechanisms. One mechanism involves the release of ions such as calcium, soluble silica, and phosphate, which leads to the formation of a biomimetic apatite surface layer on the glass. Another mechanism is the incorporation of therapeutically active ions into the glass composition, which broadens the application range of these materials.

The bioactivity mechanisms of bioactive glasses include the following five stages:

1. Ion exchange: Modifier cations in the glass exchange with hydronium ions in the body fluids.
2. Hydrolysis: Breakage of silicate bridges, forming silanol groups, and disrupting the glass network.
3. Formation of silica gel layer: A layer of silica gel forms on the bioactive glass surface.
4. Crystallization of hydroxyapatite: Hydroxyapatite, a bone-like mineral, forms on the surface of the bioactive glass.
5. Interaction with biological entities: After the formation of the hydroxyapatite layer, the bioactive glass interacts with blood proteins, growth factors, and collagen, promoting the growth of new bone onto and between the bioactive glass structures [93] [80] [72].

2.5.3 Evidence on the ion dissolution, antimicrobial, and angiogenic activity of bioactive glass:

Evidence of elemental release from bioactive glass (BAG):

Since the introduction of Hench 45S5 bioglass 1971 [94], bioactive glass system with composition SiO_2-Na_2O-CaO-P_2O_5 such as 45S5 (45% SiO_2, 24.5% Na_2O, 24.5% CaO, 6% P_2O_5 by weight %) and S53P4 (53% SiO_2, 23% Na_2O, 20% CaO, and 4%, P_2O_5 by weight%), have been extensively researched for their antibacterials and biological activities, particularly due to their osteostimulation property. In addition to these, other glass system with different composition have also been studied for their potential in various biomedical application. Currently, around 25 products based on these and other bioactive glass composition are commercially available, as summarised in [95].

The in vitro Ions (elemental) release and apatite formation is studies in different solution mostly simulated body fluid (SPF) but also in tris (hydroxyethyl) aminomethane (Tris) and cell culture media [74]. Researchers studied the ions releases of the glass composition from the bioactive glass for dissolution kinetic and hydroxyapatite (HCA) layer formation of bioactive glass both 45S5 melt derived and S58 sol-gel derived bioactive glasses [75] [96]. The mentioned studies investigate the glass concentration to form (HCA), the result suggest not to exceed the 0.002 g ml^{-1} in SPF for the 45S5 compared to the 0.0015 g ml^{-1} for the S58. This difference is attributed to the dense nature of the melt derived 45S5 in contrast to the mesopores surface structure of the sol-gel derived S58. The mesopore on the surface of the sol-gel glasses act as preferred HCA nucleation niche [75]. Another study investigated the texture and particles size effect on the dissolution in two solution SPF and cell culture

media the study suggest achieving controlled release of the glass compositions by varying the particles sizes, fine particles is favourable than coarse, and confirm the surface texture in the porous sol-gel S58 has quicker and more dense (HCA) layer than the melt derived 45S5 [96]. These invitro studies and many helped in determine the rate of the 45S5 bioglass dissolution matches the bone formation process which make the bioglass perfect substitution materials for the bone [81].

Antimicrobial activity of bioactive glasses

Numerous studies has shown the effectiveness of bioactive glass against bacteria without any ions addition in the SiO_2- Na_2O- CaO- P_2O_5 bioactive glasses, prove that they retain some antimicrobial activity, due to the releases of the Na^+ and Ca^{++} ions with combination of H_3O^+ protons result in pH increase in the environment around the dissolved glass [47]. S53P4 bioactive glass showed a potent antimicrobial activity alone and has increased when mixed with dentine powder [97]. Storr et al in 1998 studied the S53P4 against broad supra- and sub- gingival bacteria and has great antibacterials affect [61]. 45S5 in a study in 2001 investigates the antibacterial effect of the 45S5 bioglass against subgingival bacteria showed the ability of the 45S5 to kill the targeted bacteria _first time reported according to the author. The same study investigate whether the antibacterial effect of the 45S5 is pH dependent by adjusting the pH, prove the affect is pH dependent [98]. Mostly, published papers almost agreed that the high pH has the great impact on the antimicrobial effect of the original bioactive glasses especially 45S5 and S53P4 summarised in [99]. In conclusion the antibacterial activity of the mentioned bioactive glass is attributed to the dissolution and exchange of the ions lead to the increase of pH.

Angiogenesis of bioactive glass.

In addition to the antimicrobial activity of the bioactive glasses, they show an angiogenic properties in an in vivo and in vitro studies summarised in review published in 2010 [100]. In the review they summarized the effect of the bioactive glass specially 45S5 on the release of angiogenic growth factor that help in forming the blood vessels vascular endothelial growth factor (VEGF) in an in vitro study with samples containing or coated with 45S5. The review similarly mentioned in vivo studies looked at certain bioactive glasses either alone or coated on polyglycolic acid, sponge collagen, and VEFG-releasing PLGA scaffolds for tissue engineering (TE) application all showed an increased vascularisation but not with PLGA polymer or Glass ceramic scaffold derived from 45S5. These conflict in the result could be related to the size, distribution, and the properties of the scaffold, shape, and the pores. Despite that there is a confirmation that incorporation of certain bioactive glasses have stimulates the formation of blood vessel [100]. In recent review by Kargozar et al 2018, it emphasises the important of angiogenesis in the tissue engineering and how bioactive glasses satisfied the three requirements for bone regeneration: osteoconductivity, osteoconductivity and osteointegrativity. The review also confirms that latest in vitro studies has confirm the secretion VEGF, from studies where bioactive glasses were coated on different biomaterials. The review emphasise that the concentration and the size of the bioactive glass particles are affecting the angiogenic activity. The S53P4 showed an improved in VEGF secretion with smaller particle (1-2 mm) in comparison to larger particle size (2-3.15 mm), where high dose of 45S5 (0.1-10 wt.%) inhibit the VEGF. The article also reviewed the angiogenic properties of other glasses based on borate, phosphate as network former, and doped glasses where all have been proven

to promote angiogenesis in an in vitro and in vivo studies. Copper as dopped element in the glass proven to help angiogenesis in vitro and in vivo [101].

Dopped and substitution elements and their actions:

Extensive research has established the ability of the bioactive glasses of releasing dopped or substituted ions particularly one with the therapeutic and antibacterials properties such Ag, Zn, and Cu. Bellantone *et al* in 2000 were the first to report silver ions release with antibacterial affect from the sol-gel bioactive glass [43, 44]. Substitution/doping bioactive glass with bivalent metallic cations Zn, Mg , Cu, Sr to improve physical and bioactivity of the glasses [102].

In a research studying the effect of adding Zn and Mg substitution 45S5 on the ions release form glasses in two pH value on the release of Zn and Mg from in two different solution, one at natural pH 7.4 (Tris buffer) and acidic pH 4 (acetic acid/sodium acetate), founds that the Zn containing bioglass has dissolved rabidly in pH 4 solution suggesting the use of this Zn containing bioglass behaviour as controlled delivery device releasing Zn when needed at low pH environment such bacterial environment benefiting from the antibacterial property of the Zn [103]. This finding were also confirmed with low concentration of Zn in another study [104]. It is important to highlight that the type of solution choice is essential to the purpose of the investigation and could change the result, (e.g., pH that affect the element release), this study suggest using such changes (substitution with Zn and Mg) in the bioactive glass composition to reach therapeutic application [105].

Copper containing bioactive glasses (Cu) also has been proven in multiple studies it has an antibacterial and angiogenic properties when dopped or substituted in the

bioactive glasses. As the copper by itself has inherent antibacterial effects discussed in section 2.4 among other elements, it is succeeded as choice for its angiogenic affect in the bioactive glasses which is fundamental in the tissue engineering research. The addition of Cu by 2 and 5 mol % to the bioactive glass SiO_2-CaO system sol-gel mesoporous bioactive glass MBG significantly increased the antibacterial effect in addition to enhancing the angiogenic, and osteostimulation [106] [107]. Copper also studied with another element incorporated in the bioactive glass such as Mg, Zn, Sr, k, and Co for improved antimicrobial and bioactivity, and osteostimulation. An in vivo study on 2013 of bioactive borate glass (1393B3), conclude low amount of dopped CuO (0.4 wt.%) has no significant on the bone formation on rat calvarial defect but rather the shape of the glass particles (trabecular has more bone formation) [108]. Recently in vitro study the Cu affect in (0106-B1-BG) a borosilicate glass, showed an increase in the secretion of the proangiogenic marker protein in Cu-doped BGs, but the in vivo showed no significant increase in formation of new blood vessel in BG contains 5 % (wt. %) copper the highest in the study [109]. Sol-gel (70S1) bioactive glass low Cu substituted at 0.5, 1, and 1.5 by mol. % demonstrate a great inhibition against *E. coli* and *S. aureus* with the (70S 1.5 Cu 10 mg/mL [88]. Lastly, the addition of copper doped bioactive glass borosilicate glass (SBA3) as filler in PMMA cement (10 wt.%) to enhance the antimicrobial were successful without changing the properties of the cement [46]. Although the bioactive glasses are dominant in the bone regenerative research. It has its own share in wound healing when incorporation with copper and bivalent elements. In vitro and In vivo suggest that copper containing bioactive glass are promising [110] [111].

In conclusion section 2.5.3 above in the literature review showed that there is strong evidence for ion release from bioactive glasses having effects on biological systems. This was all the more so for substituted bioactive glasses, where specific oxides were frequently incorporated into glasses with the purpose of adding or enhancing a desirable feature, for example antimicrobial activity. Various metal ions have been added to bioactive glass systems to impart antimicrobial activity, including silver [112] , zinc, gallium [113] and copper ([114], (Binduhayyim 2021)). Valency may also be a factor, where Cu^{+} and Cu^{2+} may elicit different effects. In this study, copper (ii) oxide (CuO) was selected to substitute for CaO in the parent 45S5 bioactive glass composition for a number of reasons:

- This is a relatively under-researched composition, where a recent thesis from Sheffield (Binduhayyim 2021) showed promising antimicrobial activity at only 2.5 mol% substitution without a negative effect on *in vitro* biocompatibility.
- In addition to antimicrobial activity, Cu^{2+} ions are associated with angiogenesis i.e. the growth of new vascularisation around a bioglass implant [115]. This feature may be especially important in MRONJ, where vascularisation has the potential to enhance both bone and soft tissue healing.

2.5.4 Bioactive glasses manufacturing

bioactive glass is manufacture through two main methods melt-quench and sol-gel:

1. **Melt-quench.**

the melt-quench route in which the glass compositions are melted in crucible at high temperature around 1300 °C in furnace in platinum [116] or alumina crucible [117] [118], then quenched in water for frit glass see section 4.1 and 5.1 or cooled in graphite mould (annealed) for a bulk glass in different shapes [79].

One issue to consider with the selection of the melt route is that crucible type may become incorporated into the glass at low concentrations, where they have the potential to alter glass properties. For example, alumina from a crucible may undermine bioactivity via reducing glass solubility and introduce specific toxicity to bone. The Al^{3+} species will reduce the number of non-bridging oxygens in the glass, while any release of these ions may cause bone mineral defects and cell death. The potential for contamination of the glasses made in this study will be carefully considered.

Alumina crucibles are widely employed in glass melting including for bioactive glasses, on account of their low cost and stability at high temperatures. While there is a risk of contamination of the glass with Al_2O_3, it is generally understood that low levels (up to 1.5% wt./wt.), will not reduce bioactivity [93]. Alumina crucibles were therefore selected for this work, but the presence of Al_2O_3 would be determined post-melt using XRF, and ICP-OES. It is important to consider the influence of alumina contamination, as Al_2O_3 has been shown to affect properties including solubility and bioactivity (refs). This is via effects on glass structure that include (1) elimination of some non-bridging

oxygens to form a more compact glass network [93] and (2) stronger ionic cross linking and an increase in the number of octahedrally coordinated Al^{3+} ions [119]. The presence of low levels of Al_2O_3 may even have beneficial effects on a bioactive glass, including improving processing by increasing the working window between glass transition temperature and the onset of crystallisation [120] There are also well-known negative effects of aluminium ion release from biomaterials, established by Howard Carter in 1997 [121] and confirmed by Mark Blades [122]. Hence characterisation of glass and subsequent properties (e.g., ion release) should consider Al_2O_3, studies used alumina crucible showed a post melt of Al_2O_3 [117] [123]. No studies of bioactive glasses suggest that Al_2O_3 contributes to antimicrobial activity.

2. Sol-gel.

The second method is the sol-gel route where the glass precursors are dissolved and chemically react to form a gel then heat treated at low temperature (600-700 °C) to rapidly remove water leaving inorganic components in form of glass introduced by Li et al. 1991 for bioactive glasses [124] [125]. While sol-gel offers several advantages including low-temperature processing, there are risks (e.g., leaving residual cytotoxic materials in the in final product).

Although the route Hench bioglass was manufactured through melt-quench it is the most traditional method, the sol-gel route has its fair share in glass manufacturing in the research. In contrast to melt route the sol-gel is low temperature method.

Both methods have been explored to enhance the bioactive glasses properties such as improving tendency of crystallization, widening the working window (the difference between glass transition and glass crystallization temperatures), and improve

bioactivity of the glass through dropping or substitution of the glass modifier Na_2O and CaO with alkali and alkaline earth metal oxide or transition metal.

Substitution versus doping of Bioactive glasses.

Both doping and substitution bioactive glasses with metal ions produces a variation of glass to enhance physical, mechanical, and biological characteristics of the glass. Various metal ions have been incorporated in the glass's matrix reviewed in the literature which is divided into two main categories: transition metal (e.g., Ag, Zn, Cu) and alkaline / alkali earth metal (e.g., Sr, Ca, Mg) mainly to enhance crystallisation and improve the biological and introduce or improve the antimicrobial property to the glass. The incorporation of metal oxide like copper, strontium, zinc, and manganese into the glass matrix can tailor the release of therapeutic ions, thereby improving the material's functionality for bone regeneration and wound healing applications. Substitution involves partially replacing one metal oxide with another on a molar basis, whereas doping refers to the addition of extra oxides.

Table 2-5 has example of the doping and substitution of bioactive glass studies. One issue arises when reviewing the literature for substitution and doping is the differences in the titles form the methodology implied. In the doped column in Table 2-5 it shows that highlighted numbers of papers have in their title terms doped / doping but when reviewing the methodology, it is suggested that they substitute in molar basis, and some are substituted in weight percent.

It seems the term doping has been used interchangeably with substitution as in the studies in the Table 2-5 discussing the doping with an specific oxide Mg, Zn, Cu, Sr, and Br but the methodology involves substitution for mostly Ca, but also Si, and Na by

molar basis and weight base of the glass oxide compositions which is in both weight and mole indication for a form of substitution. These terminology nuance highlighting the focusing on the enhancement of the material rather than the precise chemical methodology employed. These interchangeable uses of the terminology could be misleading because the confusion arises when articles refer to "doping" in their titles but describes methodologies that involve substitution, either in molar or weight percent terms.

Table 2-5. An example of studies involved doping and substitution methodolgy and weather if the title matches the methodology for doping and substitution**.** The unmatched method to title are highlited with notes.

oxide	Doping	Substitution
Copper	Evaluation of borate bioactive glass scaffolds as a controlled delivery system for copper ions in stimulating osteogenesis and angiogenesis in bone healing [78]. Note: This study specifically indicates the wt.% addition of copper based on the glass weight. Dissolution of borate and borosilicate bioactive glasses and the influence of ion (Zn, Cu) doping in different solutions [126]. Note: Although the title mentioned doping the glasses composition table in method suggested substitution by wt.%.	A comparative in vitro and in vivo analysis of the impact of copper substitution on the cytocompatibility, osteogenic, and angiogenic properties of a borosilicate bioactive glass [109]. Note: This study substitutes on a wt.% basis.

Magnesium	Evaluation of zinc and magnesium doped 45S5 mesoporous bioactive glass system for the growth of hydroxyl apatite layer [127] Mesoporous bioactive glass nanoparticles doped with magnesium: drug delivery and acellular in vitro bioactivity [128]. Odontogenic and anti-inflammatory effects of magnesium-doped bioactive glass in vital pulp therapy [129] Note: Although the title says doped, the methods suggested substitution by mol% for Na study[127] , and Ca in study [128], and in [129] For Ca. An In Vitro Evaluation of the Biological and Osteogenic Properties of Magnesium-Doped Bioactive Glasses for Application in Bone Tissue Engineering [130] Note: This study doped the original glass formula with 6 mol% MgO extra. Synthesis and characterization of magnesium-lanthanum dual doped bioactive glasses [131] Note: In this study the method indicates substitution by wt.% for Ca and Si when increasing MgO and La2O3.	Bio-response of copper-magnesium co-substituted mesoporous bioactive glass for bone tissue regeneration [135]. Influence of low amounts of zinc or magnesium substitution on the ion release and apatite formation of Bioglass 45S5 [104]. Preparation and in vitro investigation on bioactivity of magnesia-contained bioactive glasses [136]. Novel antibacterial Cu/Mg-substituted 58S-bioglass: Synthesis, characterization and investigation of in vitro bioactivity [137] . MgF2- containing glasses as a coating for titanium dental implant. I-Glass powder [138].

	Osteogenic Potential of Magnesium (Mg)-Doped Multicomponent Bioactive Glass: In Vitro and In Vivo Animal Studies [132] Note: methodology suggest substitute by mol%. Electrospun flexible magnesium-doped silica bioactive glass nanofiber membranes with anti-inflammatory and pro-angiogenic effects for infected wounds [133]. Effects of Mg and Zn on the surface of doped melt-derived glass for biomaterials applications [134].	

Strontium	Strontium-Doped Bioactive Glass Nanoparticles in Osteogenic Commitment [139]. Effects of strontium-doped bioactive glass on the differentiation of cultured osteogenic cells [140]. Note: the method suggests substitution for both studies. [140] used the term substitution in conclusion. Binary Doping of Strontium and Copper Enhancing Osteogenesis and Angiogenesis of Bioactive Glass Nanofibers while Suppressing Osteoclast Activity [141]. Note: Sr substituted for Ca then Cu is dopped to the glass. New strontium-based bioactive glasses: physicochemical reactivity and delivering capability of biologically active dissolution products [142]. Note: the methodology is suggesting substitute by wt.%.	Influence of strontium for calcium substitution in bioactive glasses on degradation, ion release and apatite formation [143]. Preparation, characterization and in vitro biological response of simultaneous co-substitution of Zr+4/Sr+2 58S bioactive glass powder [144].

Doping of metal oxides in bioactive glasses significantly influences their bioactivity, enhancing properties such as osteogenesis, angiogenesis, and antibacterial activity. However, the substitution of metal oxides on a molar basis can offer advantages over doping, particularly in terms of network connectivity and bioactivity. This response

explores the effects of doping and substitution in bioactive glasses, focusing on their impact on bioactivity and network connectivity.

In conclusion, while both doping and substitution of metal oxides in bioactive glasses can enhance bioactivity, substitution often provides additional benefits in terms of network connectivity and mechanical properties. This makes substitution on molar basis a potentially more advantageous approach for applications requiring long-term stability, durability and ensuring the bioactivity by calculating the network connectivity mention in section 2.5.1. However, the choice between doping and substitution should be guided by the specific requirements of the intended application, considering factors such as desired bioactivity, mechanical properties, and degradation rates.

2.6 Poly (methyl methacrylate) PMMA

PMMA, or poly (methyl methacrylate), is an amorphous thermoset with high strength, rigidity, and excellent light transmission. Due to its good transparency, chemical stability, and electrical insulation, it is used in various fields such as aviation, architecture, medical treatment and optical instruments [145] [146] . It has been found that the mechanical properties of PMMA, such as tensile strength and fracture surface energy, increase with increasing molecular weight [147]. In recent years, efforts have been made to improve the toughness of PMMA without compromising its other properties. One method is to produce PMMA composites within situ engineered nanofibrils of thermoplastic polyester elastomer (TPEE), which significantly improve the toughness of PMMA while maintaining its strength, stiffness and transparency [148].

PMMA in dentistry

Poly (methyl methacrylate) (PMMA) is widely utilised in dentistry for various applications, including artificial teeth, dentures, crowns, fillings, and dental restorations, owing to its excellent biocompatibility, aesthetics, and cost-effectiveness [149] [150]. Despite its advantages, PMMA faces challenges such as weakness in hydrolytic degradation due to the enzyme and saliva in the oral environment, poor fracture toughness, and a lack of antibacterial activity [151]. In study of surface deterioration on samples collected from patients and control new dentures base materials. Research study conclude the deterioration happens because of saliva, microbial and enzymes metabolize where data has been obtained from the samples through component analysis, volatile analysis and hardness testing [152]. To address these

limitations, researchers have explored diverse strategies, such as the incorporation of nanofillers and reinforcement additives into PMMA matrices [153] [154] [155].

Studies have investigated the integration of metallic nanoparticles, metal oxide nanofillers, and carbon-based nanomaterials into PMMA to enhance its properties, including reducing water absorption and improving thermal and flexural characteristics [156]. Furthermore, efforts have been directed towards the development of antibacterial PMMA resins by incorporating natural antibacterial agents and protein-repellent agents, aiming to prevent oral diseases like denture stomatitis and gingivitis [157].

PMMA based composite.

Recent advancements in PMMA research have explored the integration of ε-poly-L-lysine (ε-PL) and 2-methacryloyloxyethyl phosphorylcholine (MPC) to create antibacterial PMMA resins that exhibit antibacterial activity without compromising mechanical properties, thus holding promise for dental applications [158]. Additionally, the incorporation of 2-methacryloyloxyethyl phosphorylcholine (MPC) and quaternary ammonium dimethylamino hexadecyl methacrylate (DMAHDM) in PMMA has resulted in a protein-repellent and antibacterial dental resin with sustained antibacterial performance [159].

Moreover, the inclusion of nanomaterials such as titanium dioxide nanoparticles (TiO_2NPs), halloysite clay nanotubes (HNTs), and graphene doped PMMA resin has demonstrated improvements in PMMA performance, including increased stiffness and reduced colonisation by Candida albicans [160]. The use of graphene-doped PMMA resin has shown enhanced physical-chemical properties and antimicrobial potential,

making it a promising option for computer-aided design and computer-aided manufacturing (CAD/CAM) dental applications [161] [162].

In the realm of bone cement, PMMA finds extensive utility in dentistry for applications like denture base resin, temporary dental restorations, and as a filler or base material. Notably, PMMA composite incorporating Y_2O_3 powder exhibits promising outcomes, showing enhanced cell proliferation and the quality of osteoblastic bone formation in vitro, positioning it as a potential material for bone cement in orthopaedic and orthodontic implants.

While PMMA offers substantial advantages, it is not without limitations, including weakness in hydrolytic degradation, poor fracture toughness, and a lack of antibacterial activity. Nonetheless, PMMA remains a versatile and cost-effective dental composite material with the potential for continuous improvement through innovative reinforcement techniques.

3 Aim and objectives.

To summarise, MRONJ is a painful and unpleasant condition for patients, many of whom are suffering from underlying conditions (e.g., cancer) that already have a debilitating impact on quality of life. Current treatments are frequently unsatisfactory, and this is largely therefore an unmet clinical need in dentistry. Advances in biomaterials research and manufacturing present an opportunity to develop a new approach, in particular copper-substituted bioactive glasses with predicted antimicrobial properties. The aim of this study was to develop copper-substituted bioactive glasses that could be used in the manufacture of a “therapeutic” component as part of a custom prosthesis to suppress the growth of pathogens while facilitating tissue regeneration in MRONJ sites in the mouth. The specific objectives were therefore:

- To design copper-substituted bioactive glasses based on the substitution of CaO with CuO and evaluate the melt process as a means of fabricating glasses with a higher concentration of copper than has been described previously.
- To produce and fully characterise a series of copper-substituted glasses using the melt quench route - including 45S5 bioactive glass as a reference material - applying x-ray diffraction (XRD) to confirm their glassy nature, and thermal analysis to investigate glass transition temperature and any crystallization events.
- To prepare and characterise glass powders suitable for use in preparation of acrylic composites (using grinding and sieving followed by scanning electron microscopy / SEM).
- To evaluate the release of component ions from reference and experimental bioactive glasses, including sodium, calcium, copper and silicon.

- To investigate the relative antimicrobial properties of these novel glasses using a range of organisms including clinical isolates.
- Finally, to carry out a preliminary investigation of in vitro biocompatibility of experimental materials using cell lines that are relevant to this application in the oral cavity.

On completion of this series of studies, it will be known if these new biomaterials have potential for the treatment of MRONJ. Further knowledge related to the preparation of copper-containing glasses, and the reactions of cultured bacteria and cells, will also have been generated. This work therefore has clinical potential.

4 Materials and Methods.

Two series of glasses based on the Hench 45S5 bioactive glass were synthesised by melt quench route and characterised for compositional and structure characterisation. Then the glasses were tested for antimicrobial activity against *Actinomyces Oris* bacteria. A composite of PMMA and the bioactive glass were produced by 30 % wt. of glass, and a biocompatibility assay was performed using direct cell contact and Prestoblue analysis with two cell lines MG63 and L929.

4.1 Glasses synthesis and substitution.

45S5 is the most highly published bioactive glass composition, with extensive studies on structure and properties. It has also been used commercially in several products including synthetic bone graft substitutes and toothpaste, providing further real-world evidence of human safety and biocompatibility. Most importantly though, a previous thesis in the group (R Bindahayim) provided strong evidence that 45S5 had greater antimicrobial activity than S53P4 which was the parent glass for a synthetic bone graft with claimed antimicrobial properties (BoneAlive®). Finally, several studies had been published on substitution of oxides in the 45S5 formulation, showing that it was feasible to prepare modified compositions with this parent glass (substitution involves replacing one metal oxide with another on a molar basis, whereas doping refers to the adding of additional oxides). For these reasons, 45S5 was selected for the studies in this research project.

Series 1

Series 1 has four glasses based on the 45S5 Hench bioactive glass, where the CuO is substituted for CaO as follow: 45S5 bioactive glass (45S5), 1 mol % Cu substituted

bioactive glass (Cu 1), 2.5 mol % substituted bioactive glass (Cu 2.5), and 5 mol % Cu substituted bioactive glass (Cu 5) Table 4-2.

Series 2

To investigate the release of Cu, new glasses were produced in which the molar proportion of Na_2O was increased in substitution of CaO in the glass. After carful reviewing the literature to determine the highest Na_2O incorporated in the glass, two glasses were designed with 30 mol% Na_2O. first one is based on the 45S5 described above in series 1 labelled as (4530) and the second is based on the 5 mol% Cu glass labelled as (305). The highest Na_2O mol % was determined after looking at the literature of the highest possible amount of the Na_2O were added to the glass [65].

The materials (reagents that provide the required oxide) used in glasses synthesis summarised in Table 4-1 were used by the calculation of the batch in Table 4-2 and Table 4-3

Table 4-1. Reagents used in glass synthesis.

Reagent	Molecular formula	Molecular weight ($g.mol^{-1}$)	supplier
sand	SiO_2	60.08	Sigma Aldrich (UK)
Sodium carbonate	$NaCO_3$	105.9888	Sigma Aldrich (UK)
Calcium carbonate	$CaCO_3$	100.0869	Sigma Aldrich (UK)
Dicalcium phosphate	$CaHPO_4$	136.06	Sigma Aldrich (UK)
Copper (II) oxide	CuO	79.545	Sigma Aldrich (UK)

Glasses design and synthesis:

The glasses series were synthesised using a melt-quench route based on Hench bioglass formula: 45 wt.% SiO_2, 24.5 wt.% CaO, 24.5 wt.% Na_2O and 6.0 wt.% P_2O_5. Firstly, the 45S5 bioglass was prepared as described by Hench (2006). Then the copper substituted glasses series based on the bioglass system (SiO_2-Na_2O-CaO-P_2O_5) designed by adding copper to the glass system substituting CaO at 1 mol%,2.5 mol%, and 5 mol%, then series 2 were further substituted of Na_2O for CaO in addition to CuO shown in Table 4-2.

The glass melting was performed in alumina crucibles. Every reagent providing the oxide composition shown in Table *4-3* was calculated and weighed on a precise electronic scale for each glass patch. The reagents were mixed in a glass jar gently until a visually homogeneous batch was observed. The batch was poured into an alumina crucible (Almath crucibles Ltd.) and was transferred to laboratory chamber furnaces (Elite LTD) at room temperature. Then the furnace programmed to reach 1450 °C in 5°C/min and held for 1 hour to ensure the molten glass. The molten glass in the crucible immediately poured into a stainless-steel bucket of cold water to obtain the frit shape glass. The frit was then placed in a dryer oven at 70°C for 24 hours. The dried glass frits were then transferred into a mortar and manually reduced to a smaller particle size about 5 mm. Additionally to produce fine powder with small particle size, the coarse glass frit was processed for 10 minutes at 200 rpm in a rotatory ball miller (Retsch PM100, Germany) with 80 ml grinding bowls and nine 15 mm tempered zirconia balls to ensure fine ground powder. Finally, the powder was sieved through a series of sieves ranging from 150 µm to 45 µm sieve (Endecotts Ltd., UK.)

Table 4-2. The mol % and wt. % composition of the synthesised glasses.

glass label	SiO_2		Na_2O		CaO		P_2O_5		CuO	
	mol%	wt.%	mol%	wt.%	mol%	wt.%	mol%	wt.%	mol%	wt.%
	Series one									
45S5	46.1	45	24.3	24.5	26.9	24.5	2.6	6	0	0
Cu 1	46.1	45	24.3	24.5	25.9	23.40	2.6	6	1	1.3
Cu 2.5	46.1	45	24.3	24.5	24.4	22	2.6	6	2.5	3.2
Cu 5	46.1	45	24.3	24.5	21.9	19.60	2.6	6	5	6.3
	Series two									
4530	46.4	45	30	30	21	19	2.6	6	0	0
305	47.4	45	30	29.3	15	13.30	2.7	6	5	6.4

Table 4-3. Reagents batch calculation in grams for each glass series.

reagents	Sand	Sodium carbonate	Calcium carbonate	Dicalcium phosphate	Copper oxide
Oxide supplied	SiO_2	Na_2O	CaO	P_2O_5 + CaO	CuO
Series one					
45S5	45.01	41.83	35.31	11.50	0
Cu 1	44.82	41.84	33.32	11.50	1.30
Cu 2.5	44.60	41.36	30.82	11.50	3.20
Cu 5	44.10	41.02	26.53	11.50	6.30
Series two					
4530	45	51.27	25.46	11.50	0
305	45	50.07	15.28	11.50	6.40

Glass powder disc making:

The discs around 12 mm diameters were produced using the hydraulic press. 0.56 grams of glass powder is put inside the press mould then pressed at 2 tons for 1 minute for each disc.

4.2 Bioactive glass characterization.

4.2.1 Differential Scanning calorimetry (DSC)

DSC is a thermal analysis technique used to determine the glass transition temperature (Tg) and glass crystallisation temperature (Tc) for glass-ceramics materials. DSC measures the heat flow in and out of the sample while it is subjected to controlled temperature change, using a reference sample for comparison.

For this study the SDT 650® instrument was used. The instrument came with an edited pre-programmed modulated DSC run. In each run, 20 mg of glass frit was placed in a 90 µm alumina crucible and mounted on the SDT 650® instrument as per the machine's instructions. The reference sample used in the analysis was an alumina sample. The DSC program is set to the following parameters: ramp rate of 10°C /min, and temperature range of 50-1000 °C.

4.2.2 X-ray diffraction (XRD).

XRD is a characterising technique used to assess the internal structure of materials including glasses using X-ray radiation. X-ray with known wavelength is directed onto the materials which then the material depending on its internal structure diffracts the X-ray, which then detected by the XRD machine's detector. During the analysis, the X-ray source or the sample table is rotated to change the diffraction angle by 2Θ. The

intensity of the diffracted X-ray is measured, and the diffraction data are recorded. The data analysed by the machine using Bragg's law.

In this study PANalytical Aeris fully automated XRD machine was used to study the glass structure. The glasses in powder form were placed on the sample mount provided with the machine and positioned on the designated area on the instrument. Then the 10 minutes rotating scan is selected and initiated according to the manual instruction. As soon as the analysis started, the data were recorded and displayed by the machine. The data were subsequently transferred using a USB flash drive.

4.2.3 X-ray fluorescence XRF

X-ray fluorescence (XRF) as an elemental compositional detection technique. XRF relies on the detection of energy emitted by electrons as they transition from higher energy levels to fill vacant electron shells in atoms. This energy emission occurs when the electrons are displaced by incident X-rays.

The energy emitted by the electrons during this process is specific to each element in the periodic table. By measuring and analysing the emitted energy, the elemental composition of a given sample can be determined. This is because the energy signatures or characteristic X-ray spectra emitted by the electrons correspond to specific elements.

In XRF analysis, the sample is typically bombarded with X-rays, which cause the displacement of electrons from their orbits. As the displaced electrons return to their original positions, they emit characteristic X-rays, and their energies are measured by the XRF detector. By comparing the detected energy values to known energy

signatures of elements, the presence and relative concentrations of different elements in the sample can be identified and quantified.

XRF is widely used in various fields, including material analysis, environmental monitoring, geology, archaeology, and forensics, due to its non-destructive nature and ability to provide rapid and quantitative elemental analysis.

In this study the XRF analysis was conducted to compare the weight percent (wt.%) of oxides between the theoretical composition and the XRF results after melting. Two machines were used for the analysis: the Nixon XRF machine for the first four synthesised glasses, and the Primus IV XRF machine for the new high sodium glasses.

4.2.4 Scanning Electron Microscopy SEM and Energy Dispersive Spectroscopy (EDS).

Scanning Electron Microscopy (SEM) and Energy Dispersive Spectroscopy (EDS) are surface elemental analysis technologies used for materials. They are based on exciting atoms with an electron beam and measuring the energy released during electron transitions. The basic concept involves an electron beam exciting an inner-shell electron of an atom, causing it to escape from its orbit. As a result, an electron from a higher energy shell drops to occupy the vacant electron shell, releasing energy in the form of X-rays that is detected with a detector in the SEM machine. Each element has its characteristic X-ray wavelengths or energies, which act as unique fingerprints.

The detected X-rays are then analysed and compared with a database of known X-ray energies for different elements. This comparison allows for the identification of the elements present in the sample surfaces. SEM-EDS technology is highly useful for

determining the elemental composition of materials at the surface level and comparing it with the theoretical composition. However, it's important to note that while it provides valuable semi-quantitative information, factors such as sample surface topography and electron beam interaction volume can affect the accuracy of the quantitative analysis. Therefore, SEM-EDS is considered a partially quantitative method.

Overall, SEM-EDS is a powerful tool in materials science, allowing researchers to investigate and understand the elemental makeup of various materials at the microscopic level.

In the SEM EDS analysis, several parameters were adjusted to study the compositions of the glasses. These parameters include the voltage intensity (HV) ranging from 15 to 20 kV, beam intensity at values of 8, 9, and 15, electron detection using scattered electron (SE) or backscattered electron (BSE) modes, and specifying the detection for specific elements Si, Na, Ca, P, and Cu. Additionally, the analysis could be performed on a specific area or spot.

The results showed that the highest quantity of elements was detected at higher HV settings with backscattered electron detection and specific element detection. Increasing the HV allows the electron beam to penetrate deeper into the sample, reaching elements that are further from the surface, up to around 5 micrometres deep. The beam intensity affects the scan speed, where lower beam intensity results in more time spent in scanning but does not significantly affect the result. Therefore, a faster scan with higher beam intensity was preferable.

4.2.5 Fourier transform infrared spectroscopy (FTIR).

FTIR is a chemical characterisation analysis technique based on the infrared interaction with the materials. The structural characteristics of bioactive glasses especially the presence of bridging oxygens (BO) and non-bridging oxygens (NBO), play a crucial role in determining their bioactivity and interaction with biological environments. Fourier Transform Infrared (FTIR) spectroscopy is a powerful tool for analysing these structural features, particularly the stretching vibrations associated with Si-O bonds. Understanding this relationship is essential for the design and optimization of bioactive glasses for various biomedical applications.

The samples are placed in the machine between an infrared (IR) source and detector. When the infrared light from the source is passing through the sample, the sample absorbs some or all the infrareds. At the other end, a detector detects the amount of IR passing through the sample which is subsequently plotted to create an IR spectrum. The IR spectrum shows the frequencies where the light absorbed by the sample indicates the vibration of the bond between the compound's atoms. Each chemical compound has its own bonds vibration detected by IR that make it a chemical fingerprint. The spectrum graph of any sample can be compared with the database to identify any compounds appearing in the sample. FTIR is a straightforward technique due to the vast number of identified chemical in the spectral libraries that could be used to compare the spectrums and identify the materials.

In this study, the Spectrum two instrument from PerkinElmer was used for the FTIR analysis. The analysis aimed to observe any chemical changes between the glasses where Cu was substituted for CaO in the glass composition. The goal was to

investigate the effects of substituting CaO with CuO on the chemical properties of the glasses in comparison to the parent 45S5 glass.

4.2.6 Inductively coupled plasma optical emission spectroscopy ICP-OES.

Series 1

The ion release study was conducted to determine the quantity of ions released in deionized water using inductively coupled plasma optical emission spectroscopy (ICP-OES). Deionized water was chosen to eliminate any background ions that could interfere with the measurements. The study design involved collecting data at three time points: 24 hours, 72 hours, and 168 hours. Four types of glasses were investigated: 45S5, 1% Cu-substituted 45S5 (Cu 1), 2.5% Cu-substituted 45S5 (Cu 2.5), and 5% Cu-substituted 45S5 (Cu 5).

Series 2

An element release study was performed to investigate the influence of increasing Na_2O mol% on the glass dissolution.

Method:

For both glass series a ratio of 600 mg per 20 mL deionized water ratio a higher ratio than suggested in the literature 75 mg per 50 mL to amplifying the elements concentration which help in increase the test sensitivity and enhance the signal to noise ration and ensuring sufficient element concentration. Also the bioactive glass dissolution behaviour is influenced by glass concentration in the solution, element concentration increased with higher glass concentration [75] [163].

600 mg of each glass with a particle size smaller than 45 µm was weighed on an electronic scale and placed in clean 50 mL glass vials. The particle size was chosen to maximize the surface area interaction with the deionized water. Then a 20 ml of deionized water was added to each vial, which was tightly closed and placed on a rolling mixer machine. As a control, a glass vial filled only with deionized water was included. The study was performed in triplicate, and each group of vials was numbered 1, 2, and 3.

At each time point, the glass vials were removed from the rolling mixer machine and placed on a bench to allow the glass particles to settle at the bottom of the vials. A Falcon tube, numbered to match the designated vials, was mounted on a holding rack. The contents of each glass vial were carefully poured through an 11 µm pore size cellulose filter paper (Whatman) into the Falcon tube without disturbing the settled glass particles. The filtered liquid was visually checked for clarity, and if necessary, it was filtered again through a clean filter paper into a fresh Falcon tube. The Falcon tube was then closed securely and stored in the refrigerator for analysis. The glass vials were refilled with approximately 20 ml of fresh deionized water, tightly closed, and placed back on the rolling mixer machine for the next time points. In case any filter paper contained trapped glass particles, the paper was washed with fresh deionized water and returned to the designated glass vials.

The samples were analysed using an IPS OES machine, with approximately 5 ml of liquid per run per sample. The collected data were averaged, and each averaged time point was added to the previous one to obtain cumulative data.

4.3 PMMA and bioactive glass composite.

PMMA was used to determine the maximum loading amount of glass to produce a packable composite mixture. Self-cure poly (methyl methacrylate) denture base material ProBase® form ivoclar vivadent was used at ratio 1.5: 1 of powder (g) to liquid (L) was per the manufactures recommendation for pouring technique. 30% weight of glass was the maximum loading glass in the PMMA. The glass was weighed and then mixed with PMMA powder then the MMA liquid added to the powder mixture and mixed. The composites mixture was then packed in a silicone mould to produce the composite discs. The mould was left to cure overnight prior to the experiments.

4.3.1 Composite Characterization.

The PMMA composite characterised for its surface roughness and surface hardness using contact profilometers, and diamond indentation hardness tester for Vickers hardens (Hv) respectively. These characterisation methods chosen to investigate the effects of adding the glasses to the PMMA. Surface roughness and hardness are crucial tests to ensure the new composite are meeting the standards for dental applications. The standards ensuring good selecting guidelines for clinicians and enhancing patients care and outcomes include durability, aesthetics, and biocompatibility.

Surface hardness.

VX Vickers hardness indenters (Foundrax, UK) used to measures surface hardness. The machine dents the samples by diamond shape indenter then measures how deep the indenters penetrate the surface. applied force equal to 10 Kg and 10 second dwelling time and recoded as surface hardness measured in (Kg/mm^2). Vickers

hardness test (Hv) performed three times on three 9 mm disc samples from each PMMA and glass / PMMA composites, five groups as PMMA sample is the control. The three reads were averaged, and the statistical analysis perfumed in Graph Pad Prism using one way ANOVA for significant differences.

Surface roughness.

To measure the surface roughness TR200 profilometers, a mechanical contact profilometer machine used to measure the surface roughness arithmetic average roughness (Ra) in micrometre (µm). The TR200 profilometers has diamond tips with 5 µm radius and it is mounted at 90-degree angle on micro stylus. The resolution 0.001 µm. The surface roughness measured by the stylus travelled across short distance on the surface of the sample. Four groups' samples of glass / PMMA and PMMA samples as controls. Two 9 mm disc samples from each PMMA and, glass / PMMA group measured twice for surface roughness. The reading recoded and averaged for each sample and the statistical analysis perfumed in Graph Pad Prism using one way ANOVA for significant differences.

Elemental release.

Elemental release from Cu 5 / PMMA discs composite in deionised water was carried out to determine the release of the glasses element especially copper to investigate copper release from the composite mentioned in 4.3. The study protocol kept the same as described above for the glass element release study in section 4.2.6, but the study performed for seven days. The samples were: three composite Cu 5/ PMMA sample, three just deionised water, and three PMMA discs sample.

4.4 Antimicrobial activity.

4.4.1 Materials and preparation.

Series 1

The antimicrobial study carried out only on the glass only. To study the antimicrobial activity of series 1 glasses, the agar disc diffusion methods were performed in aseptic workstation with clinical isolate *Actinomyces Oris,* and lab based *Actinomyces Oris MF1* Gram-positive bacterium and the Gram-negative *Prevotella Bucca,* a clinical isolate bacterium summarized in **Table 4-4**.

Series 2

For series 2 glasses only *A oris* MF1 tested to evaluate the antimicrobial of the high sodium glasses 4530 and 305 compared with the original glasses 45S5 and Cu 5 glasses also using the same method and materials described in section 4.4.

The materials for preparing the agar and the broth are listed in Table 4-5. Fastidious anaerobe blood (FAB) agar and Brain heart infusion BHI broth were used to grow and test the microorganisms.

Table 4-4. List of the bacteria used in the antimicrobial activity and their origin.

Organisms	Gram stain	Origin
Actinomyces Oris MF1	Positive	School of clinical dentistry Lab strain microorganism
Actinomyces Oris	Positive	Clinical isolate Sheffield school of clinical dentistry reference 20/WS/0165
Prevotella Bucca	Negative	

Table 4-5. Materials used to prepare the agar and the broth in 400 ml Deionized water (DH_2O) volume.

Reagent	Ratio	Supplier
Agar		
Fastidious anaerobe (agar)	18.4 g in 400 ml DH_2O	NEOGEN
Horse blood	20 ml / 400 ml agar	Sigma-Aldrich
broth		
Brain heart infusion (broth)	18.8 g in 400 ml DH_2O	Sigma-Aldrich
Yeast extract	2g / 400 ml DH_2O	OXOID
Hemin	2 ml / 400 ml DH_2O	
Vitamin K	400 µl / 400 ml DH_2O	

To prepare the agar plate the reagent ratio in **Table 4-5** were placed in glass jars then autoclaved. After autoclave the agar was melted in a microwave and stored in a 55°C water bath to reduce the agar temperature. In an aseptic workstation the horse blood was added to the agar at 20% v/v. 20 ml of the horse blood was added to 400 ml of agar and gently stirred until homogenised. The agar was poured in the plate immediately afterwards, around 20 ml of agar for each plate.

To prepare the broth culture, 200 ml BHI Broth was prepared according **Table 4-5** and autoclaved. The broth was used to prepare the inoculum and growing the bacteria.

4.4.2 Antimicrobial testing

Table 4-4The bacteria in **Table 4-4** were grown in FAB agar plate using streak methods from frozen stocks and left in an anaerobic incubator at least 24 h at 37°C to

grow and form a colony. The *Prevotella Buccae* clinical isolate needed at least three days to grow and form colonies. These checked visually every 48h.

When appropriate colonies formed, one colony was swapped with a sterilized plastic loop, inoculated in 10 ml of the prepared BHI broth in a 25ml sterilized glass vile and put on an anaerobic incubator at 37°C overnight. From the inoculum, FAB agar plates were lawned with 200 µl of inoculated BHI broth using a plastic spreader. The optical density (OD) for the inoculum kept at 0.1, the 12 mm glass disc was placed on each agar plate or group of 3.

The plates were then placed in the anaerobic incubators at 37°C overnight for the *Actinomyces sp* and 48h for the *Prevotella sp*. The plate was checked for the inhibition zone after 24 hours and picture taken with the phone perpendicularly mounted above the plate with a referenced ruler. For the *Prevotella sp* the plate was put back in the incubator for another 24 hours if the inhibition zone were not definitive. Inhibition zone measurements were performed on ImageJ (Fuji) software.

4.5 Cell viability assay

Cell viability was performed to investigate the cytotoxicity of the glasses-PMMA composites. Direct contact methods with MG63 and L929 using PrestoBlue™ with the four groups of bioactive based glasses-PMMA composite and control PMMA.

PrestoBlue™ is a viability dye which can diffuse in and out of cells. The dye is resazurin (which is the substrate and blue in colour). In the presence of living cells, the dye can be reduced by the cells (in the cytoplasm and mitochondria) to the fluorescent product resorufin (which is pink in colour). The resulting mixture of resazurin and resorufin will turn the dye a shade of purple colour. The dye can be fully reduced to a

bright pink-but this amount of resorufin is too great to be measured in the Tecan plate reader. Presto blue assay performed to compare the cell viability between the 4 samples of composite against the PMMA sample.

Materials:

Table 4-6 shows the materials and cell lines used in the experiment with their volume percentage (%).

Table 4-6. Show the cell lines and the materials used in the.

Cells	Type	Media	Supplements % v/v of DMEM
MG63	Osteosarcoma cells have fibroblast morphology.	DMEM (Sigma Aldrich)	1% v/v penicillin-streptomycin. 1% v/v L-alanyl-l-glutamine. 10% v/v Foetal bovine serum (FBS).
L929	Fibroblast cell.		
Other reagents and uses			
Reagents		Uses	
trypsin-ethylenediaminetetraacetic acid (Gibco)		Detach the cell from the flask.	
Prestoblue™ (Thermo Fisher)		cell viability reagent 10% (v/v)	

Method:

All the following procedures are performed in the cell culture hood under antiseptic procedure with autoclave and sterilise instruments. The cells in the culture flask and in the plate were incubated at 37 ºC, 95% air / 5% CO2 atmosphere incubator.

Media preparation:

The culture media prepared for the cell culture and experiment using materials and the ratio shown in Table 4-6. The supplements were added to a DMEM bottles and

gently mixed then kept in the fridge. Before use, the media culture was placed in 37 ºC water bath.

Dye mixture preparation for cell viability:

The dye mixture was prepared by mixing culture media prepared above and adding 10% PrestoBlue dye to the culture media. This aliquot dye mixture was added by 800 microliters to each well of cell cultures in the experiment.

Experiment design:

For each group of cells five 24 well plates were used to perform direct contact cell viability each plate divided as follow:

1. **Experimental samples:** Three wells containing the discs of the materials with the cells.
2. **Control 1**: Three empty wells contain only culture media. This is a control to measure how much the PrestoBlue dye will change colour in the absence of cells or material.
3. **Control 2:** three wells containing discs of material without cells. This will show if material can affect the PrestoBlue dye.
4. **Control 3:** Three wells containing cells only (no discs of material). This control will show the maximum level of dye conversion will get from the cells in the absence of any of material. This control reading will be subtracted from the fluorescence value reading from the experimental control.

The remaining empty wells filled with 1 ml of PBS Figure 4-1.

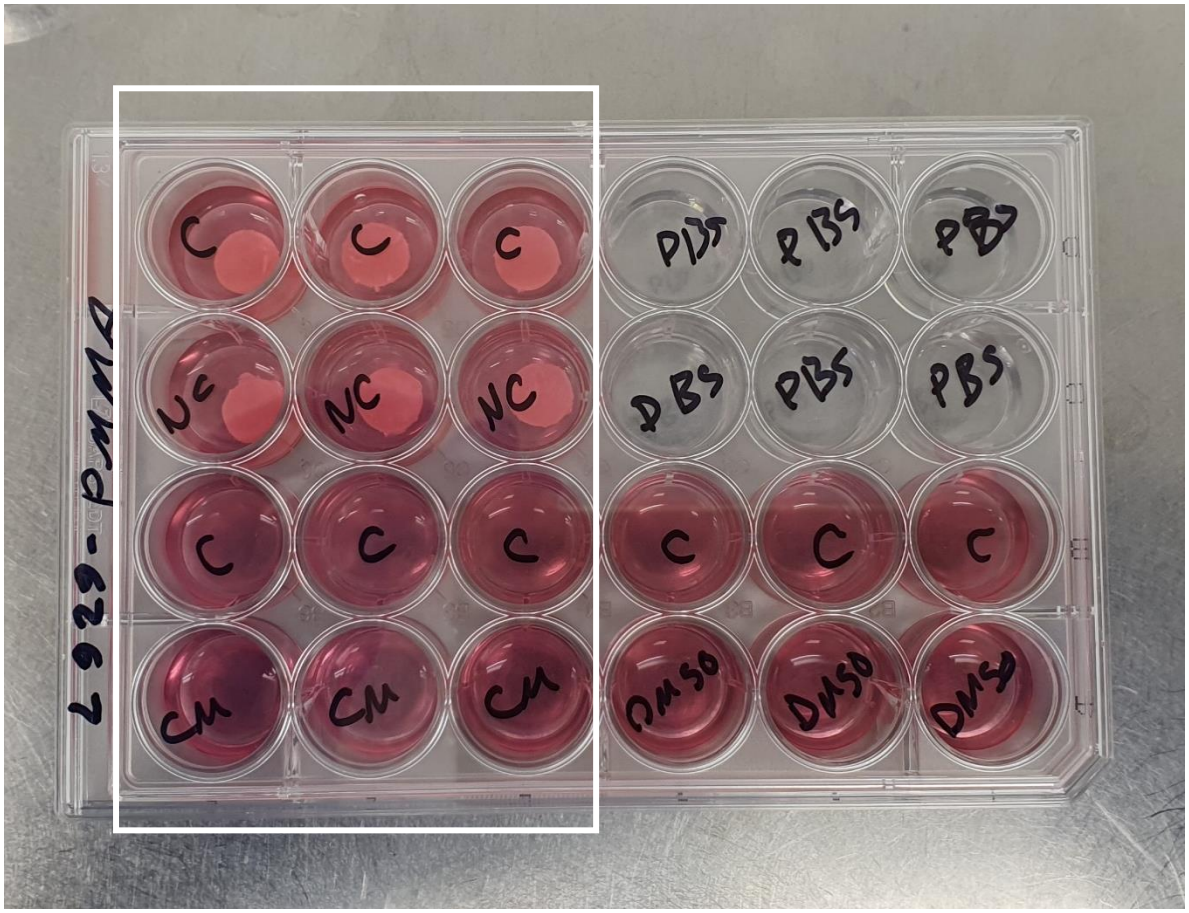

Figure 4-1. Sample images show the design of the experiment and the composites discs in the wells. the ladling was used to identify the well during the experiments. In the white box the designed experiment: 1st row experimental samples materials and cells, 2nd row control 1 materials with no cells, 3rd Control 2 cells only, 4th row Control 3 culture media only. Labels (C) Cell, (NC) no cell, (CM) Culture media only, (PBS) phosphate-buffered saline, (DMSO) Dimethyl sulfoxide_ not used in the study.

Cell culture and seeding:

Both MG63 and L929 cell passaged and split in five T75 culture flasks in culture media prepared form Table 4-6. After cells culture reached complete confluent in the T75 flasks by checking under the light microscope, the cells were detached by adding 4 ml of trypsin-ethylenediaminetetraacetic acid and incubated for 5-10 minute and checked under the microscope to ensure the cells were detached. Later 400 microliters added to the culture to inhibit the trypsin then all the cell culture content from the five flasks were transferred in 50 ml centrifuge tube fresh PBS and centrifuged at 1000 rpm for 5 minutes. The tube was checked for the cell pallet and carefully discard the supernatant. The cells pallet then resuspends in 10 ml of fresh media. Cells were counted using hemocytometer and the light microscope from the fresh cell suspension to estimate the needed amount from the cell suspension for seeding in the wells.

The seeding count was $2x10^5$ cells for each of the wells described above in the experiments design. The plates were then incubated for 24 h in the incubator at 37 ºC, 95% air/5% CO2 atmosphere to let the cells attach to the bottoms of the wells. After the 24 h incubation the cells were checked under the light microscope for confluent and attachment. The discs were gently placed in the designated wells, three discs in the cell well and three in the culture media only wells. The plates were placed back in the incubators for 48h and kept undisturbed to insure no movement of the discs over the cells.

Cell viability using PrestoBlue™

After the 48h plates incubation, the culture medium was gently removed from the wells then 800 microlitres of the PrestoBlue™ mixture was added to the wells containing

cells and the discs, culture media and the discs, the cells only, and the culture media only wells. Afterward, the plates were placed back in the incubator. The colour changes of the dye during the incubation were checked periodically for colour changing turning from blue to a pink/purple in the wells containing cells. The incubation took approximately one hour. At this point, 3 lots of 200 microlitres removed of the incubation medium of each sample wells and the controls wells to individual wells of a 96 well plate each well of the 96 well plate contains 200 microlitres of sample.

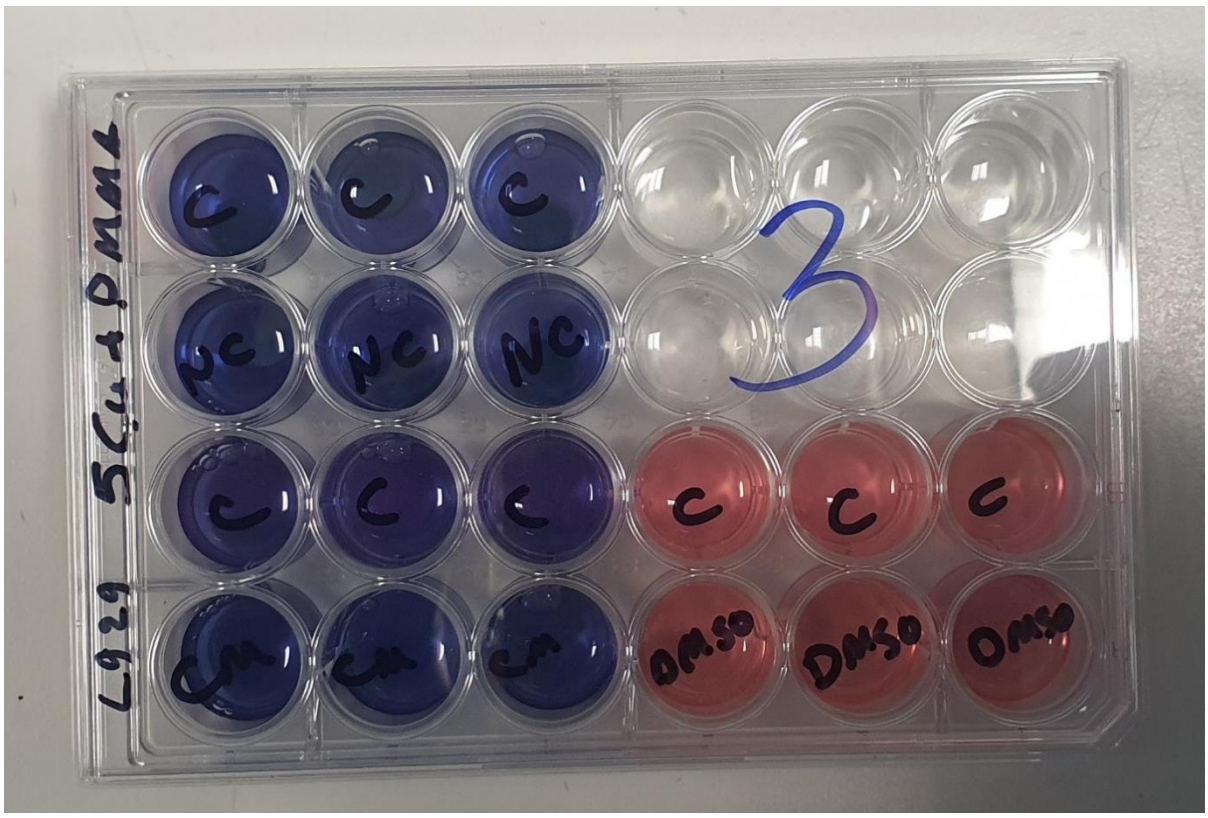

Figure 4-2. Sample image from the experiment (L929 Vs Cu 5 composite) show the Prestoblue dye in the wells. The colour change from blue to the purple indicate cell viability. There is no colour change in the Cell with the discs first row because there was no cell activity in the Cu 5 composite sample indicate no cell viability.

The 96-well plate was then placed into the TECAN Infinite M Nano for determining the fluorescence of the product resorufin at an excitation wavelength of 560 nm, and emission wavelength of 590 nm using 80% gain on the plate reader.

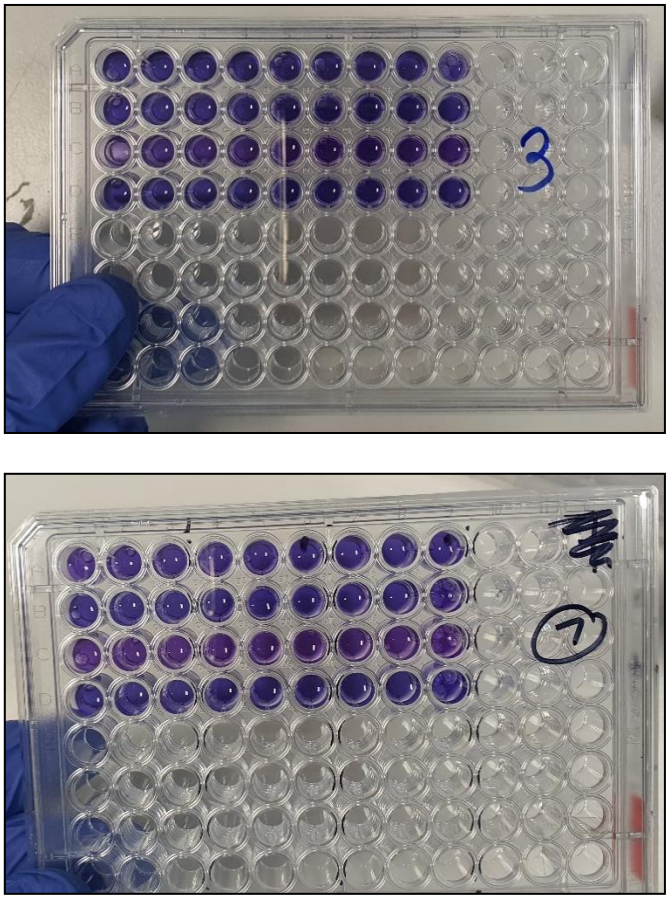

Figure 4-3. Sample images from the experiment of the 96 well plate properad for the TECAN. Top images obtained from the same plate in Figure 4-2 Cu 5 composite, only the 4th row has purple colour as described in the previous figure. Bottom image represent the 45S5-PMMA Vs MG63 plate, the first row has a slight colour change form blue to purple.

The data was then prepared using Excel Microsoft. The read from the empty well (media with no cells) were averaged and then subtracted from all the reads. The data from each sample then averaged to give the average value. The statistical analysis performed using GraphPad Prisms for one-way ANOVA test for significant differences P value 0.05.

5 Results

5.1 Bioactive glass synthesis.

Visual examination of the 45S5 glass frit after melt quench characterized with transparent colour. The Cu 1 substituted glass has transparent light blue colour. The Cu 2.5 glass has a darker blue than the Cu 1 while the Cu5 has the darkest colour among all glass dark blue green colour. All glasses showed homogeneous colour across the frit.

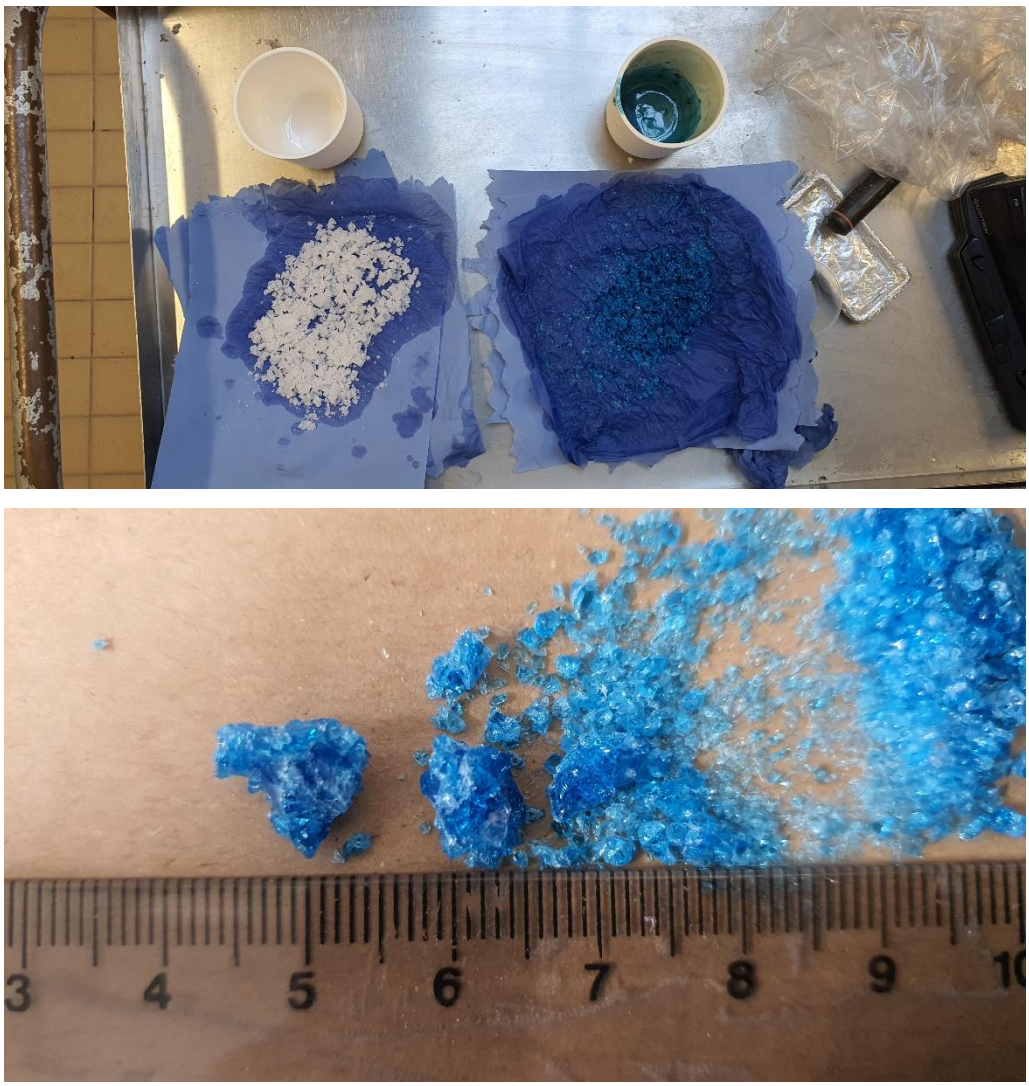

Figure 5-1. The glass frit after melt quench processes at the top, left white is 45S5 and the right blue is 1%mol Cu, the bottom dried sample glass frit with a ruler reference for the frit size.

5.2 Bioactive glasses characterisation.

5.2.1 X-ray diffraction (XRD).

Series 1

XRD is an important analysis for determining the internal crystal structure of glasses. The broad peak between 25 θ and 40 θ in **Figure 5-2** is a clear indication that the glasses are in the amorphous state. There are no sharp peaks that would indicate a crystalline phase in the glass.

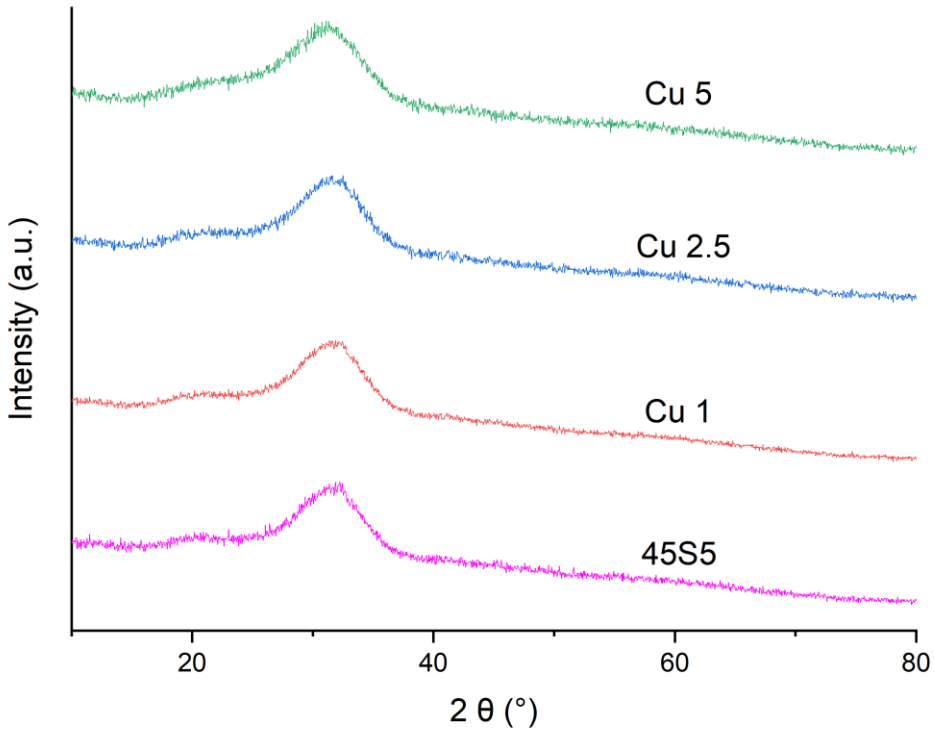

Figure 5-2 The XRD pattern of the glasses shows the amorphous state. No signs of crystallisation (sharp peak).

Series 2

The graph of the XRD Figure 5-3 indicates an amorphous structure of the 4530 and 305. The amorphous structure showed in the graph as one hump between 25Θ and 40Θ.

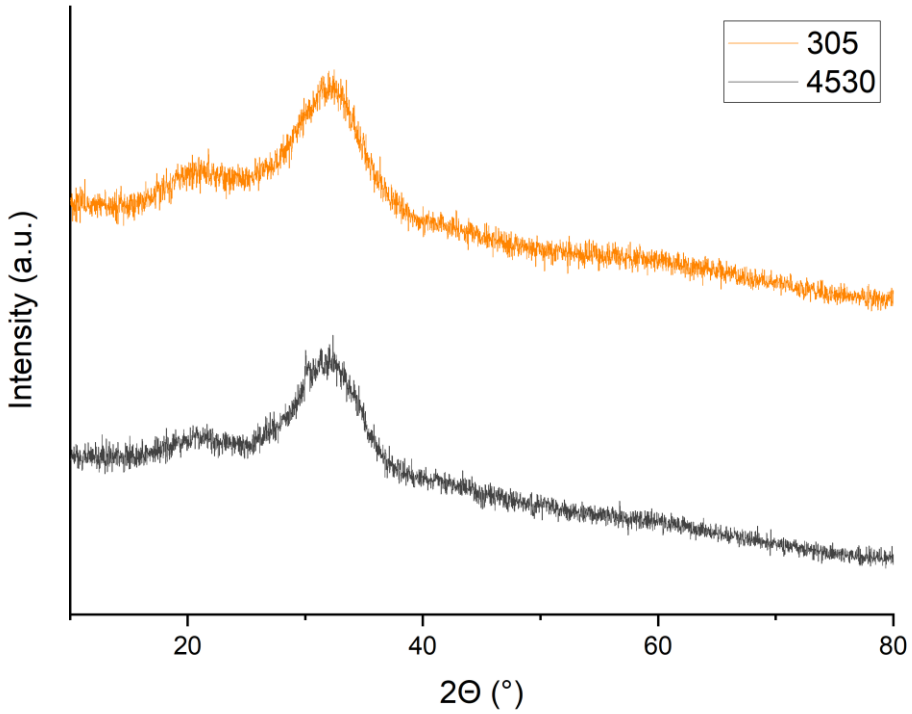

Figure 5-3. The one hump XRD pattern of the high Na_2O glasses shows the amorphous state. No signs of crystallisation (sharp peak).

5.2.2 X-ray fluorescence (XRF)

Series 1

The data from the XRF are shown in Table 5.1, which compares the molar percentage (mol %) of the theoretical formula and the mol % after melting. Due to limitations of the instrument, the element sodium is not detectable. The results show that the Cu content in the post-melt increases with increasing substitution and the Ca content decreases which confirm the substitution. The post melt molar percentage of the XRF data does not match the theoretical molar percentage. The post melting mol% percentage appears to be 4-5 times higher than the theoretical mol% and the P content is significantly lower than the theoretical and are decreases with the increased of Cu substitution. The Si mol% in the post-melt content is higher than the theoretical in Cu 1 glass and it is lower in the Cu 2.5 and Cu 5

Table 5-1. XRF data shows the mol % composition of the glasses post melting (XRF mol %) in comparison to the theoretical mol % (T mol%). (Nd) not detectable (N/A) not applicable.

Element	Si		Na		Ca		P		Cu	
Glasses /analysis	T mol %	XRF mol%	T mol %	XRF mol %	T mol%	XRF mol %	T mol %	XRF mol %	T mol %	XRF mol %
45S5	46.1	N/A	24.3	N/A	26.9	N/A	2.6	N/A	0	N/A
Cu 1	46.1	53.43	24.3	Nd	25.9	39.40	2.6	1.2	1	5.88
Cu 2.5	46.1	31.42	24.3	Nd	24.4	58.62	2.6	1.0	2.5	11.6
Cu 5	46.1	32.49	24.3	Nd	19.60	51.52	2.6	1.05	5	14.92

Series 2

The XRF data compares the percentage molar composition after melting (XRF mol%) of the glass with the theoretical percentage molar composition (T mol%). In this study, the Primus IV XRF instrument provided more accurate mol% percentages of the glass after melting. The Si XRF showed slightly lower mol% than the theoretical percentage. The XRF mol% of Na is also significantly lower with 66% deviation from the theoretical mol% for both glasses. In contrast, the mol% of Ca after melting is higher than the theoretical mol% after melting, by 129% for 4530 and by almost 144% for 305 glass. However, the XRF mol% in the 305 glass is lower than in the 4530 glass, which could confirm the substitution. The phosphorus is close to the theoretical mole % with a reduction of 31%. The Cu XRF mol % is also significantly higher than the T mol% by 152% increases.

Table 5-2. XRF molar percentage post melt (XRF mol%) and theoretical molar percentage (T mol%) of the high Na_2O glass 4530 and 305. XRF data obtained by (Primus IV XRF instrument).

Element	Si		Na		Ca		P		Cu	
Glasses /analysis	T mol %	XRF mol%	T mol %	XRF mol %	T mol%	XRF mol %	T mol %	XRF mol %	T mol %	XRF mol %
4530	46.4	42.01	30	9.41	21	45.43	2.6	3.1	0	0
305	47.4	39.50	30	10.18	15	32.48	2.7	2.6	5	15.18

Table 5-3. XRF molar percentage post melt (XRF mol%) and theoretical molar percentage (T mol%) of the high Na_2O glass 4530 and 305. XRF data obtained by Niton XL3t the Na sodium is not detectable (Nd) with this machine.

Element	Si		Na		Ca		P		Cu	
Glasses /analysis	T mol %	XRF mol%	T mol %	XRF mol %	T mol%	XRF mol %	T mol %	XRF mol %	T mol %	XRF mol %
4530	46.4	50.25	30	Nd	21	47.75	2.6	1.9	0	0
305	47.4	49.13	30	Nd	15	36.59	2.7	1.8	5	12.6

Aluminium

In addition to the detected elements of the glass composition there were a small amount aluminium detected. This is because of using alumina crucible in the making of the glass. The detected alumina in wt.% is about 0.55 detected by Niton XL3t. while Al_2O_3 detected by Primus IV XRF are between 1.4 and 1.2 wt.%. these percentages are discussed in the literature above if the using of the alumina crucible will affect the bioactive properties of the glass. Which conclude these weight percentages are safe and it should not affect the glass bioactive properties [93].

5.2.3 Differential scanning calorimetry (DSC).

Series 1

Figure 5-4 shows The DSC graph indicating the glass transition temperature (Tg) and peak crystallisation temperature (Tc). The onset Tg for 45S5 glass is around the 556°C. The Tg for the Cu substituted glasses is decreasing with the increase in Cu substitution. The Tc peak for the 45S5 is at 829°C and similarly the Tc for the Cu glasses are decreased but with no systematic decrease with the increase in Cu substitution. The least Tc among the Cu glasses was observed for the Cu 1 glass at around 737 °C and

the highest for Cu 2.5 at around 800°C. The Tc onset temperature differ from the peak where this temperature indicates the beginning of the crystallization. It is crucial for further glass treatment to not reach this temperature in glass annealing. The highest onset was observed around 785 °C for 45S5 glass where the lowest onset temperature was for Cu 1 glass around 710 °C.

In the DSC graph Figure 5-4, an indentation is appearing after the glass transition in the diagram is very noteworthy. This indentation only appeared in the copper-containing glasses and could indicate a different glass phase.

Table 5-4. Shows DSC analysis approximate Tg and Tc onset and Tc peak for the glasses rounded to the nearest true number.

Glasses	Tg onset °C	Tc onset °C	Tc peak °C
45S5	556	785	829
Cu 1	519	710	737
Cu 2.5	503	756	800
Cu 5	501	742	757

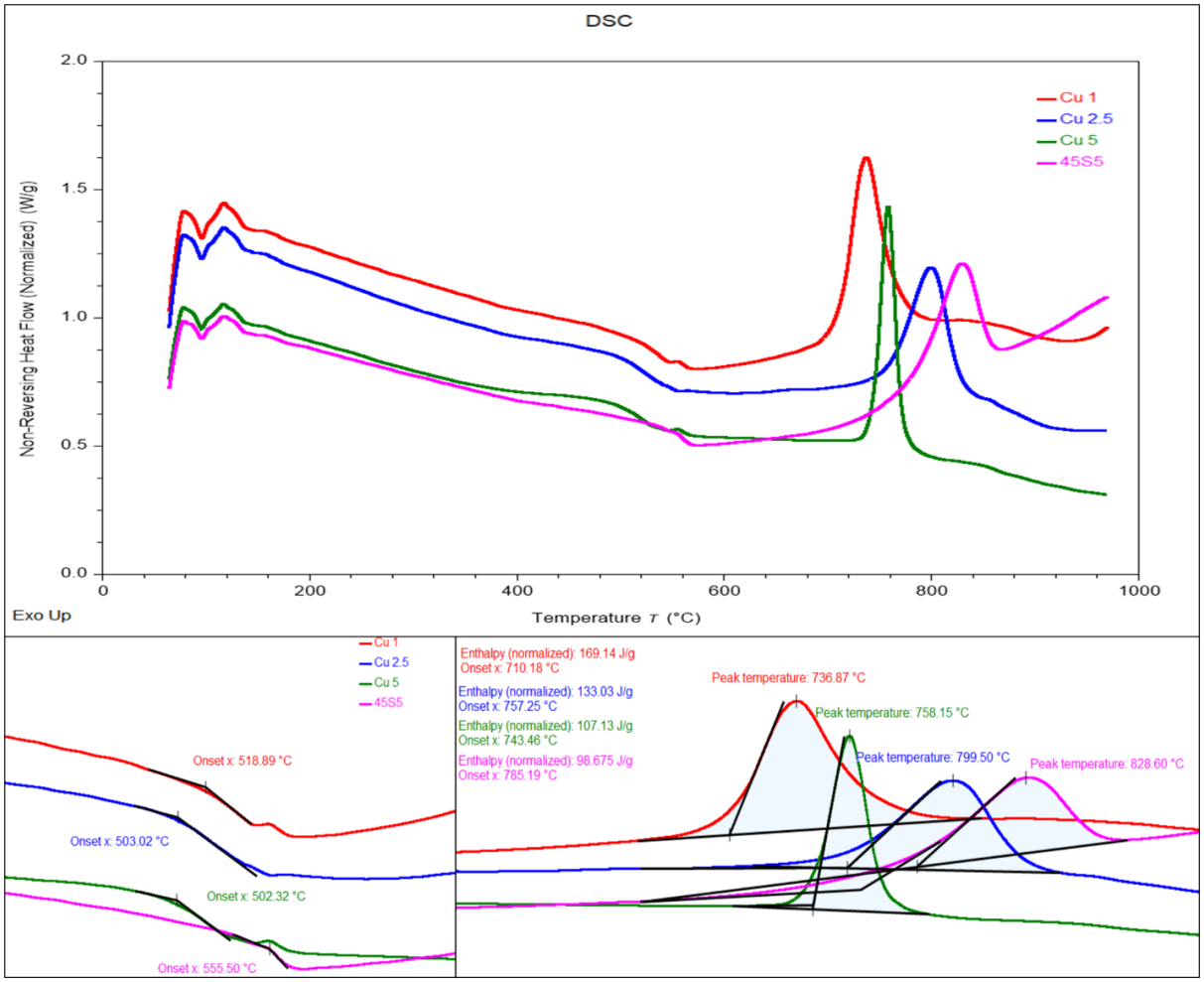

Figure 5-4. Differential scanning calorimetry (DSC) graph of all glass obtained by SDT 650® (Waters™). The sample run at 10°C /min ramp rate to 1000°C for DSC under N gas. The top show the typical DSC curve of glasses. Bottom left shows the glass transition (Tg) analysis and the onset of the (Tg). Bottom right show the peak hight and the onset of glass crystallisation analysis. The analysis performed in Trios TA® (Waters™) software provided from the company. The second indentation is clearly visible on the bottom left specially on the Cu 1 and Cu 5 glasses, where there is no sign of indentation on the 45S5 after the glass transition dip.

Series 2

The DSC showed the glass transition (Tg) and the glass crystallisation (Tc) point in the graph Figure 5-5. The Tg were lower than the series 1 glasses Table 5-4. The Tg onset for the 4530 were around the 501 °C, and the 305 glass was around 443 °C lower than any glass in this project. The Tc also were lower than the Series 1 glasses for both glasses, where the 4530 onsets at around 690 °C and peaked around 717 °C and the 305 glass has lower onset at around 611 °C and peaked around 630 °C. temperature are listed in Table 5-5. There was also an indentation in the graph after the glass transition dip Figure 5-5.

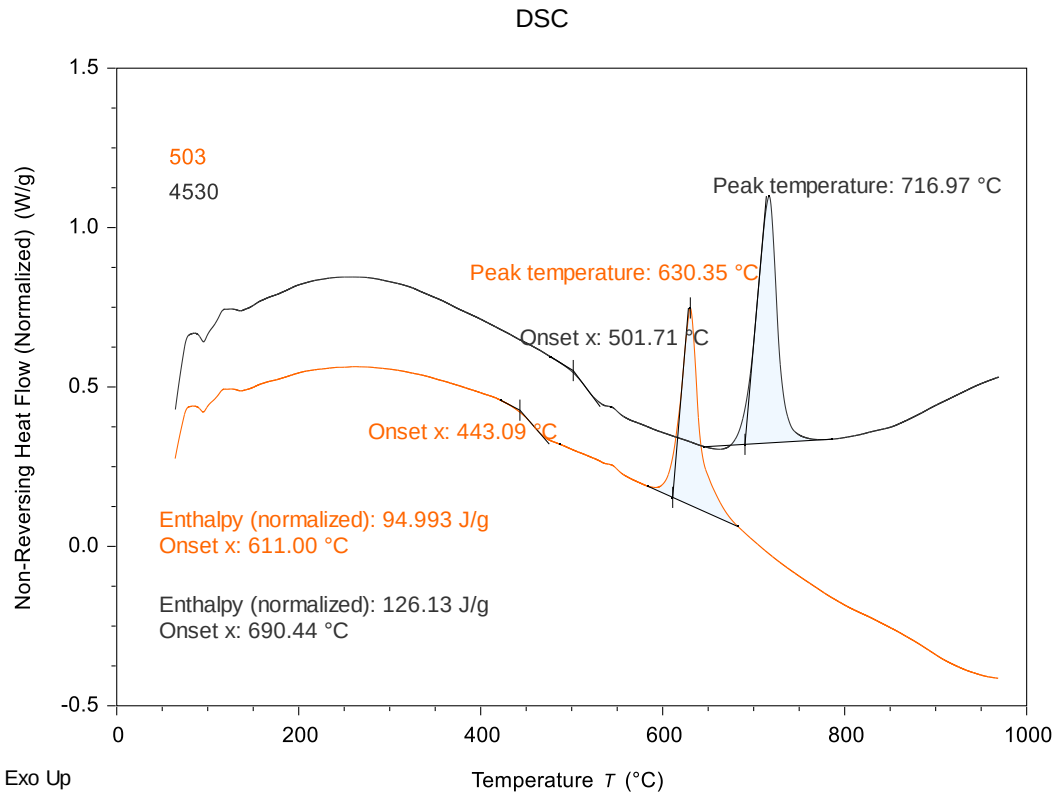

Figure 5-5. The DSC graph of the 4530 and the 305 shows the analysis of the onset of Tg and Tc and the also the hight peak of Tc. The Tg onset for 4530 glass is around 501 C and the Tc onset around 690 °C, the 503 glass Tg onset is around 443 °C and the onset of Tc is around 611 °C

Table 5-5. DSC temperature for the 4530 and 305 glasses rounded to the nearest true number obtain from the analysis of the DSC graph. The second indentation clearly seen after the glass transition dip in the 4530 and in the 305 closer to the Tc peak.

Glasses	Tg onset °C	Tc onset °C	Tc peak °C
4530	501	690	717
305	443	611	630

5.2.4 Scanning electron microscopy (SEM / EDS).

The SEM / EDS analysis confirm the presence of the element used for glasses synthesis **Figure 5-6**. In 45S5 glass the Si, Na, Ca, and P are present, also in addition, the Cu in the Cu glasses appeared in close. The Cu wt.% increases respectively with the increase in the Cu % in the glass theoretical formula and the Ca wt.% decreases subsequently which confirm the substitution the Cu glasses.

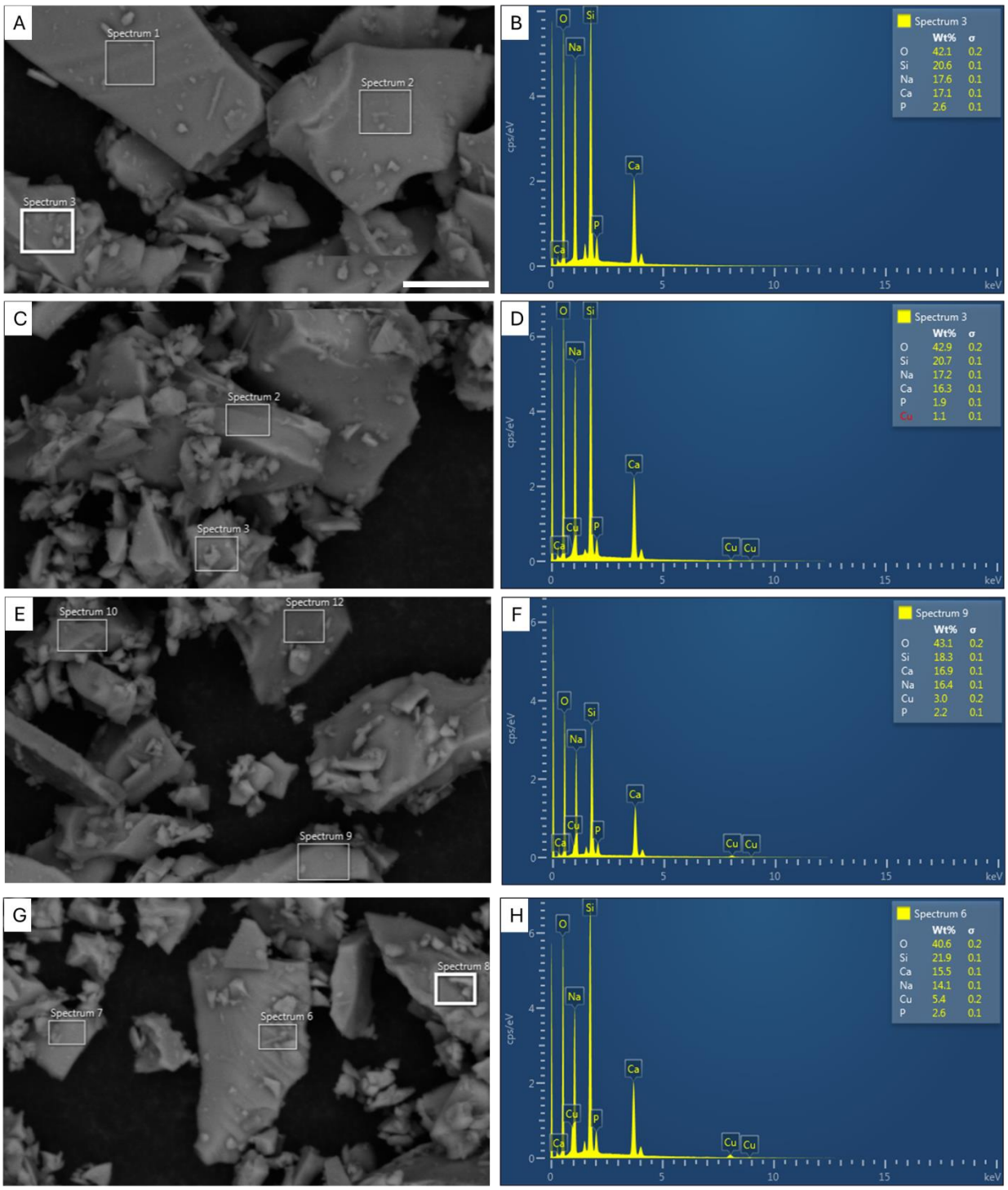

Figure 5-6. SEM images of the glass's frits in the study and the corresponding EDS analysis in the blue boxes showing the weight percentage of the elemental analysis of the bioactive glass composition Si, Ca, Na, P, and Cu. (A) 45S5, (C) Cu 1, (E) Cu 2.5, and (G) Cu 5.

5.2.5 Fourier transform infrared spectroscopy (FTIR).

Figure 5-7 shows the IR spectra that characterize with six distinctive peaks for all glasses. Because of the 45S5 glass has two network formers $(SiO_4)^{4-}$ and phosphor-oxygen $(PO_4)^{3-}$ the FTIR spectra is easily and precisely identified [164]. The band around the wavenumber 1460 cm^{-1} is assigned to carbonate group $(CO_3)^{2-}$ as reported at the literature [123]. This band is clear in all glasses except in Cu 5 glass were showed flat. The next band group centred around 1000 cm^{-1} and 900 cm^{-1} is a Si-O-Si stretch [96] [164] showed clearly in all glasses with slight intensifying in the peak with the Cu content increase in the glass. Around the 700 cm^{-1} a broad peak referred to amorphous phosphate [123]. Lastly the peak around 460 cm^{-1} appointed to Si-O-Si bend.

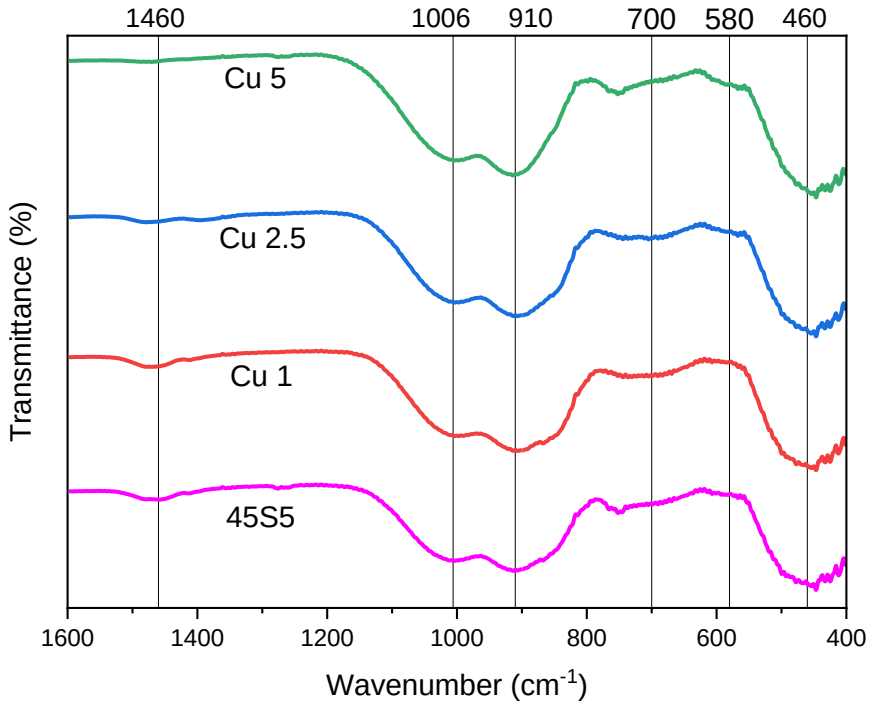

Figure 5-7. FTIR spectra for all glasses showing the band and their group signed by vertical line from left 1460 (carbonate group $(CO_3)^{2-}$),1000 and 910 (Si-O-Si stretch), 700 (amorphous phosphate), 580, and 480 (Si-O-Si bend).

5.2.6 Inductively coupled plasma optical emission spectroscopy ICP-OES.

Series 1

The effect of Cu substitution on the kinetic of glass dissolution and ion release is shown on Figure 5-8 to Figure 5-12. The result signifies the Cu substitution reduce the ion release in general.

Silicon [Si] release

The release of [Si] element implies the dissolution of the bioactive glass because it is the main network former of BG. In Figure 5-8 the Si element decrease systematically among the glasses in an inverse relation of Cu substitution. Highest release could be observed in 45S5 glass at around 11 mg/L while the lowest by almost half is for Cu 5 glass is around 6.6 mg/L at 186 hours.

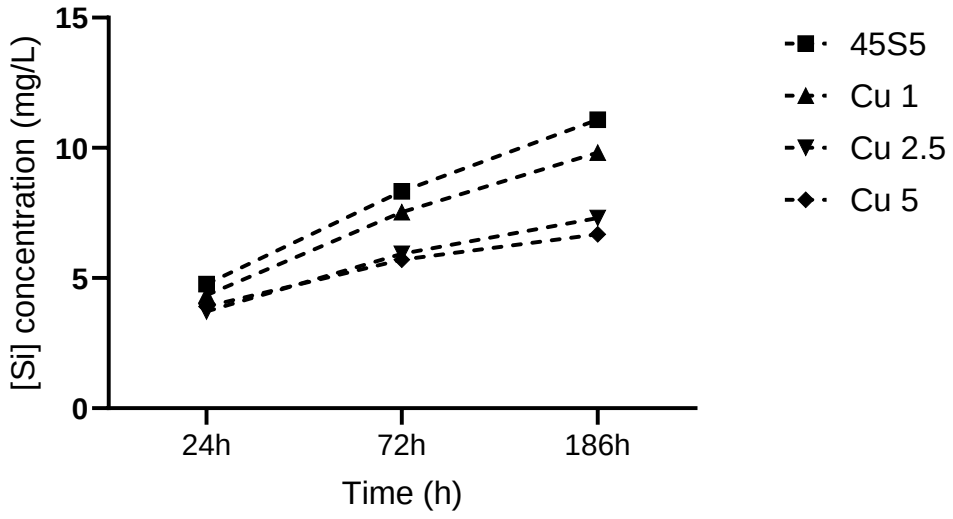

Figure 5-8. Silica [Si] concentration in deionised water measured from series 1 glasses dissolution over time determined using ICP-OES.

Sodium [Na] release

The [Na] release in Figure 5-9 showed continuous releases over the time observed. The Cu 1 and Cu 2.5 reflect the highest releases of Na element among all glasses. The highest in the 24 h time point recorded around 128 mg/L for the Cu1 and Cu 2.5 while the lowest were for the 45S5 at 95 mg/L. The highest recorded was after 186 h for Cu 1 glass around 212 mg/L.

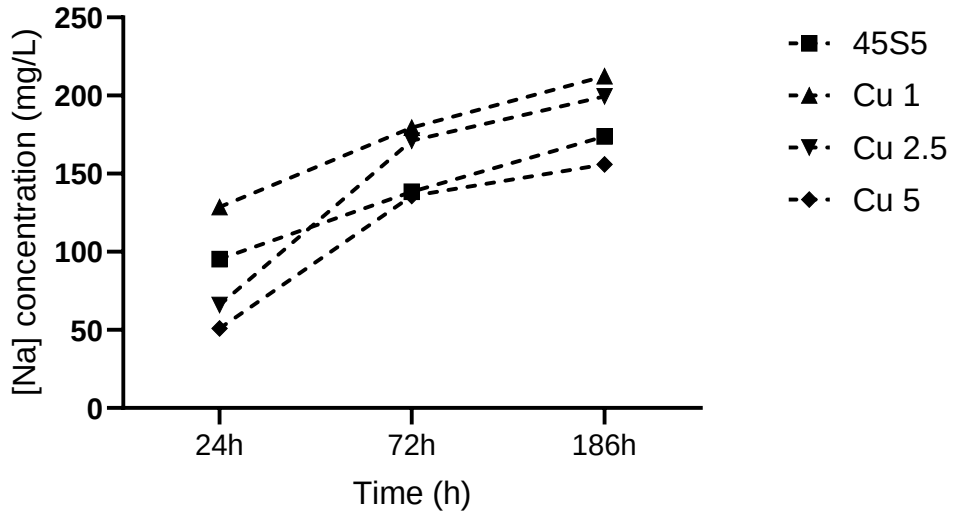

Figure 5-9. Sodium [Na] concentration in deionised water measured from series 1 glasses dissolution over time determined using ICP-OES.

Calcium [Ca] release

The substitution of the Cu with Ca shows the reduction of the Ca element release in Figure 5-10 confirm the substitution. In the 24 h reading the 45S5 glass was the highest around 18 mg/L and the lowest at 12 mg/L for Cu 5 glass. The trend is continued until 186h timepoint.

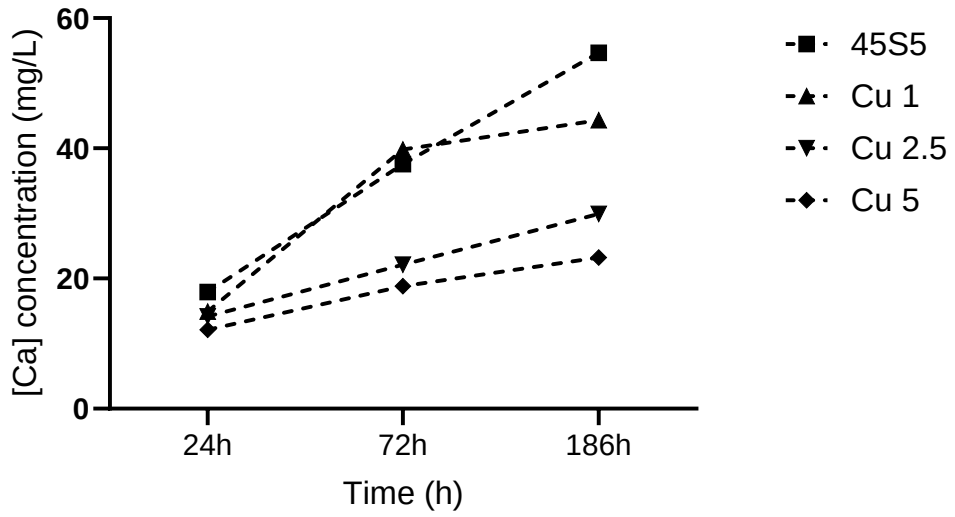

Figure 5-10. Calcium [Ca] concentration in deionised water measured from series 1 glasses dissolution over time determined using ICP-OES.

Phosphorus [P] release

The phosphate element release shown in **Figure 5-11** a trend among all glasses in correlation to the substituted in over 24 h and 72 h is dependent on Cu increases. The Cu 5 shows the highest release at 24 h about 0.8 mg/L with steady release across the time point. All the other glass shows similar result around 0.45 mg/L at the 24 h point. The same trend observed over the 72 h Cu5 highest then Cu 2.5, Cu 1, 45S5, respectively. After the 72 h the Cu 2.5 and 45S5 show an upward trend over 186h with the highest release recoded for Cu 2.5 around 1.28 mg/L. The Cu 5 and Cu 1 glasses shows a steady trend across the study period.

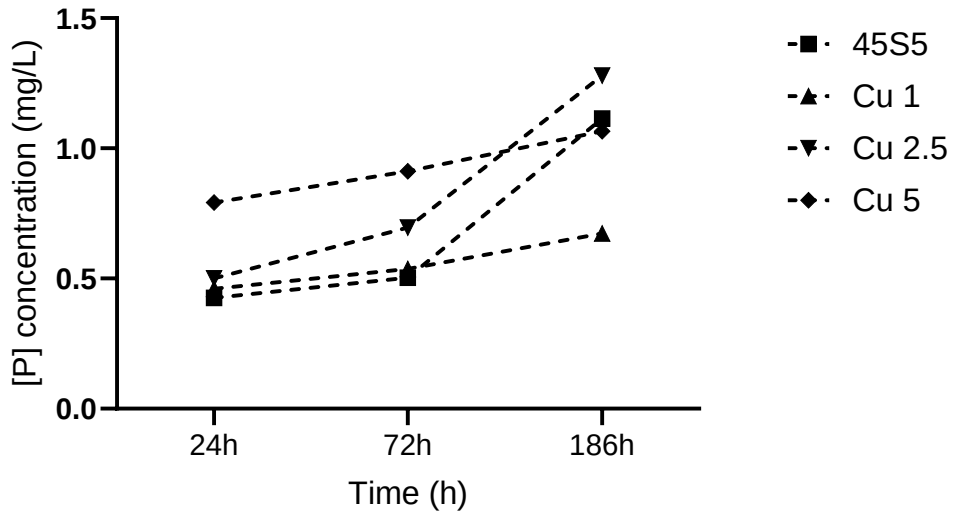

Figure 5-11. Phosphorus [P] concentration in deionised water measured from series 1 glasses dissolution over time determined using ICP-OES.

Copper [Cu] element release

Copper Element release is shown in Figure 5-12 for Cu containing glasses. The release difference among the glasses is following the Cu content. The highest release is associated with the Cu 5 glasses and the lowest for Cu 1. All glasses show steady releases during the study period 186h. The highest [Cu] element release is associated with Cu 5 after 186h at 0.9 mg/L while the lowest release at 186h was around 0.5 mg/L for the Cu 1 glass.

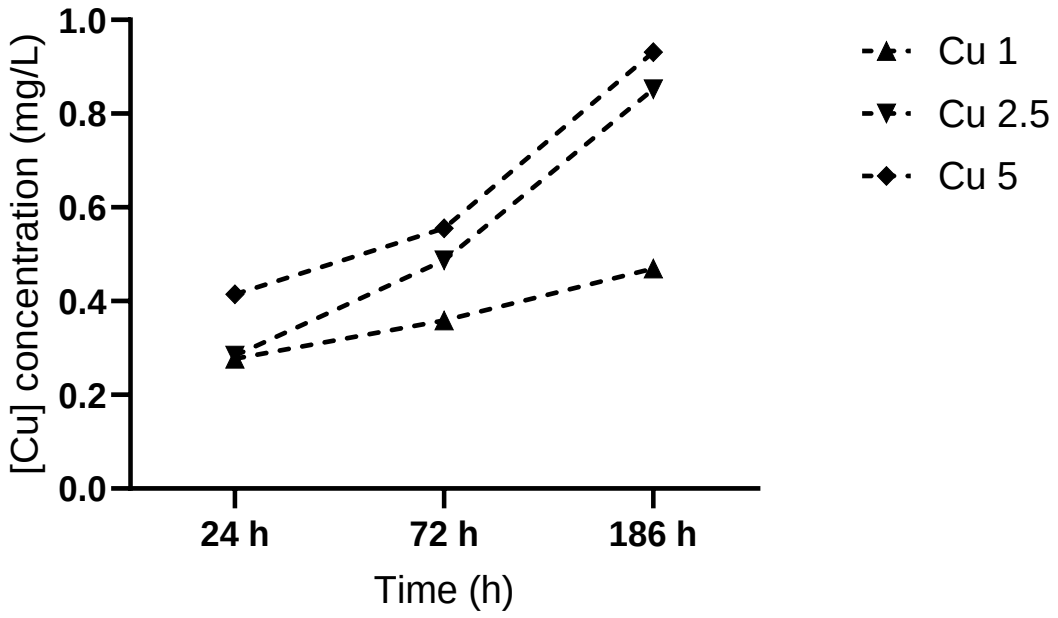

Figure 5-12. Copper [Cu] concentration in deionised water measured from series 1 glasses dissolution over time determined using ICP-OES.

Series 2

The element release was measured using ICP-OES to investigate the effect of increasing Na_2O on the kinetic of the element release over three time point were illustrated from Figure 5-13 to Figure 5-17

Silicon [Si] element release

The silicon element releases illustrated in Figure 5-13 for both 4530 and 305 glasses. The increased Na_2O molar percentage in the 4530 reflect in the high sodium element release across the time point compared to the rest of the glasses. The 305 which contain Cu shows a huge reduction in the Si element release across the time point of the experiment compared to the 4530. The difference in the release is about 83.5 % reduction between the 4530 and 305 after 186 h. This effect of Cu substitution

reducing the Si element release is observed in the series 1 glasses described above Figure 5-8 .

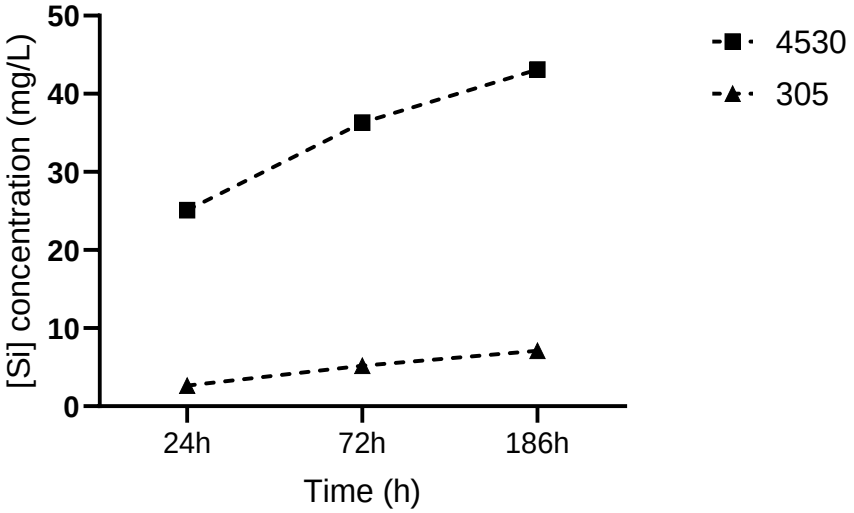

Figure 5-13. Silicon [Si] Concentration in deionised water measured from series 2 glasses dissolution over time determined using ICP-OES.

Sodium [Na] element releases

Figure 5-14 shows the release of Na element. The copper containing 305 glass shows a similar effect on the release of Na element as on the Si, whereby the Na release in the 305 glass is reduced by 67 % compared to the 4530-glass Na release. The Na element release of the 4530 glass is over 1000 mg/L, which is also significantly higher than the four glasses in series 1 Figure 5-9.

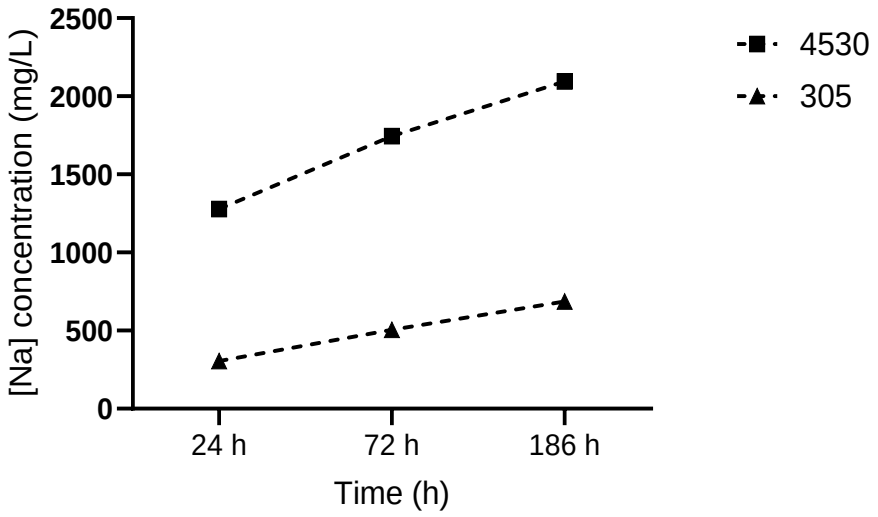

Figure 5-14. Sodium [Na] concentration in deionised water measured from series 2 glasses dissolution over time determined using ICP-OES.

Calcium [Ca] element release

As expected, the release of Ca element is low in the 305 glass and reflects the Ca reduction due to the substitution with Cu. The release trend in 4530 increased from 24 hours to 72 hours and remained on a plateau until 186 hours. The release trend for the 305 glass is constant over the entire period of the experiment Figure 5-15.

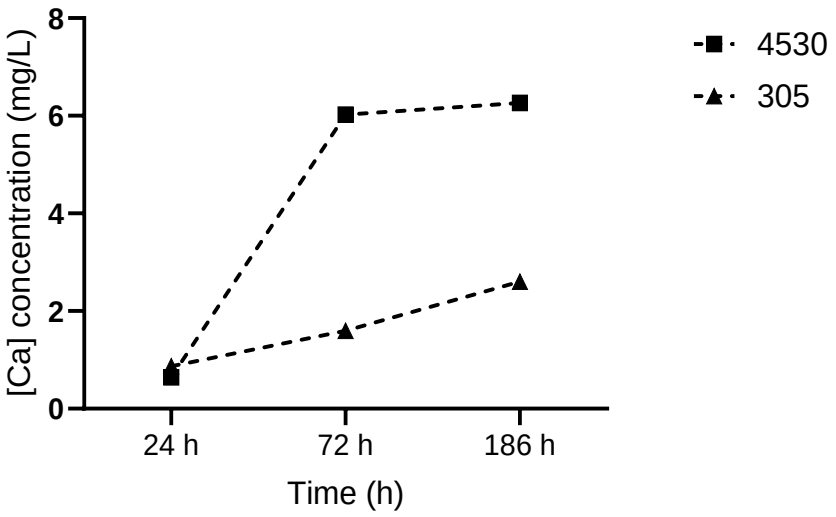

Figure 5-15. Calcium [Ca] Concentration in deionised water measured from series 2 glasses dissolution over time determined using ICP-OES.

Phosphorus [P] element release

The release of P element Figure 5-16 is higher in glass 4530 than in glass 305 and increases after 72 hours. In contrast, glass 305 shows a consistent trend across all time points from 24 hours to 186 hours. The difference between the two glasses in the release of P element is not as great as for the previously mentioned element.

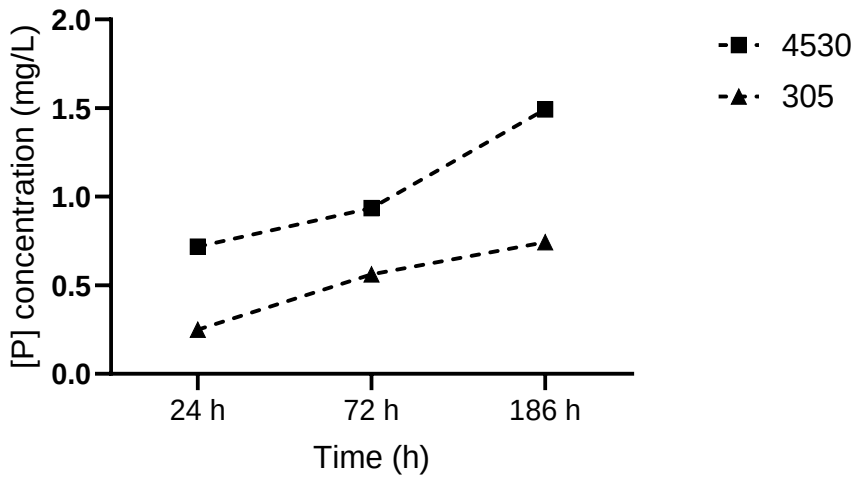

Figure 5-16. Phosphorus [P] Concentration in deionised water measured from series 2 glasses dissolution over time determined using ICP-OES.

Copper [Cu] element release

The release of Cu element from the 305 was the lowest among the 3 previous glasses containing Cu element: Cu 1 glass, Cu 2.5 glass and Cu 5 glass Figure 5-17 It shows an approximately 53 % reduced difference in release compared to the highest Cu element release from the Cu 5 glass after 186 hours. The trend of Cu element release in the 305 showed an increase after 72 hours. This trend is also seen for Cu 2.5 and Cu 5, while Cu 1 shows an almost flat trend of Cu element release.

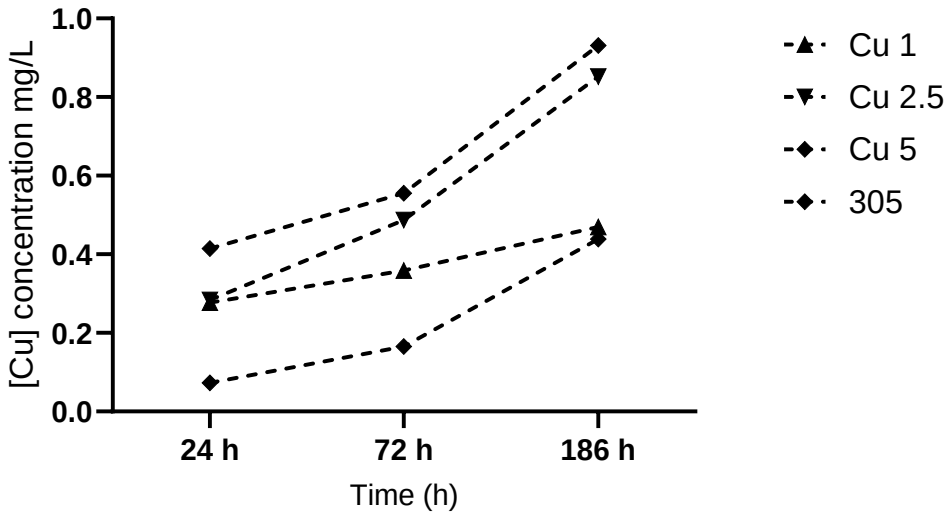

Figure 5-17. Copper [Cu] Concentration in deionised water from series 1 glasses containing Cu (Cu 1, Cu 2.5, and Cu 5) and series 2 glass containing Cu (305) over time determined using ICP-OES.

5.3 PMMA and bioactive glass composite.

The maximum loading wt.% was determined by different loading weights of the glass in the PMMA series of loadings trails ranged from 80 wt.% to 20 wt.%. Four glass loaded composites of 30 wt.% glass PMMA produced: 45S5 PMMA, Cu 1 PMMA, Cu 2.5 PMMA and Cu 5 PMMA Figure 5-18.

Figure 5-18. Image of the composites disc sample of the four different composites of 30 % w/w glass PMMA. From the left, 0 PMMA (control), 45S5 PMMA, Cu 1 PMMA, Cu 2.5 PMMA, and Cu 5 PMMA.

5.3.1 Composite Characterization.

Surface roughness

The surface roughness of the composite materials was evaluated to understand the impact of bioactive glass and copper content on surface morphology. The baseline PMMA exhibited a mean surface roughness of 1.745 µm, with relatively low variability (standard deviation of 0.1996 and a standard error of 0.08149). The addition of bioactive glass (BG-PMMA) increased the mean surface roughness to 2.211 µm, with a wider variability reflected in a standard deviation of 0.6075.

The incorporation of copper into the composite matrix resulted in a progressive reduction in surface roughness. The Cu 1% composite had a mean roughness of 1.873 µm (standard deviation: 0.4285), which further decreased to 1.486 µm for the Cu 2.5% composite (standard deviation: 0.1829). The Cu 5% composite exhibited the lowest

mean surface roughness of 1.266 µm, with moderate variability (standard deviation: 0.2345).

Statistical analysis using one-way ANOVA and Dunnett's multiple comparisons test indicated that only the Cu 5% composite demonstrated a statistically significant reduction in surface roughness compared to PMMA (*adjusted p = 0.0173*). The differences observed for BG-PMMA, Cu 1%, and Cu 2.5% composites were not statistically significant, with adjusted p-values exceeding the threshold of significance ($\alpha = 0.05$) **Table 5-6** and **Figure 5-19**.

These findings highlight the potential of copper incorporation, particularly at the 5% level, to enhance surface smoothness. Such improvements in roughness are critical for reducing bacterial adhesion and improving wear resistance, particularly in dental applications.

Surface hardness

The surface hardness of the composite materials was measured to assess the impact of bioactive glass and copper content on mechanical properties. The results showed that the baseline PMMA exhibited the lowest surface hardness, with a mean value of 33.24 kg/mm² (standard deviation: 8.115, standard error of mean: 2.705).

The addition of bioactive glass (BG-PMMA) increased the mean surface hardness to 44.91 kg/mm² (standard deviation: 18.05, standard error of mean: 6.017), with the widest range of values (66.60 kg/mm²), indicating higher variability.

Further increases were observed in the composites containing copper. The Cu 1% composite had a mean surface hardness of 50.69 kg/mm² (standard deviation: 13.48, standard error of mean: 4.494), while the Cu 2.5% composite achieved the highest

mean value of 52.19 kg/mm² (standard deviation: 13.77, standard error of mean: 4.590). However, a slight decrease was recorded for the Cu 5% composite, which had a mean surface hardness of 49.23 kg/mm² (standard deviation: 18.57, standard error of mean: 6.190).

Statistical analysis using one-way ANOVA and Dunnett's multiple comparisons test revealed that only the Cu 2.5% composite showed a statistically significant improvement in surface hardness compared to PMMA ($p = 0.0345$). The differences observed for other samples (BG-PMMA, Cu 1%, and Cu 5%) were not statistically significant, as indicated by their overlapping error bars and adjusted p-values above the threshold of significance ($\alpha = 0.05$) **Figure 5-20.**

Table 5-6. The average measurement of the roughness of different glass and PMMA composites. The asterisk denotes the significant difference ($p<0.05$) between PMMA, and the Cu 5 composite determined by one-way ANOVA analysis and Tukey's test.

	PMMA	BG composite	Cu1 composite	Cu 2.5 composite	Cu 5 composite
Mean	1.745	2.211	1.873	1.486	1.266*
Std. Deviation	0.1996	0.6075	0.4285	0.1829	0.2345

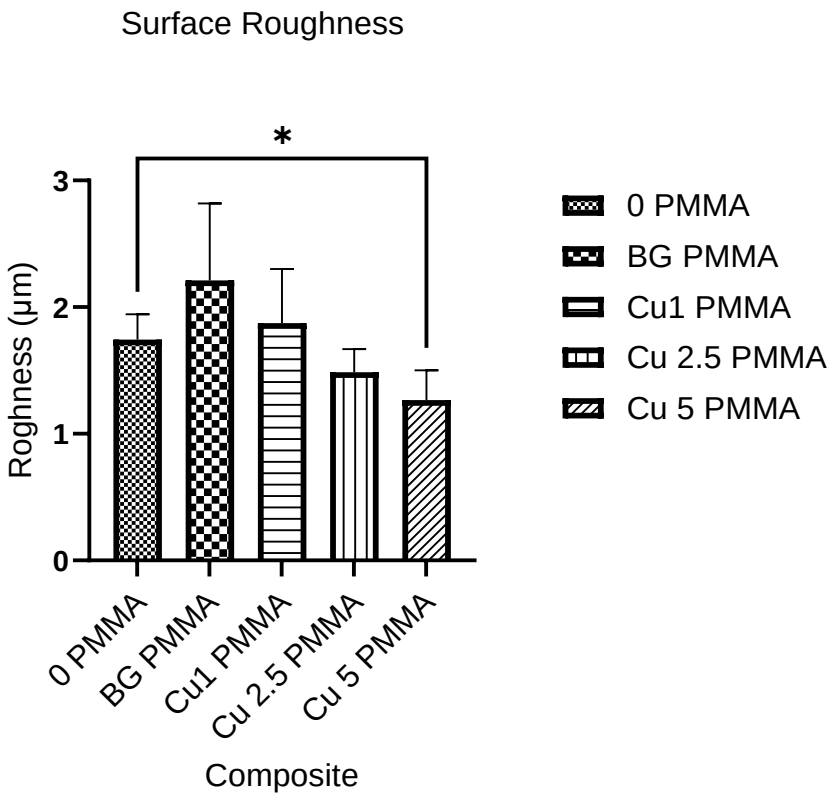

Figure 5-19. Bars chart for the surface roughness of the four composites and the PMMA control. The bars compare the surface hardness of the composite in comparison to the PMMA control. There is a slight decrease in surface roughness among the study group. significant difference between 0 PMMA and Cu 5 PMMA. Each bar represents an average of three reading on three sample (n = 3).

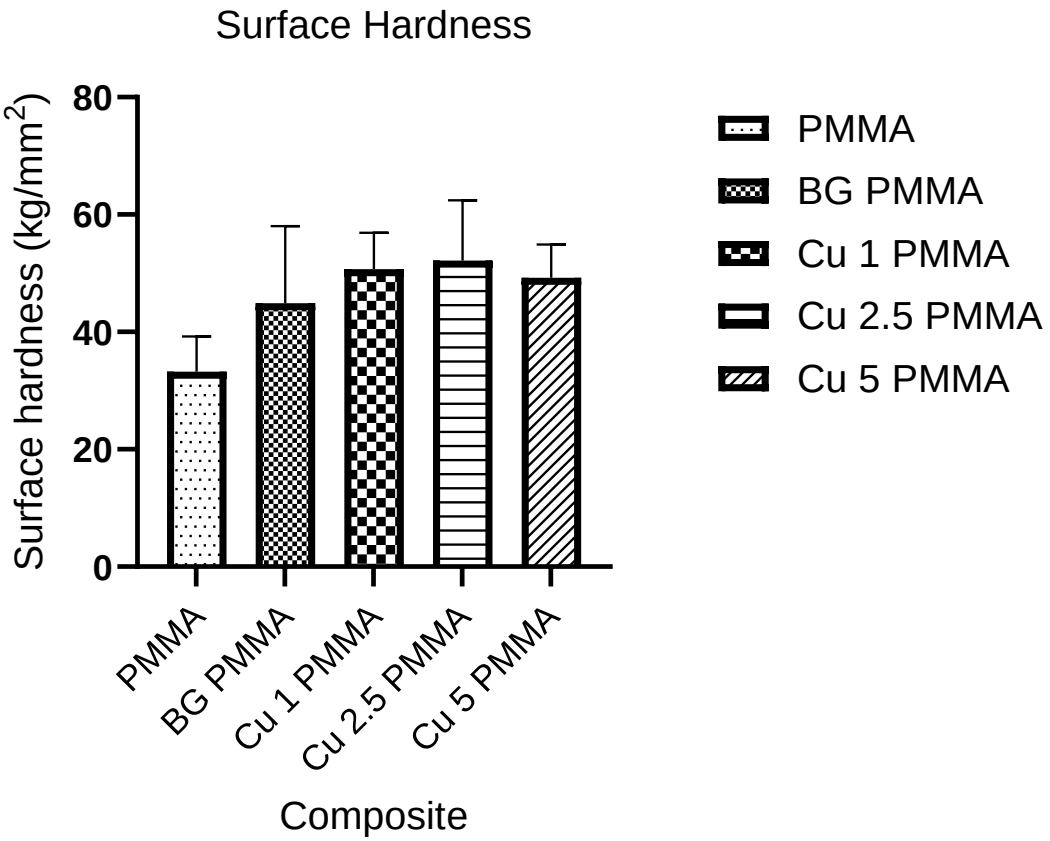

Figure 5-20. Bars chart for the surface hardness of the four composites and the PMMA control. The bars compare the surface hardness of the composite in comparison to the PMMA control. There is a slight increase in surface hardness but no significant difference between or among the control and the study group. Each bar represents an average of three reading on three sample (n = 3).

Composite elemental release

An element release study was conducted to evaluate the release of copper (Cu), calcium (Ca), and sodium (Na) from the composite of 30 % wt. Cu 5 / PMMA over a 7-day period using ICP-OES, under conditions similar to the glass-only study, in deionized water. The results indicated negligible copper release, with an average value of 0.0097 mg/L. In contrast, calcium and sodium showed significantly higher release values of 10.8 mg/L and 32.47 mg/L, respectively. These findings suggest that the incorporation of copper into the composite does not result in substantial leaching under the conditions tested.

Table 5-7. Elements concentration (mg/L) in deionised water measured from glass / PMMA composite over seven days determined using ICP-OES.

Sample / element concentration (mg /L)	[Ca]	[Na]	[Cu]
Cu 5 / PMMA discs	10.854	32.473	0.0097

5.4 Antimicrobial activity.

Series 1

The agar disc diffusion test was performed over Actinomyces oris (clinical isolate) and Actinomyces MF1 (laboratory strain) using 12 × 2 mm pressed powder glass discs to investigate the glasses' antimicrobial activity over 24 hours of incubation.

The copper-substituted bioglasses showed an improvement in antibacterial activity against both bacterial strains. The mean inhibition zones are presented in

Table 5-8 and **Figure 5-21** and **Figure 5-22** for (clinical isolate) and (MF1 strain). The data demonstrate that increasing copper substitution generally enhances the antimicrobial activity.

For the A. oris clinical isolate, the glass with 5 mol% Cu exhibited the highest inhibition zone (30.3 mm), significantly larger than both the parent 45S5 glass (25.1 mm) and the 2.5 mol% Cu glass (24.6 mm) ($p<0.05$, one-way ANOVA).

For the *A. oris* MF1 strain, the 2.5 mol% Cu glass displayed the highest inhibition zone (28.5 mm), which was significantly larger than the inhibition zone for the 45S5 parent glass (23.6 mm) ($p<0.05$, one-way ANOVA). No significant differences were observed between other compositions.

These data suggest that the copper-substituted glasses have the potential for local antimicrobial effects, likely due to the release of antimicrobial ions (Cu^{2+}), particularly in glasses with higher copper content.

Table 5-8 Mean inhibition zone from agar disc diffusion in (mm).

Glass\ Bacterial	*A oris* (clinical isolate)	*A oris* MF1 (lab strain)
45S5	25.1	23.6
Cu 1	27.4	27.3
Cu 2.5	24.6	28.5
Cu 5	30.3	27.7

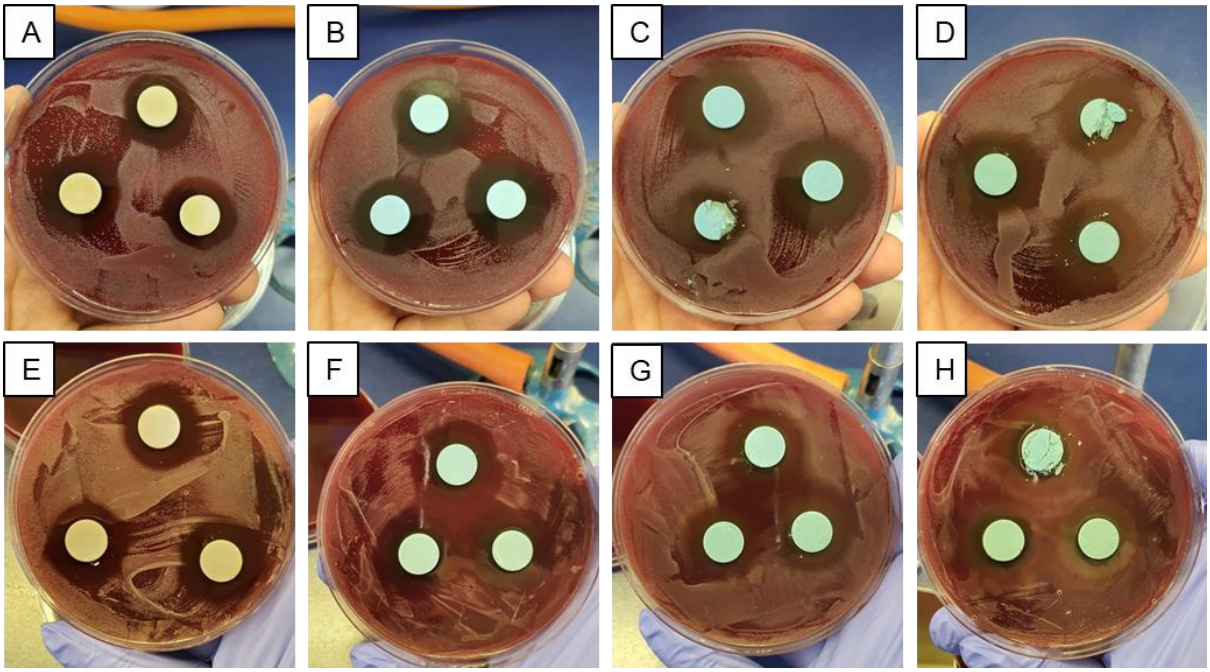

Figure 5-21. Pictures of the Agar disc diffusion assay of two different *Actinomyces oris* strain on fastidious anaerobe blood agar blates for series 1 glasses. A-D *Actinomyces* MF1 laboratory strain, E-H *Actinomyces oris* clinical Isolate. A, E 45S5, B, F Cu 1, C, G Cu 2.5, D, H Cu 5. The inhibition zone appears as a clear halo around the bioactive glass samples.

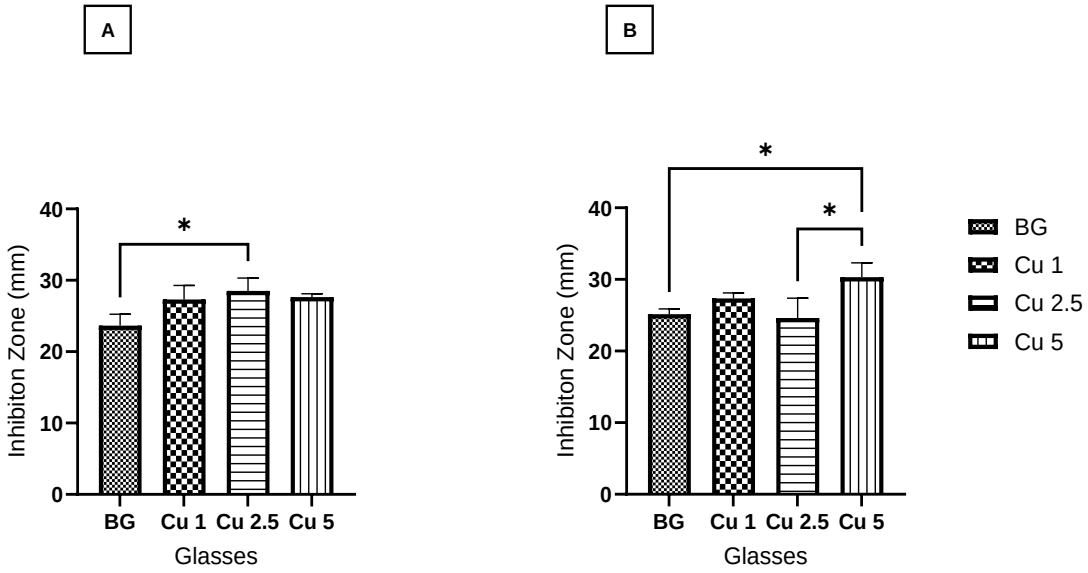

Figure 5-22. Inhibition of two strains of *Actinomyces oris* by Cu-substituted bioactive glasses. The data shown is the inhibition zones around glass samples using (A) *Actinomyces oris MF1* and (B) clinical isolate *Actinomyces oris* from an MRONJ patient. The data shown is an average of three sample (n = 3) for each bioactive glass and the error bar is standard deviation. All bioactive glasses showed an inhibition zone greater than 20 mm for both strains. The asterisks denote the statistically significant (P value <0.05) obtained by one way ANOVA test and Tukey's multi comparison test.

Series 2

The antimicrobial activity of the agar disc diffusion test of the high sodium glasses 4530 and 305 shows a larger zone of inhibition against the laboratory strain *Actinomyces Oris* MF1 compared to the glasses 45S5 and Cu 5. The zone of inhibition increases by 82.5 % for 4530 compared to 45S5, which is a significant difference at $P < 0.05$ as determined by a one-way ANOVA test. The average zone of inhibition for 45S5 is about 24 mm and for 4530 about 44.5 mm. For the copper-containing glasses, the zone of inhibition is increased by 65% for 305 glasses compared to Cu 5, with the average zone of inhibition in mm being 51.86 and 31.44 respectively.

Between the high Na glasses, 4530 and 305 there were a significant difference in the zone of the inhibition in favour to 305-glass. The average increase is about 16.5 %.

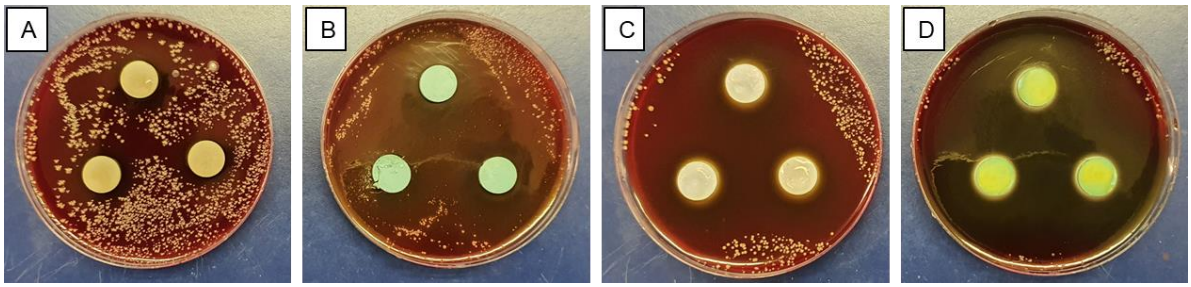

Figure 5-23. Pictures of the Agar disc diffusion assay of *Actinomyces Oris* MF1 laboratory strain on fastidious anaerobe blood agar blates against series 2 glasses: A 45S5. B Cu 5, C 4530, and D 305

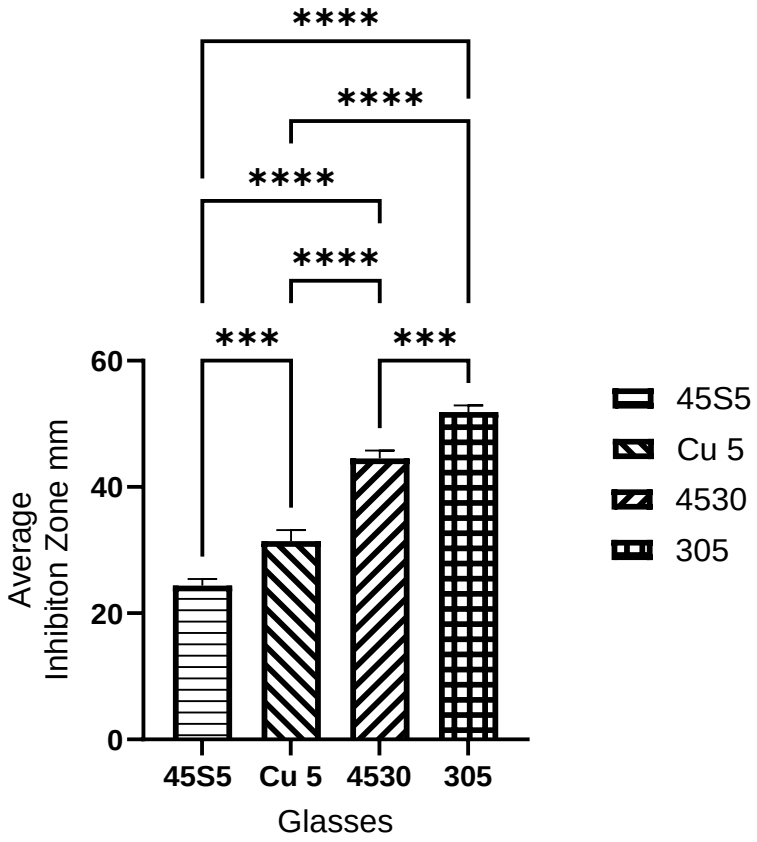

Figure 5-24. Antibacterial activity bars chart comparing antimicrobial activity between high Na_2O (4530), and Cu containing glass (305) and the 45S5 bioglass and Cu 5 glasses against *Actinomyces Oris* MF, by agar disc diffusion test measuring the inhibition zone in mm. The bars chart shows an upward trend of inhibition as the Cu and Na increased. The asterisk denotes the statistically significant (P value <0.05) obtained by one-way ANOVA test and Tukey's multi-comparison test. Error bars for standard deviation**.**

5.5 In vitro biocompatibility of composite.

The cell viability direct cells contact for 48h using Prestoblue dye assay with two cell lines, MG63 cell line has fibroblast morphology from cancer patient with osteosarcoma, and L929 mouse fibroblast cell. There were used to examine the cytotoxicity of the four 30% w/w bioactive glasses PMMA composite and PMMA disc as control. All the four composites showed decline in cell viability in both cell lines. The result shows a decrease in cell viability with the increase of the Cu ions concentration in the bioactive glasses, compared with the PMMA control group.

In the glasses composite groups, the BG composite is the most viable composite with the L929 cell with steady decrease among the glasses group with the increase of the Cu ions in the glass composition. The Cu 1 composite recorded the highest viability of the MG63 cells. Noticeably the Cu 5 glass shows almost no cell viability in both cells. The PMMA group showed the most viability in both cells.

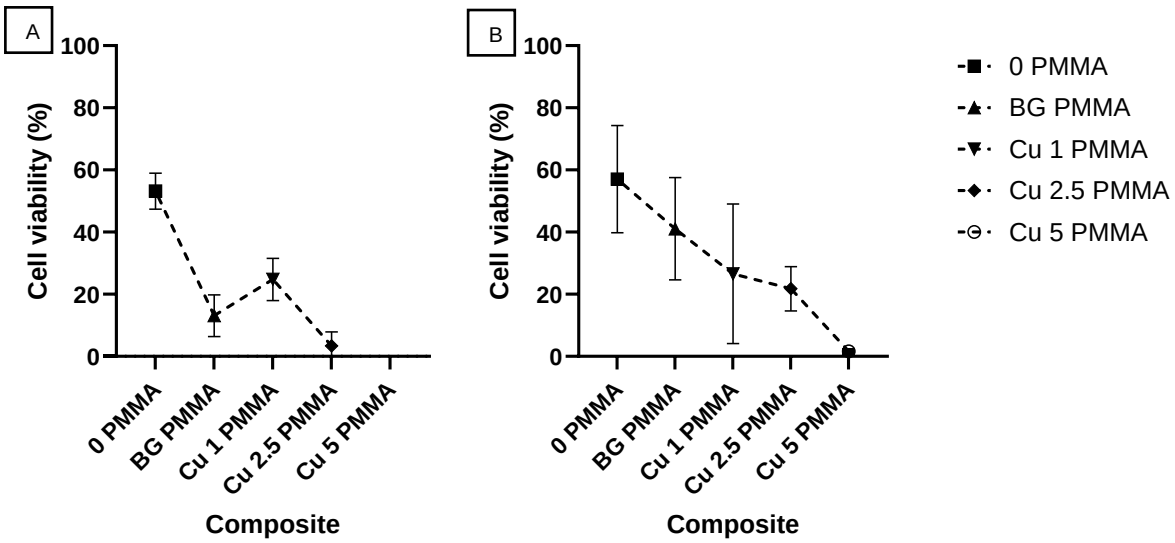

Figure 5-25. Cell viability percentage Prestoblue® assay of 48 - hours period. The lines show the cell viability percentage between the four bioactive glasses PMMA composite 30% w/w and the control 0 PMMA with two cell lines (A) MG63 and (B) L929. The lines downward trends demonstrate a dose dependent between the Cu content and cell viability. The asterisk denotes the statistically significant (P value <0.05) obtained by one-way ANOVA test and Tukey's multi comparison test. Error bars are of the standard deviation.

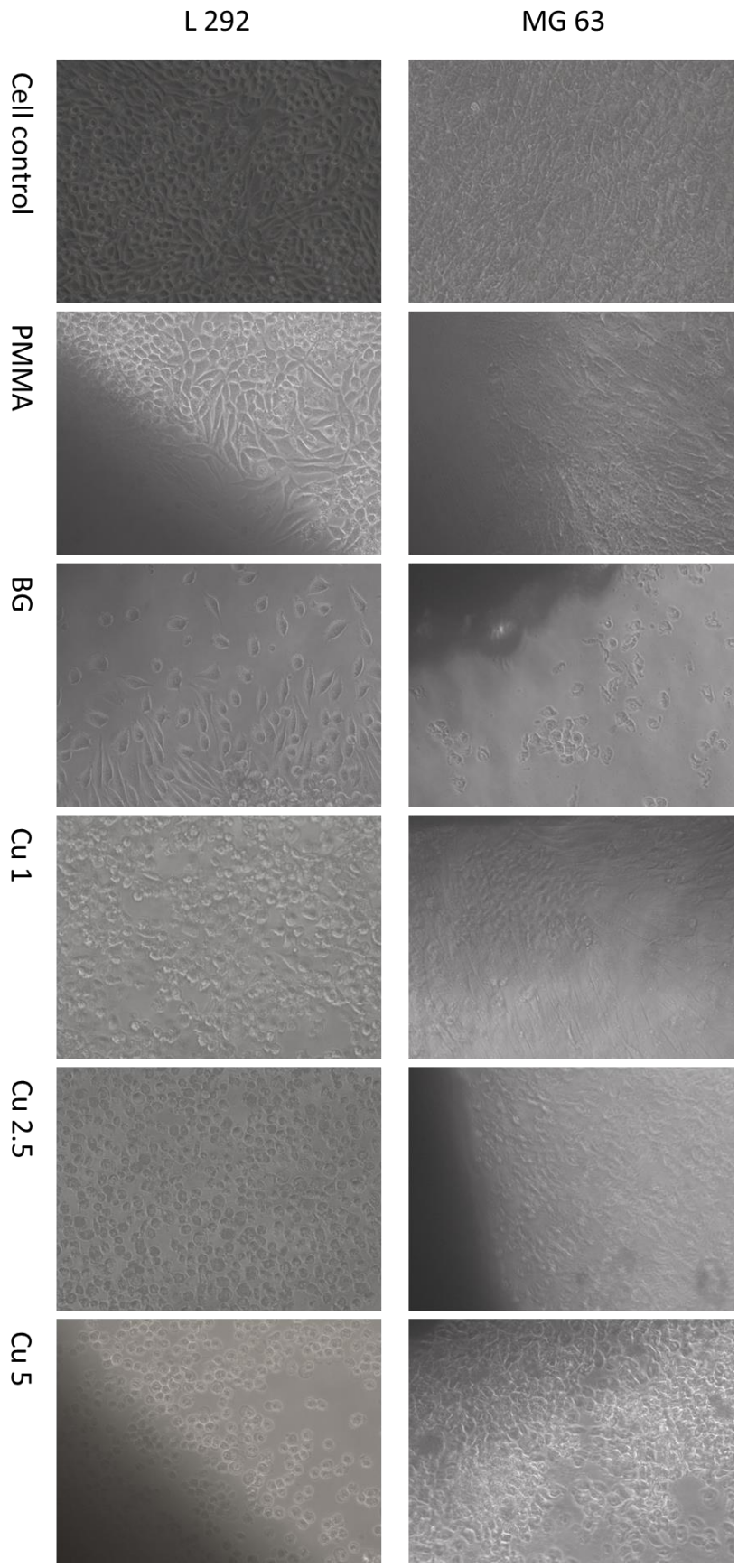

Figure 5-26. Images of cells after 48h of cell contact assy. images taken next to the disc (black shadow in the images).

6 Discussion

6.1 Glasses composition and characterization:

Two series of glasses in this project were produced based on the Hench Bioglass formula through the melt-quench route using alumina crucible. First series consist of four partially substitute the calcium oxide (CaO) with copper oxide (CuO) in 0, 1, 2.5, and 5 mol %. Second series have two glasses with soda (Na_2O) increased to 30 mol% substituted for CaO and a new 5 mol % CuO and 30 mol % Na_2O for CaO. Bioactive glass substitution is a process used to enhance the properties of the glasses, and the biological interference with the body. From designing and manufacturing point of view of the glasses, most recent studies are either dopped or substitute the glass modifier usually CaO with alkaline oxide or transition metal oxide for example the MgO and ZnO respectively to the glass [80] [82] [68], see section 2.5.4. The melt-quench rout selected over the sol-gel to avoid any residual might be left from the sol-gel method also the original Hench's Bioglass was firstly and commonly produced through the melt route.

X-ray diffraction (XRD)

All the glasses series 1 and series 2 produced in this study are characterised for their composition and structure. To exhibit the structure of the glass X-ray diffraction (XRD) used. XRD is non-destructive structural analysis commonly used with glass and ceramics to study the internal structure and determine the phase of the crystallisation. The XRD graph shows the glass has an amorphous structure for both glass series in the **Error! Reference source not found.** and Figure 5-3 **Error! Reference source not found.**obtained by the PANalytical Aeris XRD. This glassy structure graph is

characterised by one hump which represents the amorphous state of the materials. That proves the substitution for soda for copper oxide through the melt quench route did not affect the glassy structures. It is important for the bioactive glass not to crystallized because the crystal structure is harder to dissolve then, less or slow bioactivity of the glass.

Thermal analysis

The DSC thermal analysis Figure 5-4 and Figure 5-5 was also performed to study the effect of substitution of copper by investigating thermal behaviour of the substitution. Two temperature points were observed, the glass transition temperature (Tg) and glass crystallisation temperature (Tc). The result shows reduction in both temperatures compared to the parent glass. This reduction could be explained by the introduction of copper through the concept of glass modifier which might suggest the copper is disrupting the structure of the glass that leads to less energy needed to reach the Tg. lower Tg indicates more soluble glass which is important to this type of application in this study to ensure rapid delivery of the antimicrobial agent (copper). The Tg for the 45S5 bioactive glass produced in this study (556 degree C) which is slightly higher than generally reported by leading groups (around 540 degrees C) [165].

Moreover, The Tg has reduced with all copper-substituted glasses (including series 2 glass high sodium) in comparison to the parent glass 45S5, suggesting that alumina contamination from using alumina crucible was not excessively influencing this physical property compared to copper substitution, where Al_2O_3 would typically increase Tg for the reasons outlined in the literature review. There were an indentation observed in the DSC graph appeared only in the copper substituted glass in both

series Figure 5-4 and Figure 5-5 might suggest that there is another glass phase which might explain the lack of the Cu element release the ICP-OES elements release study will be discussed later.

Series 2

To investigate the effects on the solubility of the glass, a new glass formula (series 2) was prepared with a 5.7 mol% increase in Na_2O mol%, from 24.3 % to 30 % (mol%) as a substitute for CaO to investigate whether the increase in Na improves the release of Cu ions, Wallace *et al* 1999 Na_2O is a crucial for the solubility and bioactivity of bioactive glasses as it is more disruptive for the glass network and its show clearly by reducing the glass transition temperature greatly shown in **Figure 5-5** in this project [87]. Remarkably, the substitution of CuO in the series 2 glass also influences reducing the release of Na ions and Si ions illustrated in section **5.2.6**. This mysterious effect of Cu on the restriction the release of the other ions could indicate the formation of insoluble species probably copper phosphate in the glass lattice that make it poorly soluble. Also, because of using alumina crucible, aluminium element release was determined using ICP-OES, where the levels were consistently low ranging from 0.3 to 1.1 ppm (not shown). Overall, the evidence was that all glasses produced using alumina crucibles were contaminated with Al_2O_3 where some physical properties may be influenced, but not at levels associated with a deleterious effect on bioactivity or antimicrobial properties described in section 2.5.4 in melt quench using alumina crucible [93].

X-ray fluorescence analysis

An XRF analysis was carried out for the elemental composition of the glasses showed in **Table 5-1**, although the study was limited. The analysis showed that the elements in the glass are consistent with the theoretical formula. The XRF data shows an increase in copper and a decrease in calcium, which is due to substitution. Due to the limitation of the instrument used, no sodium was detected. The lightest element that could be detected was magnesium. The result shows that the XRF Cu content is 4-5 times higher than the theoretical formula content. This could be related to the limitations of the instrument, as the data shown **Table 5-1** are normalised and the sodium element is missing from the analysis. Hence, alternative investigation used to confirm the elemental composition.

SEM-EDS

The SEM-EDS in section 4.2.4 is a surface elemental analysis used to confirm the elemental composition in these glasses. The increase in copper ions wt.% and the decrease in the calcium ions is an indication of the substitution. In addition to the presence of the other ions Si, Na, and P confirm the composition of the glasses post melt process. The XRF data also showed a trace of Al_2O_3 which contribute to the use of alumina crucible in glass making. The literature review suggested that alumina contamination from crucibles used in the melt fabrication of bioactive glasses had the potential to affect glass properties including bioactivity (see section 2.5.4). XRF post-melt analysis therefore included quantification of Al_2O_3, where the results showed contamination in the range of 0.5 to 1.4 wt.% (see section 0). This is below the levels associated with a reduction in bioactivity (1.5 wt.%), although it is plausible that even

these low levels may influence bioactive glass properties as outlined in the literature review. Several studies report on this, including Melchers *et al* who confirmed that this level of alumina contamination had no negative effects on bioactive glasses in a mesoporous system [166].

FTIR

The FTIR data shown in Figure 5-7 showed no significant difference between the Cu glasses and the parent glass. There were two major bonds bands that appeared in the graph for all glasses. The first is a representation of the Si-O- 1NBO around 1020-1050 cm-1 (Q3) and 920-960 cm-1 (Q2) represent the Si-O- 2NBO. The presence of the Q2 and Q3 species detected by FTIR as vibration band in the glass is an indication of its bioactivity and the connectivity of the glass. This similarity of the bonds could indicate that the substitution did not affect the Q structure in the tetrahedral system of the silicate. The Qn structure of the silicate glass is crucial in the bioactive glass such as bioglass because the Qn (n) indicate the number of bridging oxygen (BOs) in the bioactive glass since the since the non-bridging oxygen bond Si-NBOs are favourable to the glass dissolution and ions exchanges [167].

6.2 Inductively coupled plasma optical emission spectroscopy ICP-OES.

The ICP-OES element release study was conducted using deionized water to eliminate potential interference from background elements that could arise in simulated body fluid see (**section2.5.3**). This approach ensured accurate quantification of cumulative ion concentrations over the testing period. However, while the use of deionized water allows for a controlled study of ion release, it does not replicate biologically relevant environments. Simulated body fluids (SBF) or acidic

bacterial suspensions could provide a more realistic representation of clinical conditions, as these solutions simulate interactions with physiological ions and pH fluctuations. Future studies using such media would help determine whether copper's release behaviour differs in vivo, where pH and ion exchange could influence ion mobility and bioactivity.

The results demonstrated that copper substitution significantly influences the release behaviour of key ions from the bioactive glasses. Calcium (Ca) and silicon (Si) release decreased progressively with increasing copper substitution. The parent 45S5 glass released a cumulative calcium concentration of 54.66 mg/L at 186 hours, while the 5% Cu glass released significantly less, at 23.23 mg/L. Similarly, silicon release from the 45S5 glass reached 11.08 mg/L, while the 5% Cu glass released only 6.68 mg/L. These reductions confirm that calcium was successfully substituted by copper in the glass matrix, leading to a more stable silica network with reduced solubility. This finding aligns with earlier studies on nano-Cu mesoporous bioactive glass [168] , which also observed a reduction in silicon release with copper addition.

Interestingly, sodium (Na) release showed a more complex trend. The 45S5 glass exhibited a cumulative release of 173.82 mg/L at 186 hours, while the 1% Cu glass released 212.48 mg/L, suggesting initial network disruption due to copper incorporation. However, at higher copper substitution levels, such as 5% Cu, sodium release decreased to 155.91 mg/L, indicating a stabilization of the glass network with increased copper content. This stabilization is further supported by the absence of crystallization in the XRD analysis, which confirmed that no crystalline phases formed in the glasses.

The controlled release of copper (Cu) ions was also observed, with the 5% Cu glass releasing 0.90 mg/L at 186 hours. This sustained release of copper highlights its potential for antimicrobial functionality. Phosphorus (P) release showed variability, with the 2.5% Cu glass releasing the highest concentration (1.28 mg/L), possibly reflecting interactions between phosphate groups and the modified glass network.

These results challenge the notion that the addition of modifier cations such as Cu would disrupt the glass network and increase solubility. Instead, copper substitution appears to enhance the stability of the glass matrix, as evidenced by the reduced release of structural ions like sodium and silicon. The lack of crystallization further supports the conclusion that the glasses remain in an amorphous state, even with copper substitution. While the formation of a secondary glass phase or other species cannot be entirely ruled out, their detection may be difficult given the relatively low copper content in the compositions.

6.3 Antibacterial activity of the glasses

Two species of bacteria were selected for the antimicrobial study: *Actinomyces oris* (Gram-positive), believed to be a primary bacterial species associated with medication-related osteonecrosis of the jaw (MRONJ), and *Prevotella* (Gram-negative), based on their prevalence in MRONJ-related bacterial environments as reported in the literature (see section 2.3.1). The antimicrobial activity of the bioactive glasses was tested using the agar disc diffusion method, which is commonly employed to assess the efficacy of antimicrobial materials [169] [170]. Agar disc diffusion is widely used due to its simplicity and cost-effectiveness, allowing rapid assessment of antimicrobial activity by measuring inhibition zones. However, it lacks the ability to determine minimum inhibitory concentration (MIC) values, which are essential for

understanding the potency of the antimicrobial agent [171]. Additionally, the method can be subjective and may not be suitable for slow-growing bacteria [172]. In contrast, Serial dilution methods, including broth and agar dilution techniques, provide quantitative MIC data and are more precise for assessing bacterial susceptibility [173, 174]. These methods are labour-intensive but allow evaluation of a broader concentration range, enabling a better understanding of dose-response relationships [172]. The choice of method depends on study objectives, with disc diffusion suitable for preliminary screening and serial dilution preferred for detailed analysis [171, 175]. The characteristics of the bioactive glass powder, including solubility and interaction with the agar medium, may influence the choice of method. For instance, its diffusion behaviour can affect the results, highlighting the need to carefully match the method to the material properties [99, 176]. While this study used agar disc diffusion due to its practicality, further investigations using serial dilution could provide complementary insights into the antimicrobial efficacy of the glasses.

In this study, the potential of bioactive glass and its copper-substituted variants was evaluated against *A. oris* laboratory strain MF1 and a clinical isolate from MRONJ patients. The results showed that all glasses exhibited antimicrobial activity.

For series 1, the glass with 5 mol% Cu displayed the largest inhibition zone against the clinical isolate *A oris,* with an average size of 30.31 mm, significantly exceeding both the baseline 45S5 composition (25.15 mm) and the 2.5 mol% Cu glass (24.62 mm) ($p<0.05$, one-way ANOVA). This represents an improvement of approximately 20 % compared to 45S5. Similarly, for the MF1 strain, the 2.5 mol% Cu glass exhibited the highest antimicrobial activity with an average inhibition zone of 28.50 mm, significantly larger than that of the 45S5 glass ($p<0.05$, one-way ANOVA). This

corresponds to an increase of approximately 20 % compared to 45S5, while no significant differences were observed between other glasses **Figure 5-22**.

The mean inhibition zones observed in this study exceed 5 mm in several cases (e.g., 5 mol% Cu against the clinical isolate), which are notably larger than those reported in previous studies on antimicrobial biomaterials [177] [53] [170]. These findings highlight the effectiveness of the agar diffusion method for evaluating the antimicrobial properties of bioactive glasses. Furthermore, the addition of copper as an antimicrobial agent appears to enhance bacterial inhibition, particularly in MRONJ-related bacterial environments.

The antimicrobial activity of 45S5 glass has been well-documented, primarily attributed to the release of sodium ions upon dissolution. Sodium ions raise the pH of the surrounding environment [99], creating oxidative stress conditions unfavourable for bacterial growth. However, copper incorporation introduces additional antimicrobial properties, as copper ions can disrupt bacterial cell walls and inhibit metabolic processes [51] [37]. Notably, ion release studies conducted in deionized water revealed negligible copper ion release from the glasses, emphasizing the critical role of environmental factors.

The high-sodium glasses (Series 2) demonstrated a marked improvement in antimicrobial activity compared to the regular glasses (Series 1). The high-sodium glass 4530 exhibited an 82.5% larger inhibition zone against the laboratory strain MF1 than the parent glass 45S5, with average inhibition zones of 44.5 mm and 24 mm, respectively. Similarly, the high-sodium copper glass 305 outperformed the 5 mol%

Cu glass (Cu 5), with a 65% increase in inhibition zone size, averaging 51.86 mm compared to 31.44 mm.

Literature indicates that acidic conditions, such as those found in bacterial environments, can enhance the release of sodium and copper ions from the glass surface. This pH-dependent ion release likely amplifies the antimicrobial activity observed in both Series 1 and Series 2 glasses, with the increased sodium content in Series 2 further promoting ion release and enhancing bacterial inhibition [88]. The observed lack of copper release in deionized water highlights the importance of pH in activating ion release. Acidic bacterial environments likely promote the release of transition metal ions, such as Cu^{2+}, which are critical for the antimicrobial performance of these glasses. This is supported by the superior performance of the high-sodium glasses, which leverage both their increased sodium content and the acidic bacterial milieu to achieve enhanced antimicrobial efficacy. These findings underscore the importance of bioactive glass composition and the target environment when designing antimicrobial materials. Further studies are needed to quantify ion release dynamics in acidic conditions and confirm their contribution to the observed antimicrobial efficacy.

6.4 Composite characterisation

Surface hardness

The surface hardness of the composite materials demonstrated an overall increasing trend with the addition of bioactive glass and copper, suggesting enhanced mechanical performance. The baseline PMMA exhibited the lowest mean surface hardness, while the inclusion of bioactive glass (BG-PMMA) resulted in a noticeable, though not statistically significant, increase. Further improvement was observed with

the incorporation of copper, where the Cu 2.5% composite achieved the highest mean surface hardness. Statistical analysis using one-way ANOVA and Dunnett's multiple comparisons test indicated that this improvement was significant compared to PMMA ($p = 0.0345$).

However, the Cu 5% composite showed a slight decrease in surface hardness compared to the 2.5% composite, and this reduction was not statistically significant. This plateau or decline in hardness at higher copper content could be attributed to microstructural changes, such as clustering or uneven distribution of copper particles, which may offset the benefits of copper inclusion.

It is important to note that these measurements were conducted on unpolished, as-prepared samples. Surface irregularities inherent to the as-prepared state may have influenced the hardness values, introduced variability and potentially underestimated the material's true hardness. In comparison, studies in the literature often use polished samples, which yield more uniform and consistent hardness values. As such, direct comparisons to the literature must be approached with caution, and future studies should consider testing both polished and unpolished samples to better contextualize these findings.

The observed trends highlight the potential of the Cu 2.5% composite as an optimal formulation for enhancing the mechanical performance of denture base materials. Improved surface hardness is critical for wear resistance and durability, making this composite particularly suited for dental applications.

Surface roughness

The surface roughness of the composite materials revealed contrasting trends compared to hardness. The baseline PMMA exhibited a moderate mean roughness, which increased significantly with the addition of bioactive glass (BG-PMMA). This increase in roughness may be due to the introduction of inorganic particles within the polymer matrix, leading to a less uniform surface.

In contrast, the incorporation of copper into the composite progressively reduced surface roughness, with the Cu 5% composite achieving the smoothest surface. Statistical analysis confirmed that this reduction in roughness for the Cu 5% composite was statistically significant compared to PMMA ($p = 0.0173$), while the changes for other composites (Cu 1% and Cu 2.5%) were not significant. The smoother surface observed at 5% copper content may result from improved particle dispersion or matrix densification, minimizing surface irregularities.

However, these results must be interpreted because the samples were tested in their as-prepared state without polishing. Unpolished surfaces are expected to exhibit higher roughness values compared to polished samples, as residual irregularities from the fabrication process remain. This distinction could explain differences between the current results and smoother roughness values reported in the literature. While the trends observed here are meaningful, future studies should include polished samples to provide a more accurate basis for comparison and better assess the material's true surface morphology.

These findings underscore the importance of surface smoothness in dental applications, where reduced roughness can lower bacterial adhesion and enhance

patient comfort. The results suggest that the Cu 5% composite may provide a dual benefit of improved biocompatibility and functionality, even in its as-prepared state.

6.5 Composite Cell viability study

Four glass PMMA composite discs and PMMA discs as control were tested for cell viability on two types of cells. The result shows decrease in cell viability with the increase in CuO in the glass composition. The composite with the Cu 5 shows no sign of cell viability while the 45S5 has shown cell viability see result 5.5. As the concentration of the Cu in the glass increased the percentage of the cell viability decrees. This suggest that Cu is toxic to these cells at higher copper concentration 5 mole %. In MG 63 there were significant deference between the 0 PMMA and all the glass group. The only significant differences among the glass group observed only between Cu 1 PMMA and Cu 2.5 PMMA, there were no cell survival with Cu 5 PMMA. In the L929 the significant between the 0 PMMA Cu 5 composite only, and among the glass there were significant differences between BG composite and 5 Cu PMMA and 0 PMMA and 5 Cu PMMA.

In cell culture the pH value of the culture medium is crucial for the viability of the cells. It is important that the pH is controlled during cell culture. The preferred pH is between 7.2 and 7.4 and any deviation from this could affect cell viability and cause cell death [178]. The metabolic production of the cell is acidic, which can be checked by eye when the phenol red dye in the medium changes the colour of the medium [179].

In this project the decrease in the percentage of cell viability with increase of Cu in the glass see result 5.5, could indicate increased sodium release, as the glass is presumably less stable when substituted with modifier ions such as Cu++. Although

this statement is not consistent with the element release study conducted in this project, and the element releases might be obstructed by the PMMA we could conclude that the DMEM medium and the presence of the cells may have altered the environmental conditions, e.g., pH, which could also promote the release of Cu and Na ions. This could indicate a synergistic effect between the release of Na ions and Cu ions. This synergistic effect might be due to the increase release of Cu ions in acidic environments and Na ions increases alkalinity. As mentioned in the discussion of the element release results, copper phosphate could form as a secondary phase in the glass matrix during glass melting in the Cu-substituted glasses, which is soluble in an acidic environment. The occurrence of this secondary phase and the release of Cu from the assumed copper phosphate in an acidic environment must be investigated further. If true, this would favour MRONJ sites that are more acidic due to the high number of bacteria, as already discussed for antimicrobial activity.

The results from the elemental and the structural characterisation imply that the Cu addition did not affect the composition of the glass greatly, hence the lack of the Cu release in the deionized water might indicate the release of the Cu or similar earth metal elements are pH dependent. This characteristics of the metal elements release from the glass matrix in more acidic environment as shown in the antimicrobial activity increase with CuBGs could confirm the hypothesis as mentioned in [103] with Zn release were pH dependent. This is great for application where bacterial infectious environment such MRONJ are usually acidic and the CuBG has great affect in targeting the *actinomyces'* bacteria in this study.

7 Conclusion

Medication-related osteonecrosis of the jaw (MRONJ) is a debilitating and often painful condition. Current interventions may stabilize the affected site but rarely lead to complete healing. While the use of certain drugs is associated with MRONJ onset, recent findings highlight the pivotal role of a complex biofilm in driving disease progression. This understanding creates new opportunities for antimicrobial biomaterials as therapeutic interventions. Bioactive glasses hold great promise due to their intrinsic ability to promote healing and their potential for incorporating metal oxides to inhibit bacterial growth.

The aim of this research was to prepare and characterize a systematic series of bioactive glasses where calcium oxide was substituted with copper (II) oxide and evaluate their antimicrobial activity and in vitro cytotoxicity. The key findings of this experimental study are as follows:

1. **Glass Preparation and Characterization:**

Calcium oxide was successfully substituted with copper (II) oxide across a range of compositions (0–5 mol%), producing amorphous (glassy) materials confirmed by XRD analysis.

XRF demonstrated increasing copper content with substitution, while FTIR showed no significant change in the glass network structure.

Substitution of calcium oxide resulted in a proportional reduction in the glass transition temperature (Tg), consistent with the introduction of copper (II) oxide.

2. **Contamination Considerations:**

Low levels of alumina (Al_2O_3) contamination were detected in all glasses prepared using alumina crucibles. While alumina affected some physical properties, it did not account for the observed antimicrobial activity in copper-substituted glasses.

Future studies should continue monitoring contamination levels using XRD and evaluate their effects on glass properties.

3. **Elemental Release and Solubility:**

The novel copper-substituted glasses released copper ions in aqueous conditions, though the concentration was lower than anticipated and unlikely sufficient to inhibit microbial growth alone.

Copper-substituted glasses exhibited lower solubility than the parent 45S5 glass, as indicated by reduced silica release. Sodium release peaked in the 1 mol% Cu glass, while calcium and copper release were inversely proportional, aligning with the substitution mechanism.

4. **Antimicrobial Activity:**

Copper-substituted glasses inhibited Actinomyces sp. more effectively than the parent 45S5 glass, but the inhibition was not directly proportional to the degree of copper substitution. Antimicrobial activity appeared to result from a synergistic effect of copper and sodium ion release, though this was inconclusive for this series.

5. **Cytotoxicity:**

Cytotoxicity evaluation using two cell lines showed a reduction in cell respiratory rate as copper concentration increased. The L929 fibroblast cell line tolerated most compositions, with only the 5 mol% Cu glass (in an acrylic composite) eliminating cell viability.

6. **High Sodium Glasses:**

To increase solubility and potentially enhance copper release and antimicrobial activity, sodium oxide (Na_2O) content was elevated from 24.3 mol% to 30 mol% by substituting calcium oxide. These high-sodium glasses produced elevated concentrations of NaOH in solution, resulting in enhanced antimicrobial activity. However, copper release was unexpectedly reduced in these basic formulations, possibly due to the formation of an insoluble copper species within the glass matrix.

Summary

Copper-substituted bioactive glasses demonstrated significant antimicrobial activity compared to the parent 45S5 composition. However, the observed inhibition was not proportional to the degree of copper substitution, indicating other factors, such as sodium ion release and pH modulation, played a significant role. To further enhance solubility and potentially increase copper ion release, the sodium content was elevated to produce high-NaOH glasses. These compositions indeed demonstrated superior antimicrobial activity, which was primarily attributed to pH effects rather than the anticipated increase in copper release. The release of copper ions from the high-soda glasses remained limited, suggesting the potential formation of an insoluble copper species within the glass network.

The preparation of bioactive glass loaded composites shows promise for use in developing treatments for MRONJ. However, further research is needed to optimize copper release and fully harness its antimicrobial potential. Future studies should explore the effects of environmental conditions, such as pH, and investigate alternative glass compositions or fabrication methods to enhance copper release while maintaining biocompatibility and antimicrobial efficacy.

8 Future work

While progress has been made and the specific addition to knowledge summarised in the conclusions chapter, further work is needed towards preparation of a truly antimicrobial composite that supresses infection and promotes healing. The following next steps are suggested:

- Copper substitution is evidently not straightforward in bioactive glasses. While copper was incorporated as copper (ii) oxide and the melt performed without restricting air from the process, it is likely that some copper (i) ions were generated. Further work is suggested to investigate the nature of copper in the glass melt and final products.

- Further work on increasing the amount of copper in the glass series is desirable to find a composition that inhibits microbial growth more than the series reported here. This may not be an easy task, see below.

- The limited copper element release, especially in high soda compositions, was unexpected and suggests formation of an insoluble species. It was suggested that this might be a copper phosphate (Professor Robert Hill, personal communication), and further work is suggested that could include (a) solid state MAS-NMR to investigate the formation of this insoluble compound, and (b) investigation of copper element release at low (acidic) pH. The latter would be interesting, as infections are frequently acidic, and this might underpin an environmentally responsive element release mechanism.

- When an optimised formulation has been prepared and characterised, investigation of the fabrication of a custom prosthesis to locate the therapeutic biomaterial is the logical “next step”. This should ideally use additive manufacturing.

9 References

[1] J. P. Bonjour, W. Kohrt, R. Levasseur, M. Warren, S. Whiting, and M. Kraenzlin, "Biochemical markers for assessment of calcium economy and bone metabolism: Application in clinical trials from pharmaceutical agents to nutritional products," in *Nutrition Research Reviews* vol. 39, ed: Cambridge University Press, 2014.

[2] R. Baron, S. Ferrari, and R. G. G. Russell, "Denosumab and bisphosphonates: Different mechanisms of action and effects," *Bone,* vol. 48, no. 4, pp. 677-692, 2011, doi: 10.1016/j.bone.2010.11.020.

[3] T. Hasegawa *et al.*, "A multicenter retrospective study of the risk factors associated with medication-related osteonecrosis of the jaw after tooth extraction in patients receiving oral bisphosphonate therapy: can primary wound closure and a drug holiday really prevent MRONJ?," *Osteoporosis International,* vol. 28, no. 8, pp. 2465-2473, 2017, doi: 10.1007/s00198-017-4063-7.

[4] E. Eleutherakis-Papaiakovou and A. Bamias, "Antiresorptive treatment-associated ONJ," *European Journal of Cancer Care,* vol. 26, no. 6, pp. 1-11, 2017, doi: 10.1111/ecc.12787.

[5] A. Allegra, V. Innao, N. Pulvirenti, and C. Musolino, "Antiresorptive agents and anti-angiogenesis drugs in the development of osteonecrosis of the jaw," *Tohoku Journal of Experimental Medicine,* vol. 248, no. 1, pp. 27-29, 2019, doi: 10.1620/tjem.248.27.

[6] P. Marx, "Letters to the editor," *J oral maxillofac surg,* vol. 61, pp. 1115-1117, 2003, doi: 10.1080/15426432.1979.10383302.

[7] R. King, N. Tanna, and V. Patel, "Medication-related osteonecrosis of the jaw unrelated to bisphosphonates and denosumab—a review," *Oral Surgery, Oral Medicine, Oral Pathology and Oral Radiology,* vol. 127, no. 4, pp. 289-299, 2019, doi: 10.1016/j.oooo.2018.11.012.

[8] S. L. Ruggiero *et al.*, "American association of oral and maxillofacial surgeons position paper on medication-related osteonecrosis of the jaw - 2014 update," *Journal of Oral and Maxillofacial Surgery,* vol. 72, no. 10, pp. 1938-1956, 2014, doi: 10.1016/j.joms.2014.04.031.

[9] M. Kajizono *et al.*, "Incidence and risk factors of osteonecrosis of the jaw in advanced cancer patients after treatment with zoledronic acid or denosumab: A retrospective cohort study," *Biological and Pharmaceutical Bulletin,* vol. 38, no. 12, pp. 1850-1855, 2015, doi: 10.1248/bpb.b15-00385.

[10] R. A. Miksad *et al.*, "Quality of Life Implications of Bisphosphonate-Associated Osteonecrosis of the Jaw," *The Oncologist,* vol. 16, no. 1, pp. 121-132, 2011, doi: 10.1634/theoncologist.2010-0183.

[11] M. Kawahara, S. Kuroshima, and T. Sawase, "Clinical considerations for medication-related osteonecrosis of the jaw: a comprehensive literature review," *International Journal of Implant Dentistry,* vol. 7, no. 1, 2021, doi: 10.1186/s40729-021-00323-0.

[12] M. Zirk *et al.*, "The impact of surgical intervention and antibiotics on MRONJ stage II and III – Retrospective study," *Journal of Cranio-Maxillofacial Surgery,* vol. 45, no. 8, pp. 1183-1189, 2017, doi: 10.1016/j.jcms.2017.05.027.

[13] G. Campisi, S. Fedele, V. Fusco, G. Pizzo, O. Di Fede, and A. Bedogni, "Epidemiology, clinical manifestations, risk reduction and treatment strategies of jaw osteonecrosis in cancer patients exposed to antiresorptive agents," *Future Oncology,* vol. 10, no. 2, pp. 257-275, 2014, doi: 10.2217/fon.13.211.

[14] J. W. Kim, A. M. D. Alfafara, H. Y. Kim, S. Y. Kim, and S. J. Kim, "Effects of pH alteration on the pathogenesis of medication-related osteonecrosis of the jaw," *Bone,* vol. 122, no. December 2018, pp. 45-51, 2019, doi: 10.1016/j.bone.2019.02.007.

[15] M. Zirk, C. Wenzel, J. Buller, J. E. Zöller, M. Zinser, and F. Peters, "Microbial diversity in infections of patients with medication-related osteonecrosis of the jaw," *Clinical Oral Investigations,* vol. 23, no. 5, pp. 2143-2151, 2019, doi: 10.1007/s00784-018-2655-z.

[16] F. Hallmer, T. Bjørnland, G. Andersson, J. P. Becktor, A. K. Kristoffersen, and M. Enersen, "Bacterial diversity in medication-related osteonecrosis of the jaw," *Oral Surgery, Oral Medicine, Oral Pathology and Oral Radiology,* vol. 123, no. 4, pp. 436-444, 2017, doi: 10.1016/j.oooo.2016.11.011.

[17] A. Shuster, V. Reiser, L. Trejo, C. Ianculovici, S. Kleinman, and I. Kaplan, "Comparison of the histopathological characteristics of osteomyelitis, medication-related osteonecrosis of the jaw, and osteoradionecrosis," *International Journal of Oral and Maxillofacial Surgery,* vol. 48, no. 1, pp. 17-22, 2019, doi: 10.1016/j.ijom.2018.07.002.

[18] S. Pushalkar *et al.*, "Oral microbiota and host innate immune response in bisphosphonate-related osteonecrosis of the jaw," *International Journal of Oral Science,* vol. 6, no. 4, pp. 219-226, 2014, doi: 10.1038/ijos.2014.46.

[19] S. Panya *et al.*, "Role of microbiological culture and polymerase chain reaction (PCR) of actinomyces in medication-related osteonecrosis of the jaw (MRONJ)," *Journal of Cranio-Maxillofacial Surgery,* vol. 45, no. 3, pp. 357-363, 2017, doi: 10.1016/j.jcms.2017.01.006.

[20] R. E. Marx, J. E. Cillo, and J. J. Ulloa, "Oral Bisphosphonate-Induced Osteonecrosis: Risk Factors, Prediction of Risk Using Serum CTX Testing, Prevention, and Treatment," *Journal of Oral and Maxillofacial Surgery,* vol. 65, no. 12, pp. 2397-2410, 2007, doi: 10.1016/j.joms.2007.08.003.

[21] L. De Bruyn, R. Coropciuc, W. Coucke, and C. Politis, "Microbial population changes in patients with medication-related osteonecrosis of the jaw treated with systemic antibiotics," *Oral Surgery, Oral Medicine, Oral Pathology and Oral Radiology,* vol. 125, no. 3, pp. 268-275, 2018, doi: 10.1016/j.oooo.2017.11.022.

[22] G. Russmueller *et al.*, "The association of medication-related osteonecrosis of the jaw with Actinomyces spp. infection," *Scientific Reports,* vol. 6, no. January, pp. 1-8, 2016, doi: 10.1038/srep31604.

[23] X. Wei *et al.*, "Molecular profiling of oral microbiota in jawbone samples of bisphosphonate-related osteonecrosis of the jaw," *Oral Diseases,* vol. 18, no. 6, pp. 602-612, 2012, doi: 10.1111/j.1601-0825.2012.01916.x.

[24] P. Lesclous *et al.*, "Bisphosphonate-associated osteonecrosis of the jaw: A key role of inflammation?," *Bone,* vol. 45, no. 5, pp. 843-852, 2009/11// 2009, doi: 10.1016/j.bone.2009.07.011.

[25] P. P. Sedghizadeh, S. K. S. Kumar, A. Gorur, C. Schaudinn, C. F. Shuler, and J. W. Costerton, "Identification of Microbial Biofilms in Osteonecrosis of the Jaws Secondary to Bisphosphonate Therapy," *Journal of Oral and Maxillofacial Surgery,* vol. 66, no. 4, pp. 767-775, 2008/4// 2008, doi: 10.1016/j.joms.2007.11.035.
[26] E. Könönen and W. G. Wade, "Actinomyces and related organisms in human infections," *Clinical Microbiology Reviews,* vol. 28, no. 2, pp. 419-442, 2015/4// 2015, doi: 10.1128/CMR.00100-14.
[27] A. Cerrato, G. Zanette, M. Boccuto, A. Angelini, M. Valente, and C. Bacci, "Actinomyces and MRONJ: A retrospective study and a literature review," *Journal of Stomatology, Oral and Maxillofacial Surgery,* vol. 122, no. 5, pp. 499-504, 2021, doi: 10.1016/j.jormas.2020.07.012.
[28] H. M. Wexler, "Bacteroides: The good, the bad, and the nitty-gritty," in *Clinical Microbiology Reviews* vol. 20, ed, 2007, pp. 593-621.
[29] A. J. van Winkelhoff, T. J. M. van Steenbergen, and J. de Graaff, "The role of oral Bacteroides in mixed infections," *Antonie van Leeuwenhoek,* vol. 49, no. 6, pp. 145-155, 1987/11// 1987, doi: 10.1007/BF00399864.
[30] A. Tett, E. Pasolli, G. Masetti, D. Ercolini, and N. Segata, "Prevotella diversity, niches and interactions with the human host," in *Nature Reviews Microbiology* vol. 19, ed, 2021, pp. 585-599.
[31] A. M. Mitchell and T. J. Mitchell, "Streptococcus pneumoniae: Virulence factors and variation," *Clinical Microbiology and Infection,* vol. 16, no. 5, pp. 411-418, 2010, doi: 10.1111/j.1469-0691.2010.03183.x.
[32] W. Krzyściak, A. Jurczak, D. Kościelniak, B. Bystrowska, and A. Skalniak, "The virulence of Streptococcus mutans and the ability to form biofilms," *European Journal of Clinical Microbiology & Infectious Diseases,* vol. 33, no. 4, pp. 499-515, 2014/4// 2014, doi: 10.1007/s10096-013-1993-7.
[33] S. Otto *et al.*, "Bisphosphonate-Related Osteonecrosis of the Jaw: Is pH the Missing Part in the Pathogenesis Puzzle?," *Journal of Oral and Maxillofacial Surgery,* vol. 68, no. 5, pp. 1158-1161, 2010, doi: 10.1016/j.joms.2009.07.079.
[34] S. Otto *et al.*, "Osteonecrosis of the jaw: Effect of bisphosphonate type, local concentration, and acidic milieu on the pathomechanism," *Journal of Oral and Maxillofacial Surgery,* vol. 68, no. 11, pp. 2837-2845, 2010, doi: 10.1016/j.joms.2010.07.017.
[35] S. Kuroshima, M. Sasaki, and T. Sawase, "Medication-related osteonecrosis of the jaw: A literature review," *Journal of Oral Biosciences,* vol. 61, no. 2, pp. 99-104, 2019, doi: 10.1016/j.job.2019.03.005.
[36] M. J. Hajipour *et al.*, "Antibacterial properties of nanoparticles," *Trends in Biotechnology,* vol. 30, no. 10, pp. 499-511, 2012, doi: 10.1016/j.tibtech.2012.06.004.
[37] A. Singh and A. K. Dubey, "Various Biomaterials and Techniques for Improving Antibacterial Response," *ACS Applied Bio Materials,* vol. 1, no. 1, pp. 3-20, 2018, doi: 10.1021/acsabm.8b00033.
[38] H. Lucie, H. Jens, and M. Craig, "Fabrication of Electrospun Mucoadhesive Membranes for Therapeutic Applications in Oral Medicine," 2017.
[39] Z. Shi, K. G. Neoh, E. T. Kang, and W. Wang, "Antibacterial and mechanical properties of bone cement impregnated with chitosan nanoparticles,"

Biomaterials, vol. 27, no. 11, pp. 2440-2449, 2006, doi: 10.1016/j.biomaterials.2005.11.036.
[40] C. B. Huang, Y. Alimova, T. M. Myers, and J. L. Ebersole, "Short- and medium-chain fatty acids exhibit antimicrobial activity for oral microorganisms," *Archives of Oral Biology,* vol. 56, no. 7, pp. 650-654, 2011, doi: 10.1016/j.archoralbio.2011.01.011.
[41] E. Sherry, H. Boeck, and P. H. Warnke, "Percutaneous treatment of chronic MRSA osteomyelitis with a novel plant-derived antiseptic," *BMC Surgery,* vol. 1, pp. 1-3, 2001, doi: 10.1186/1471-2482-1-1.
[42] A. Man, L. Santacroce, R. Jacob, A. Mare, and L. Man, "Antimicrobial activity of six essential oils against a group of human pathogens: A comparative study," *Pathogens,* vol. 8, no. 1, pp. 1-11, 2019, doi: 10.3390/pathogens8010015.
[43] M. Bellantone, N. J. Coleman, and L. L. Hench, "Bacteriostatic action of a novel four-component bioactive glass," *Journal of Biomedical Materials Research,* vol. 51, no. 3, pp. 484-490, 2000/9// 2000, doi: 10.1002/1097-4636(20000905)51:3<484::AID-JBM24>3.0.CO;2-4.
[44] M. Bellantone, H. D. Williams, and L. L. Hench, "Broad-spectrum bactericidal activity of Ag2O-doped bioactive glass," *Antimicrobial Agents and Chemotherapy,* vol. 46, no. 6, pp. 1940-1945, 2002, doi: 10.1128/AAC.46.6.1940-1945.2002.
[45] M. T. Cunha, M. A. Murça, S. Nigro, G. B. Klautau, and M. J. C. Salles, "In vitro antibacterial activity of bioactive glass S53P4 on multiresistant pathogens causing osteomyelitis and prosthetic joint infection," *BMC Infectious Diseases,* vol. 18, no. 1, pp. 1-6, 2018, doi: 10.1186/s12879-018-3069-x.
[46] M. Miola, A. Cochis, A. Kumar, C. R. Arciola, L. Rimondini, and E. Verné, "Copper-doped bioactive glass as filler for PMMA-based bone cements: Morphological, mechanical, reactivity, and preliminary antibacterial characterization," *Materials,* vol. 11, no. 6, 2018, doi: 10.3390/ma11060961.
[47] T. Waltimo, T. J. Brunner, M. Vollenweider, W. J. Stark, and M. Zehnder, "Antimicrobial effect of nanometric bioactive glass 45S5," *Journal of Dental Research,* vol. 86, no. 8, pp. 754-757, 2007/12// 2007, doi: 10.1177/154405910708600813.
[48] H. Palza Cordero, R. Castro Cid, M. Diaz Dosque, R. Cabello Ibacache, and P. Palma Fluxá, "Li-doped bioglass® 45S5 for potential treatment of prevalent oral diseases," *Journal of Dentistry,* vol. 105, no. December 2020, 2021, doi: 10.1016/j.jdent.2020.103575.
[49] S. Shanmugam and B. Gopal, "Copper substituted hydroxyapatite and fluorapatite: Synthesis, characterization and antimicrobial properties," *Ceramics International,* vol. 40, no. 10, pp. 15655-15662, 2014, doi: 10.1016/j.ceramint.2014.07.086.
[50] N. Matsumoto, K. Sato, K. Yoshida, K. Hashimoto, and Y. Toda, "Preparation and characterization of β-tricalcium phosphate co-doped with monovalent and divalent antibacterial metal ions," *Acta Biomaterialia,* vol. 5, no. 8, pp. 3157-3164, 2009, doi: 10.1016/j.actbio.2009.04.010.
[51] A. Azam, A. S. Ahmed, M. Oves, M. S. Khan, S. S. Habib, and A. Memic, "Antimicrobial activity of metal oxide nanoparticles against Gram-positive and Gram-negative bacteria: A comparative study," *International Journal of Nanomedicine,* vol. 7, pp. 6003-6009, 2012, doi: 10.2147/IJN.S35347.

[52] F. A. Bezza, S. M. Tichapondwa, and E. M. N. Chirwa, "Fabrication of monodispersed copper oxide nanoparticles with potential application as antimicrobial agents," *Scientific Reports,* vol. 10, no. 1, pp. 1-18, 2020, doi: 10.1038/s41598-020-73497-z.
[53] C. J. Wilcock *et al.*, "Preparation and antibacterial properties of silver-doped nanoscale hydroxyapatite pastes for bone repair and augmentation," *Journal of Biomedical Nanotechnology,* vol. 13, no. 9, pp. 1168-1176, 2017, doi: 10.1166/jbn.2017.2387.
[54] M. Kazemzadeh-Narbat, J. Kindrachuk, K. Duan, H. Jenssen, R. E. W. Hancock, and R. Wang, "Antimicrobial peptides on calcium phosphate-coated titanium for the prevention of implant-associated infections," *Biomaterials,* vol. 31, no. 36, pp. 9519-9526, 2010, doi: 10.1016/j.biomaterials.2010.08.035.
[55] H. Sun *et al.*, "3D printing of calcium phosphate scaffolds with controlled release of antibacterial functions for jaw bone repair," *Materials and Design,* vol. 189, pp. 108540-108540, 2020, doi: 10.1016/j.matdes.2020.108540.
[56] V. Uskoković, C. Hoover, M. Vukomanović, D. P. Uskoković, and T. A. Desai, "Osteogenic and antimicrobial nanoparticulate calcium phosphate and poly-(d,l-lactide-co-glycolide) powders for the treatment of osteomyelitis," *Materials Science and Engineering C,* vol. 33, no. 6, pp. 3362-3373, 2013, doi: 10.1016/j.msec.2013.04.023.
[57] S. Ghosh, V. Wu, S. Pernal, and V. Uskoković, "Self-Setting Calcium Phosphate Cements with Tunable Antibiotic Release Rates for Advanced Antimicrobial Applications," *ACS Applied Materials and Interfaces,* vol. 8, no. 12, pp. 7691-7708, 2016, doi: 10.1021/acsami.6b01160.
[58] M. K. Swamy, M. S. Akhtar, and U. R. Sinniah, "Antimicrobial properties of plant essential oils against human pathogens and their mode of action: An updated review," *Evidence-based Complementary and Alternative Medicine,* vol. 2016, 2016, doi: 10.1155/2016/3012462.
[59] S. Chouhan, K. Sharma, and S. Guleria, "medicines Antimicrobial Activity of Some Essential Oils-Present Status and Future Perspectives," doi: 10.3390/medicines4030058.
[60] P. Stoor, V. Kirstilä, E. Söderling, I. Kangasniemi, K. Herbst, and A. Yli-Urpo, "Interactions between bioactive glass and periodontal pathogens," *Microbial ecology in health and disease,* vol. 9, no. 3, pp. 109-114, 1996.
[61] P. Stoor, E. Söderling, and J. I. Salonen, "Antibacterial effects of a bioactive glass paste on oral microorganisms," *Acta Odontologica Scandinavica,* vol. 56, no. 3, pp. 161-165, 1998.
[62] C. H. G. Martins *et al.*, "Assessment of antimicrobial effect of Biosilicate ® against anaerobic, microaerophilic and facultative anaerobic microorganisms," *Journal of Materials Science: Materials in Medicine,* vol. 22, no. 6, pp. 1439-1446, 2011/6// 2011, doi: 10.1007/s10856-011-4330-7.
[63] C. H. Chu, L. Mei, C. J. Seneviratne, and E. C. M. Lo, "Effects of silver diamine fluoride on dentine carious lesions induced by Streptococcus mutans and Actinomyces naeslundii biofilms," *International journal of paediatric dentistry,* vol. 22, no. 1, pp. 2-10, 2012.
[64] M.-J. Lee *et al.*, "Bioactive resin-based composite with surface pre-reacted glass-ionomer filler and zwitterionic material to prevent the formation of multi-species biofilm," *Dental Materials,* vol. 35, no. 9, pp. 1331-1341, 2019.

[65] H. Miyaji *et al.*, "Ultrasonic irrigation of periodontal pocket with surface pre-reacted glass-ionomer (S-PRG) nanofiller dispersion improves periodontal parameters in beagle dogs," *Journal of Oral Biosciences,* vol. 64, no. 2, pp. 222-228, 2022.
[66] A. Munir *et al.*, "Using copper-doped mesoporous bioactive glass nanospheres to impart anti-bacterial properties to dental composites," *Pharmaceutics,* vol. 14, no. 10, p. 2241, 2022.
[67] M. Walker and D. Parsons, "The biological fate of silver ions following the use of silver-containing wound care products - A review," *International Wound Journal,* vol. 11, no. 5, pp. 496-504, 2014, doi: 10.1111/j.1742-481X.2012.01115.x.
[68] A. Hoppe, N. S. Güldal, and A. R. Boccaccini, "A review of the biological response to ionic dissolution products from bioactive glasses and glass-ceramics," *Biomaterials,* vol. 32, no. 11, pp. 2757-2774, 2011, doi: 10.1016/j.biomaterials.2011.01.004.
[69] H. Wang *et al.*, "Evaluation of borate bioactive glass scaffolds as a controlled delivery system for copper ions in stimulating osteogenesis and angiogenesis in bone healing," *Journal of Materials Chemistry B,* vol. 2, no. 48, pp. 8547-8557, 2014, doi: 10.1039/c4tb01355g.
[70] C. J. Harrison, P. V. Hatton, P. Gentile, and C. A. Miller, "Nanoscale strontium-substituted hydroxyapatite pastes and gels for bone tissue regeneration," *Nanomaterials,* vol. 11, no. 6, p. 1611, 2021.
[71] G. Bullock, C. Miller, A. McKechnie, and V. Hearnden, "Synthetic Hydroxyapatite Inhibits Bisphosphonate Toxicity to the Oral Mucosa In Vitro," *Materials,* vol. 13, no. 9, pp. 2086-2086, 2020, doi: 10.3390/ma13092086.
[72] L. L. Hench, "Bioceramics," *Journal of the American Ceramic Society,* vol. 81, no. 7, pp. 1705-1728, 1998/07/01 1998, doi: https://doi.org/10.1111/j.1151-2916.1998.tb02540.x.
[73] G. Kirste *et al.*, "Apatite formation of substituted Bioglass 45S5: SBF vs. Tris," *International Journal of Applied Glass Science,* vol. 257, no. 4, pp. 126760-126760, 2019, doi: 10.1111/ijag.12288.
[74] G. Kirste, J. Brandt-Slowik, C. Bocker, M. Steinert, R. Geiss, and D. S. Brauer, "Effect of chloride ions in Tris buffer solution on bioactive glass apatite mineralization," *International Journal of Applied Glass Science,* vol. 8, no. 4, pp. 438-449, 2017, doi: 10.1111/ijag.12288.
[75] P. S. L. L. H. Julian R. Jones, "Dose-Dependent Behavior of Bioactive Glass Dissolution," *Journal of Biomedical Materials Research,* no. 58, pp. 720–726-720–726, 2002.
[76] A. A. Ahmed, A. A. Ali, D. A. R. Mahmoud, and A. M. El-Fiqi, "Preparation and characterization of antibacterial P2O 5-CaO-Na2O-Ag2O glasses," *Journal of Biomedical Materials Research - Part A,* vol. 98 A, no. 1, pp. 132-142, 2011/7// 2011, doi: 10.1002/jbm.a.33101.
[77] M. M. Babu *et al.*, "ZnO incorporated high phosphate bioactive glasses for guided bone regeneration implants: enhancement of in vitro bioactivity and antibacterial activity," *Journal of Materials Research and Technology,* vol. 15, pp. 633-646, 2021/11// 2021, doi: 10.1016/j.jmrt.2021.08.020.

[78] H. Wang *et al.*, "Evaluation of borate bioactive glass scaffolds as a controlled delivery system for copper ions in stimulating osteogenesis and angiogenesis in bone healing," 2014, doi: 10.1039/c4tb01355g.
[79] J. R. Jones, "Review of bioactive glass: From Hench to hybrids," *Acta Biomaterialia,* vol. 9, no. 1, pp. 4457-4486, 2013, doi: 10.1016/j.actbio.2012.08.023.
[80] H. Eckert, "Structural characterization of bioactive glasses by solid state NMR," *Journal of Sol-Gel Science and Technology,* vol. 88, no. 2, pp. 263-295, 2018, doi: 10.1007/s10971-018-4795-7.
[81] D. S. Brauer, "Bioactive glasses - Structure and properties," *Angewandte Chemie - International Edition,* vol. 54, no. 14, pp. 4160-4181, 2015, doi: 10.1002/anie.201405310.
[82] N. Gupta *et al.*, "Effects of transition metal ion dopants (Ag, Cu and Fe) on the structural, mechanical and antibacterial properties of bioactive glass," *Colloids and Surfaces A: Physicochemical and Engineering Aspects,* vol. 538, pp. 393-403, 2018/2// 2018, doi: 10.1016/j.colsurfa.2017.11.023.
[83] D. Fernando *et al.*, "Influence of network modifiers in an acetate based sol-gel bioactive glass system," *Microporous and Mesoporous Materials,* vol. 257, pp. 99-109, 2018.
[84] F. G. Mecca, D. Bellucci, and V. Cannillo, "Effect of Thermal Treatments and Ion Substitution on Sintering and Crystallization of Bioactive Glasses: A Review," in *Materials* vol. 16, ed: Multidisciplinary Digital Publishing Institute (MDPI), 2023.
[85] A. Pedone, V. Cannillo, and M. C. Menziani, "Toward the understanding of crystallization, mechanical properties and reactivity of multicomponent bioactive glasses," *Acta Materialia,* vol. 213, 2021/7// 2021, doi: 10.1016/j.actamat.2021.116977.
[86] J. Jiusti *et al.*, "Effect of network formers and modifiers on the crystallization resistance of oxide glasses," *Journal of Non-Crystalline Solids,* vol. 550, p. 120359, 2020.
[87] K. E. Wallace, R. G. Hill, J. T. Pembroke, C. J. Brown, and P. V. Hatton, "Influence of sodium oxide content on bioactive glass properties," in *Journal of Materials Science: Materials in Medicine*, 1999, vol. 10, 12 ed., pp. 697-701, doi: 10.1023/A:1008910718446.
[88] S. Akhtach, Z. Tabia, K. El Mabrouk, M. Bricha, and R. Belkhou, "A comprehensive study on copper incorporated bio-glass matrix for its potential antimicrobial applications," *Ceramics International,* vol. 47, no. 1, pp. 424-433, 2021/1// 2021, doi: 10.1016/j.ceramint.2020.08.149.
[89] R. G. Hill and D. S. Brauer, "Predicting the bioactivity of glasses using the network connectivity or split network models," *Journal of Non-Crystalline Solids,* vol. 357, no. 24, pp. 3884-3887, 2011/12// 2011, doi: 10.1016/j.jnoncrysol.2011.07.025.
[90] M. Edén, "The split network analysis for exploring composition-structure correlations in multi-component glasses: I. Rationalizing bioactivity-composition trends of bioglasses," *Journal of Non-Crystalline Solids,* vol. 357, no. 6, pp. 1595-1602, 2011/3// 2011, doi: 10.1016/j.jnoncrysol.2010.11.098.
[91] L. L. Hench and J. R. Jones, "Bioactive glasses: frontiers and challenges," *Frontiers in bioengineering and biotechnology,* vol. 3, p. 194, 2015.

[92] L. Ghasemi-Mobarakeh, D. Kolahreez, S. Ramakrishna, and D. Williams, "Key terminology in biomaterials and biocompatibility," *Current Opinion in Biomedical Engineering,* vol. 10, pp. 45-50, 2019.
[93] S. M. Rabiee, N. Nazparvar, M. Azizian, D. Vashaee, and L. Tayebi, "Effect of ion substitution on properties of bioactive glasses: A review," in *Ceramics International* vol. 41, ed: Elsevier Ltd, 2015, pp. 7241-7251.
[94] L. L. Hench, R. J. Splinter, W. Allen, and T. Greenlee, "Bonding mechanisms at the interface of ceramic prosthetic materials," *Journal of biomedical materials research,* vol. 5, no. 6, pp. 117-141, 1971.
[95] A. Shearer, M. Montazerian, J. J. Sly, R. G. Hill, and J. C. Mauro, "Trends and perspectives on the commercialization of bioactive glasses," *Acta Biomaterialia,* vol. 160, pp. 14-31, 2023.
[96] P. Sepulveda, J. R. Jones, and L. L. Hench, "In vitro dissolution of melt-derived 45S5 and sol-gel derived 58S bioactive glasses," *Journal of Biomedical Materials Research,* vol. 61, no. 2, pp. 301-311, 2002, doi: 10.1002/jbm.10207.
[97] M. Zehnder, T. Waltimo, B. Sener, and E. Söderling, "Dentin enhances the effectiveness of bioactive glass S53P4 against a strain of Enterococcus faecalis," *Oral Surgery, Oral Medicine, Oral Pathology, Oral Radiology, and Endodontology,* vol. 101, no. 4, pp. 530-535, 2006.
[98] I. Allan, H. Newman, and M. Wilson, "Antibacterial activity of particulate Bioglass® against supra-and subgingival bacteria," *Biomaterials,* vol. 22, no. 12, pp. 1683-1687, 2001.
[99] D. Zhang *et al.*, "Antibacterial effects and dissolution behavior of six bioactive glasses," *Journal of Biomedical Materials Research - Part A,* vol. 93, no. 2, pp. 475-483, 2010, doi: 10.1002/jbm.a.32564.
[100] A. A. Gorustovich, J. A. Roether, and A. R. Boccaccini, "Effect of bioactive glasses on angiogenesis: a review of in vitro and in vivo evidences," *Tissue Engineering Part B: Reviews,* vol. 16, no. 2, pp. 199-207, 2010.
[101] S. Kargozar, F. Baino, S. Hamzehlou, R. G. Hill, and M. Mozafari, "Bioactive glasses: sprouting angiogenesis in tissue engineering," *Trends in biotechnology,* vol. 36, no. 4, pp. 430-444, 2018.
[102] I. Cacciotti, "Bivalent cationic ions doped bioactive glasses: the influence of magnesium, zinc, strontium and copper on the physical and biological properties," *Journal of Materials Science,* vol. 52, no. 15, pp. 8812-8831, 2017.
[103] M. Blochberger, L. Hupa, and D. S. Brauer, "Influence of zinc and magnesium substitution on ion release from Bioglass 45S5 at physiological and acidic pH," *Biomedical glasses,* vol. 1, no. 1, 2015.
[104] R. Wetzel, O. Bartzok, and D. S. Brauer, "Influence of low amounts of zinc or magnesium substitution on ion release and apatite formation of Bioglass 45S5," *Journal of Materials Science: Materials in Medicine,* vol. 31, no. 10, 2020, doi: 10.1007/s10856-020-06426-1.
[105] R. Wetzel and D. S. Brauer, "Apatite formation of substituted Bioglass 45S5: SBF vs. Tris," *Materials Letters,* vol. 257, pp. 126760-126760, 2019, doi: 10.1016/j.matlet.2019.126760.
[106] C. Wu *et al.*, "Copper-containing mesoporous bioactive glass scaffolds with multifunctional properties of angiogenesis capacity, osteostimulation and antibacterial activity," *Biomaterials,* vol. 34, no. 2, pp. 422-433, 2013.

[107] A. Bari *et al.*, "Copper-containing mesoporous bioactive glass nanoparticles as multifunctional agent for bone regeneration," *Acta Biomaterialia,* vol. 55, pp. 493-504, 2017, doi: 10.1016/j.actbio.2017.04.012.
[108] L. Bi *et al.*, "Effect of bioactive borate glass microstructure on bone regeneration, angiogenesis, and hydroxyapatite conversion in a rat calvarial defect model," *Acta biomaterialia,* vol. 9, no. 8, pp. 8015-8026, 2013.
[109] L. A. Fiehn *et al.*, "A comparative in vitro and in vivo analysis of the impact of copper substitution on the cytocompatibility, osteogenic, and angiogenic properties of a borosilicate bioactive glass," *Journal of Biomedical Materials Research - Part A,* no. January, pp. 1-20, 2024, doi: 10.1002/jbm.a.37721.
[110] S. Zhao *et al.*, "Wound dressings composed of copper-doped borate bioactive glass microfibers stimulate angiogenesis and heal full-thickness skin defects in a rodent model," *Biomaterials,* vol. 53, pp. 379-391, 2015.
[111] J. Li *et al.*, "Preparation of copper-containing bioactive glass/eggshell membrane nanocomposites for improving angiogenesis, antibacterial activity and wound healing," *Acta biomaterialia,* vol. 36, pp. 254-266, 2016.
[112] S. Shirgill, G. Poologasundarampillai, S. Jabbari, J. Ward, and S. A. Kuehne, "Silver-doped bioactive glass fibres as a potential treatment for wound-associated bacterial biofilms," *Biofilm,* vol. 5, p. 100115, 2023/12/01/ 2023, doi: https://doi.org/10.1016/j.bioflm.2023.100115.
[113] N. Mutlu *et al.*, "Effect of Zn and Ga doping on bioactivity, degradation, and antibacterial properties of borate 1393-B3 bioactive glass," *Ceramics International,* vol. 48, no. 11, pp. 16404-16417, 2022/06/01/ 2022, doi: https://doi.org/10.1016/j.ceramint.2022.02.192.
[114] S. Chitra, P. Bargavi, M. Balasubramaniam, R. R. Chandran, and S. Balakumar, "Impact of copper on in-vitro biomineralization, drug release efficacy and antimicrobial properties of bioactive glasses," *Materials Science and Engineering: C,* vol. 109, p. 110598, 2020/04/01/ 2020, doi: https://doi.org/10.1016/j.msec.2019.110598.
[115] E. Bosch-Rué, L. Díez-Tercero, R. Rodríguez-González, B. M. Bosch-Canals, and R. A. Perez, "Assessing the potential role of copper and cobalt in stimulating angiogenesis for tissue regeneration," *PLoS One,* vol. 16, no. 10, p. e0259125, 2021.
[116] M. Plewinski, K. Schickle, M. Lindner, A. Kirsten, M. Weber, and H. Fischer, "The effect of crystallization of bioactive bioglass 45S5 on apatite formation and degradation," *Dental Materials,* vol. 29, no. 12, pp. 1256-1264, 2013, doi: 10.1016/j.dental.2013.09.016.
[117] W. Leenakul, T. Tunkasiri, N. Tongsiri, K. Pengpat, and J. Ruangsuriya, "Effect of sintering temperature variations on fabrication of 45S5 bioactive glass-ceramics using rice husk as a source for silica," *Materials Science and Engineering C,* vol. 61, pp. 695-704, 2016, doi: 10.1016/j.msec.2015.12.029.
[118] X. Lu *et al.*, "Mixed Network Former Effect on Structure, Physical Properties, and Bioactivity of 45S5 Bioactive Glasses: An Integrated Experimental and Molecular Dynamics Simulation Study," *Journal of Physical Chemistry B,* vol. 122, no. 9, pp. 2564-2577, 2018, doi: 10.1021/acs.jpcb.7b12127.
[119] A. A. El-Kheshen, F. A. Khaliafa, E. A. Saad, and R. L. Elwan, "Effect of Al2O3 addition on bioactivity, thermal and mechanical properties of some bioactive

glasses," *Ceramics International,* vol. 34, no. 7, pp. 1667-1673, 2008, doi: 10.1016/j.ceramint.2007.05.016.
[120] M. S. Araujo, A. C. Silva, J. F. Bartolomé, and S. Mello-Castanho, "Structural and thermal behavior of 45S5 Bioglass®-based compositions containing alumina and strontium," *Journal of the American Ceramic Society,* vol. 103, no. 6, pp. 3620-3630, 2020/6// 2020, doi: 10.1111/jace.17061.
[121] D. H. Carter, P. Sloan, I. M. Brook, and P. V. Hatton, "Role of exchanged ions in the integration of ionomeric (glass polyalkenoate) bone sub&tutes."
[122] M. C. Blades, D. P. Moore, P. A. Revell, and R. Hill, "In vivo skeletal response and biomechanical assessment of two novel polyalkenoate cements following femoral implantation in the female New Zealand White rabbit," *Journal of Materials Science: Materials in Medicine,* vol. 9, no. 12, pp. 701-706, 1998, doi: 10.1023/A:1008990516159.
[123] M. Montazeri, S. Karbasi, M. R. Foroughi, A. Monshi, and R. Ebrahimi-Kahrizsangi, "Evaluation of mechanical property and bioactivity of nano-bioglass 45S5 scaffold coated with poly-3-hydroxybutyrate," *Journal of Materials Science: Materials in Medicine,* vol. 26, no. 2, pp. 1-11, 2015, doi: 10.1007/s10856-014-5369-z.
[124] M. Cannio, D. Bellucci, J. A. Roether, D. N. Boccaccini, and V. Cannillo, "Bioactive glass applications: A literature review of human clinical trials," in *Materials* vol. 14, ed: MDPI, 2021.
[125] R. Li, A. E. Clark, and L. L. Hench, "An investigation of bioactive glass powders by sol-gel processing," *Journal of applied biomaterials : an official journal of the Society for Biomaterials,* vol. 2, no. 4, pp. 231-239, 1991, doi: 10.1002/jab.770020403.
[126] K. Schuhladen, X. Wang, L. Hupa, and A. R. Boccaccini, "Dissolution of borate and borosilicate bioactive glasses and the influence of ion (Zn, Cu) doping in different solutions," *Journal of Non-Crystalline Solids,* vol. 502, pp. 22-34, 2018.
[127] V. Anand, K. Singh, and K. Kaur, "Evaluation of zinc and magnesium doped 45S5 mesoporous bioactive glass system for the growth of hydroxyl apatite layer," *Journal of non-crystalline solids,* vol. 406, pp. 88-94, 2014.
[128] Z. Tabia, K. El Mabrouk, M. Bricha, and K. Nouneh, "Mesoporous bioactive glass nanoparticles doped with magnesium: drug delivery and acellular in vitro bioactivity," *RSC advances,* vol. 9, no. 22, pp. 12232-12246, 2019.
[129] Y. Zhong, C. Liu, X. Yan, X. Li, X. Chen, and S. Mai, "Odontogenic and anti-inflammatory effects of magnesium-doped bioactive glass in vital pulp therapy," *Biomedical Materials,* vol. 19, no. 4, p. 045026, 2024.
[130] F. Hohenbild, M. Arango Ospina, S. I. Schmitz, A. Moghaddam, A. R. Boccaccini, and F. Westhauser, "An in vitro evaluation of the biological and osteogenic properties of magnesium-doped bioactive glasses for application in bone tissue engineering," *International Journal of Molecular Sciences,* vol. 22, no. 23, p. 12703, 2021.
[131] H. Jodati, B. Güner, Z. Evis, D. Keskin, and A. Tezcaner, "Synthesis and characterization of magnesium-lanthanum dual doped bioactive glasses," *Ceramics International,* vol. 46, no. 8, pp. 10503-10511, 2020.
[132] S. Kargozar *et al.*, "Osteogenic potential of magnesium (Mg)-doped multicomponent bioactive glass: in vitro and in vivo animal studies," *Materials,* vol. 15, no. 1, p. 318, 2022.

[133] M. Liu *et al.*, "Electrospun flexible magnesium-doped silica bioactive glass nanofiber membranes with anti-inflammatory and pro-angiogenic effects for infected wounds," *Journal of Materials Chemistry B,* vol. 11, no. 2, pp. 359-376, 2023.
[134] E. Dietrich, H. Oudadesse, A. Lucas-Girot, Y. Le Gal, S. Jeanne, and G. Cathelineau, "Effects of Mg and Zn on the surface of doped melt-derived glass for biomaterials applications," *Applied Surface Science,* vol. 255, no. 2, pp. 391-395, 2008.
[135] A. Anand, H. Kaňková, Z. Hájovská, D. Galusek, A. R. Boccaccini, and D. Galusková, "Bio-response of copper–magnesium co-substituted mesoporous bioactive glass for bone tissue regeneration," *Journal of Materials Chemistry B,* vol. 12, no. 7, pp. 1875-1891, 2024.
[136] S. K. Arepalli *et al.*, "Preparation and in vitro investigation on bioactivity of magnesia-contained bioactive glasses," *Journal of the Australian Ceramic Society,* vol. 55, pp. 145-155, 2019.
[137] A. Moghanian *et al.*, "Novel antibacterial Cu/Mg‐substituted 58S‐bioglass: Synthesis, characterization and investigation of in vitro bioactivity," *International Journal of Applied Glass Science,* vol. 11, no. 4, pp. 685-698, 2020.
[138] A. Al-Noaman, S. C. Rawlinson, and R. G. Hill, "MgF2-containing glasses as a coating for titanium dental implant. I-Glass powder," *Journal of the Mechanical Behavior of Biomedical Materials,* vol. 125, p. 104948, 2022.
[139] A. l. J. Leite, A. I. Gonçalves, M. T. Rodrigues, M. E. Gomes, and J. o. F. Mano, "Strontium-doped bioactive glass nanoparticles in osteogenic commitment," *ACS applied materials & interfaces,* vol. 10, no. 27, pp. 23311-23320, 2018.
[140] J. Isaac *et al.*, "Effects of strontium-doped bioactive glass on the differentiation of cultured osteogenic cells," *Eur Cell Mater,* vol. 21, no. 130, p. e43, 2011.
[141] L. Weng, S. K. Boda, M. J. Teusink, F. D. Shuler, X. Li, and J. Xie, "Binary doping of strontium and copper enhancing osteogenesis and angiogenesis of bioactive glass nanofibers while suppressing osteoclast activity," *ACS applied materials & interfaces,* vol. 9, no. 29, pp. 24484-24496, 2017.
[142] J. Lao, J.-M. Nedelec, and E. Jallot, "New strontium-based bioactive glasses: physicochemical reactivity and delivering capability of biologically active dissolution products," *Journal of Materials Chemistry,* vol. 19, no. 19, pp. 2940-2949, 2009.
[143] Y. C. Fredholm, N. Karpukhina, D. S. Brauer, J. R. Jones, R. V. Law, and R. G. Hill, "Influence of strontium for calcium substitution in bioactive glasses on degradation, ion release and apatite formation," *Journal of the Royal Society Interface,* vol. 9, no. 70, pp. 880-889, 2012.
[144] A. Moghanian, M. Zohourfazeli, M. H. Mahdi Tajer, Z. Miri, S. M. Hosseini, and A. Rashvand, "Preparation, characterization and in vitro biological response of simultaneous co-substitution of Zr+4/Sr+2 58S bioactive glass powder," *Ceramics International,* vol. 47, no. 17, pp. 23762-23769, 2021/9// 2021, doi: 10.1016/j.ceramint.2020.11.139.
[145] E. Pawar, "A review article on acrylic PMMA," *IOSR J. Mech. Civ. Eng,* vol. 13, no. 2, pp. 1-4, 2016.
[146] U. Ali, K. J. B. A. Karim, and N. A. Buang, "A review of the properties and applications of poly (methyl methacrylate)(PMMA)," *Polymer Reviews,* vol. 55, no. 4, pp. 678-705, 2015.

[147] M. Yuan, D. Huang, and Y. Zhao, "Development of synthesis and application of high molecular weight poly (methyl methacrylate)," *Polymers,* vol. 14, no. 13, p. 2632, 2022.
[148] S. S. Rahman, M. B. Mahmud, A. R. Monfared, P. C. Lee, and C. B. Park, "Achieving outstanding toughness of PMMA while retaining its strength, stiffness, and transparency using in situ developed TPEE nanofibrils," *Composites Science and Technology,* vol. 236, p. 109994, 2023.
[149] J. L. Ferracane, "Resin composite—state of the art," *Dental materials,* vol. 27, no. 1, pp. 29-38, 2011.
[150] M. Shetty, H. Alva, and A. Prasad, "Provisional restorations in prosthodontic rehabilitations-concepts, materials and techniques," *Journal of Health and Allied Sciences NU,* vol. 2, no. 02, pp. 72-77, 2012.
[151] F. A. Alshahrani, F. AlToraibily, M. Alzaid, A. A. Mahrous, M. A. Al Ghamdi, and M. M. Gad, "An updated review of salivary pH effects on polymethyl methacrylate (PMMA)-based removable dental prostheses," *Polymers,* vol. 14, no. 16, p. 3387, 2022.
[152] H. Matsuo, H. Suenaga, M. Takahashi, O. Suzuki, K. Sasaki, and N. Takahashi, "Deterioration of polymethyl methacrylate dentures in the oral cavity," *Dental materials journal,* vol. 34, no. 2, pp. 234-239, 2015.
[153] M. M. Gad, S. M. Fouda, F. A. Al-Harbi, R. Näpänkangas, and A. Raustia, "PMMA denture base material enhancement: a review of fiber, filler, and nanofiller addition," *International journal of nanomedicine,* pp. 3801-3812, 2017.
[154] C. Bacali, M. Constantiniuc, M. Moldovan, V. Nastase, M. Badea, and A. Constantin, "Reinforcement of PMMA denture base resins: From Macro to Nano Scale," *International journal of medical dentistry,* vol. 23, no. 3, pp. 374-378, 2019.
[155] R. S. Jamel, M. A. Al-Murad, and E. F. Alkhalidi, "The efficacy of reinforcement of glass fibers and ZrO2 nanoparticles on the mechanical properties of autopolymerizing provisional restorations (PMMA)," *The Saudi Dental Journal,* vol. 35, no. 6, pp. 707-713, 2023.
[156] A. M. Díez-Pascual, "PMMA-based nanocomposites for odontology applications: a state-of-the-art," *International Journal of Molecular Sciences,* vol. 23, no. 18, p. 10288, 2022.
[157] P. Ramburrun, N. A. Pringle, A. Dube, R. Z. Adam, S. D'Souza, and M. Aucamp, "Recent advances in the development of antimicrobial and antifouling biocompatible materials for dental applications," *Materials,* vol. 14, no. 12, p. 3167, 2021.
[158] H. Yang, X. Xie, X. Li, and Y. Bai, "Polymethyl methacrylate resin containing ε-poly-L-lysine and 2-methacryloyloxyethyl phosphorylcholine with antimicrobial effects," *The Journal of Prosthetic Dentistry,* vol. 129, no. 1, pp. 228. e1-228. e8, 2023.
[159] L. Cao *et al.*, "Protein-repellent and antibacterial effects of a novel polymethyl methacrylate resin," *Journal of dentistry,* vol. 79, pp. 39-45, 2018.
[160] M. Cascione *et al.*, "Improvement of PMMA dental matrix performance by addition of titanium dioxide nanoparticles and clay nanotubes," *Nanomaterials,* vol. 11, no. 8, p. 2027, 2021.
[161] A. C. Ionescu *et al.*, "Physical-chemical and microbiological performances of graphene-doped PMMA for CAD/CAM applications before and after

accelerated aging protocols," *Dental Materials,* vol. 38, no. 9, pp. 1470-1481, 2022.
[162] E. J. Selva-Otaolaurruchi, L. Fernández-Estevan, M. F. Solá-Ruiz, F. García-Sala-Bonmati, I. Selva-Ribera, and R. Agustín-Panadero, "Graphene-doped polymethyl methacrylate (PMMA) as a new restorative material in implant-prosthetics: In vitro analysis of resistance to mechanical fatigue," *Journal of Clinical Medicine,* vol. 12, no. 4, p. 1269, 2023.
[163] D. Galusková, H. Kaňková, A. Švančárková, and D. Galusek, "Early-Stage Dissolution Kinetics of Silicate-Based Bioactive Glass under Dynamic Conditions: Critical Evaluation," (in eng), *Materials (Basel),* vol. 14, no. 12, Jun 18 2021, doi: 10.3390/ma14123384.
[164] B. Glass, G.-c. Fiber, M. Kochanowicz, J. Zmojda, and D. Dorosz, "Crystallization Kinetics and Structural Properties of," *materials Article,* 2020.
[165] K. Fujikura, N. Karpukhina, T. Kasuga, D. S. Brauer, R. G. Hill, and R. V. Law, "Influence of strontium substitution on structure and crystallisation of Bioglass® 45S5," *Journal of Materials Chemistry,* vol. 22, no. 15, pp. 7395-7402, 2012/4// 2012, doi: 10.1039/c2jm14674f.
[166] S. Melchers, T. Uesbeck, O. Winter, H. Eckert, and D. Eder, "Effect of Aluminum Ion Incorporation on the Bioactivity and Structure in Mesoporous Bioactive Glasses," *Chemistry of Materials,* vol. 28, no. 10, pp. 3254-3264, 2016/5// 2016, doi: 10.1021/acs.chemmater.5b04117.
[167] K. Zheng *et al.*, "Aging time and temperature effects on the structure and bioactivity of gel‐derived 45S5 glass‐ceramics," *Journal of the American Ceramic Society,* vol. 98, no. 1, pp. 30-38, 2015.
[168] K. Zheng *et al.*, "Toward highly dispersed mesoporous bioactive glass nanoparticles with high cu concentration using cu/ascorbic acid complex as precursor," *Frontiers in Chemistry,* vol. 7, no. July, pp. 1-15, 2019, doi: 10.3389/fchem.2019.00497.
[169] K. Schuhladen, L. Stich, J. Schmidt, A. Steinkasserer, A. R. Boccaccini, and E. Zinser, "Cu, Zn doped borate bioactive glasses: Antibacterial efficacy and dose-dependent: In vitro modulation of murine dendritic cells," *Biomaterials Science,* vol. 8, no. 8, pp. 2143-2155, 2020/4// 2020, doi: 10.1039/c9bm01691k.
[170] O. Thongsri *et al.*, "Enhanced remineralisation ability and antibacterial properties of sol-gel glass ionomer cement modified by fluoride containing strontium-based bioactive glass or strontium-containing fluorapatite," *Dental Materials,* vol. 40, no. 4, pp. 716-727, 2024/4// 2024, doi: 10.1016/j.dental.2024.02.014.
[171] E. Mabonga *et al.*, "Complete ciprofloxacin resistance in gonococcal isolates in an urban Ugandan clinic: findings from a cross-sectional study," *International journal of STD & AIDS,* vol. 30, no. 3, pp. 256-263, 2019.
[172] A. Senok *et al.*, "Pattern of antibiotic susceptibility in Campylobacter jejuni isolates of human and poultry origin," *Japanese journal of infectious diseases,* vol. 60, no. 1, pp. 1-4, 2007.
[173] M. De Cueto, L. Lopez, J. Hernandez, C. Morillo, and A. Pascual, "In vitro activity of fosfomycin against extended-spectrum-β-lactamase-producing Escherichia coli and Klebsiella pneumoniae: comparison of susceptibility testing procedures," *Antimicrobial agents and chemotherapy,* vol. 50, no. 1, pp. 368-370, 2006.

[174] P. Luber, E. Bartelt, E. Genschow, J. Wagner, and H. Hahn, "Comparison of broth microdilution, E test, and agar dilution methods for antibiotic susceptibility testing of Campylobacter jejuni and Campylobacter coli," *Journal of clinical microbiology,* vol. 41, no. 3, pp. 1062-1068, 2003.
[175] A. Nicodemo, M. Araujo, A. Ruiz, and A. Gales, "In vitro susceptibility of Stenotrophomonas maltophilia isolates: comparison of disc diffusion, Etest and agar dilution methods," *Journal of Antimicrobial Chemotherapy,* vol. 53, no. 4, pp. 604-608, 2004.
[176] L. Jiang, F. Wang, F. Han, W. Prinyawiwatkul, H. No, and B. Ge, "Evaluation of diffusion and dilution methods to determine the antimicrobial activity of water-soluble chitosan derivatives," *Journal of Applied Microbiology,* vol. 114, no. 4, pp. 956-963, 2013.
[177] T. E. Paterson *et al.*, "Electrospun scaffolds containing silver-doped hydroxyapatite with antimicrobial properties for applications in orthopedic and dental bone surgery," *Journal of Functional Biomaterials,* vol. 11, no. 3, 2020/9// 2020, doi: 10.3390/jfb11030058.
[178] Y. Li, A. Huang, T. Zhang, L. Wen, Z. Shi, and L. Shi, "A pH Monitoring Algorithm for Orifice Plate Culture Medium," *Applied Sciences (Switzerland),* vol. 12, no. 15, pp. 1-13, 2022, doi: 10.3390/app12157560.
[179] J. Michl, K. C. Park, and P. Swietach, "Evidence-based guidelines for controlling pH in mammalian live-cell culture systems," *Communications Biology,* vol. 2, no. 1, pp. 1-12, 2019, doi: 10.1038/s42003-019-0393-7.

Appendix:
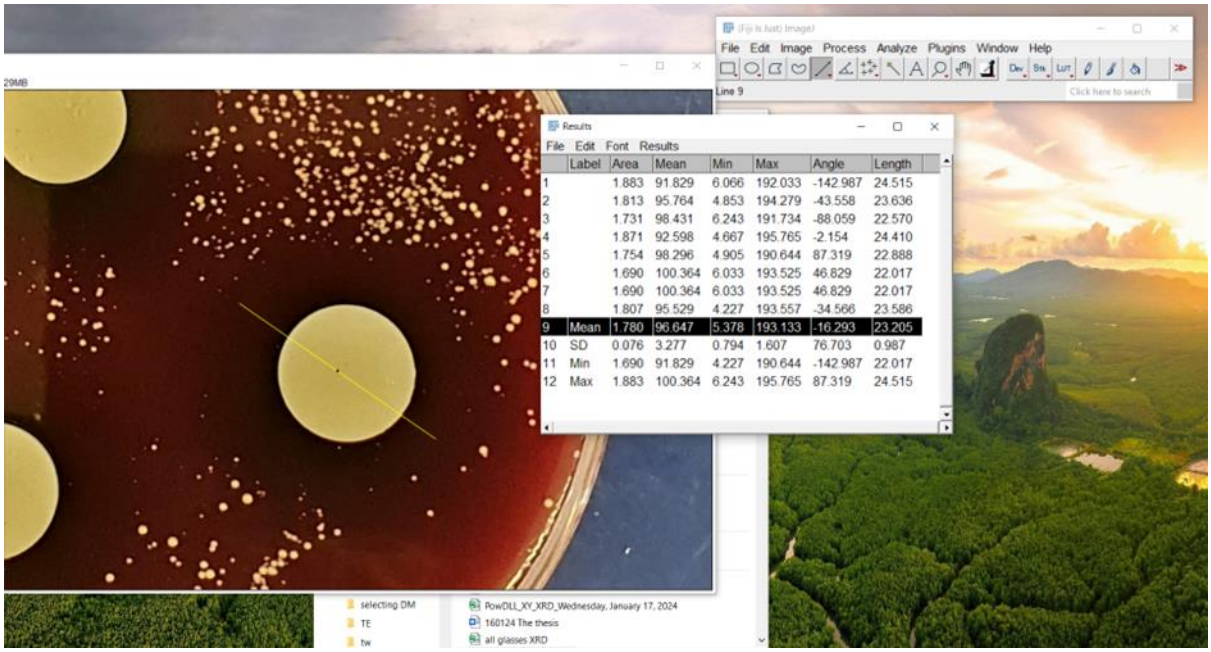
Using image J to calculate the inhibition zone